NASA TECHNICAL MEMORANDUM

NASA TM X-74008

NASA TM X-74008

(NASA-TM-X-74008) WIND TUNNEL INVESTIGATION OF THE AERODYNAMIC CHARACTERISTICS OF SYMMETRICALLY DEFLECTED AILERONS OF THE F-8C AIRPLANE (NASA) 120 p HC A06/MF A01 CSCL 01C G3/02

N77-23052

Unclas 26134

WIND TUNNEL INVESTIGATION OF THE AERODYNAMIC CHARACTERISTICS OF SYMMETRICALLY DEFLECTED AILERONS OF THE F-8C AIRPLANE

By Joseph Gera

April 4, 1977

National Aeronautics and Space Administration

Langley Research Center
Hampton, Virginia 23665

1. Report No.	2. Government Accession No.	3. Recipient's Catalog No.
NASA TM X-74008		

4. Title and Subtitle	5. Report Date
WIND TUNNEL INVESTIGATION OF THE AERODYNAMIC CHARACTERISTICS OF SYMMETRICALLY DEFLECTED AILERONS OF THE F-8C AIRPLANE	April 1977
	6. Performing Organization Code

7. Author(s)	8. Performing Organization Report No.
Joseph Gera	
	10. Work Unit No.

9. Performing Organization Name and Address	11. Contract or Grant No.
NASA Langley Research Center Hampton, Virginia 23665	
	13. Type of Report and Period Covered
12. Sponsoring Agency Name and Address	Technical Memorandum
National Aeronautics and Space Administration Washington, D. C. 20546	14. Sponsoring Agency Code

15. Supplementary Notes

16. Abstract

An investigation was conducted in the Langley 8-Foot Transonic Pressure Tunnel on a .042-scale model of the F-8C airplane at high subsonic Mach numbers and a range of angles of attack between -3 and 20 degrees. The objective of the test was to measure the effect of symmetrically deflected ailerons on the longitudinal aerodynamic characteristics. Some data were also obtained on the lateral control effectiveness of asymmetrically deflected horizontal tail surfaces.

17. Key Words (Suggested by Author(s))	18. Distribution Statement
Symmetric aileron deflections Direct lift Flap effectiveness F-8 airplane	

19. Security Classif. (of this report)	20. Security Classif. (of this page)	21. No. of Pages	22. Price*
Unclassified	Unclassified	120	$5.50

* For sale by the National Technical Information Service, Springfield, Virginia 22161

NATIONAL AERONAUTICS AND SPACE ADMINISTRATION

NASA TM X - 74008

WIND TUNNEL INVESTIGATION OF THE AERODYNAMIC CHARACTERISTICS OF SYMMETRICALLY DEFLECTED AILERONS OF THE F-8C AIRPLANE

By Joseph Gera

INTRODUCTION

One of the several active controls concepts considered for future fighter airplanes is the automatic control of wing camber. At subsonic speeds the increase of wing camber generally increases the lift coefficient at which minimum drag occurs. This results in improved combat capability; however, the highly cambered wing at supersonic speeds would result in excessive profile drag and trim drag.

The NASA F-8 digital fly-by-wire research airplane flight control system includes an automatic flap actuation mode. Ir this mode the control system computer will continuously vary the symmetric component of the total aileron commands so as to produce minimum drag throughout the flight envelope. The ailerons are displaced symmetrically in lieu of trailing edge flaps which do not exist on this airplane. The objective of the wind tunnel tests reported herein was to investigate the effect of symmetrically deflected ailerons on the lift, drag and pitching moment characteristics at high subsonic Mach numbers. A limited amount of data were also obtained with the horizontal tail surfaces displaced asymmetrically in an effort to establish their effectiveness for lateral control.

SUMMARY

An investigation was conducted in the Langley 8-Foot Transonic Pressure Tunnel on a .042-scale model of the F-8C airplane at high subsonic Mach numbers and a range of angles of attack between -3 and 20 degrees. The objective of the test was to measure the effect of symmetrically deflected ailerons on the longitudinal aerodynamic characteristics. Some data were also obtained on the lateral control effectiveness of asymmetrically deflected horizontal tail surfaces.

SYMBOLS

The forces and moments were measured in a body-axis coordinate system. The origin of the axis system is the projection of a point located at the forward 28.7 percent of the mean aerodynamic chord onto waterline 100. (See Figure 1.). The x-axis coincides with waterline 100 in the plane of symmetry.

b	wing span, .4566 m
$\bar{c}$	mean aerodynamic chord, $.151 \times 10^{-2}$ m
C_D	drag coefficient, (Drag force)/qS
C_L	lift coefficient, (Lift force)/qS
$C_{D_{\delta_f}}$	$\frac{\Delta C_D}{\Delta \delta_f}$, rad^{-1}
$C_{L_{\delta_f}}$	$\frac{\Delta C_L}{\Delta \delta_f}$, rad^{-1}
C_Y	side force coefficient, (Side force)/qS
C_l	rolling moment coefficient, (Rolling moment)/qSb
C_m	pitching moment coefficient, (Pitching moment)/$qS\bar{c}$
C_n	yawing moment coefficient, (Yawing moment)/qSb
$C_{m_{\delta_f}}$	$\frac{\Delta C_m}{\Delta \delta_f}$, rad^{-1}
M	free-stream Mach number
S	total wing area, 6.146×10^{-2} m^2

S_t	total horizontal tail surface (based on area extending to fuselage center line) 1.53×10^{-2} m^2
S_a	aileron area per surface, $.34 \times 10^{-2}$ m^2
q	free-stream dynamic pressure, N/m^2
δ_{a_L}, δ_{a_R}	left and right single surface aileron deflections, respectively, trailing edge down is positive deg
δ_e	horizontal tail deflection, defined by $\delta_e = \frac{1}{2}(\delta_{e_R} + \delta_{e_L})$ deg
δ_{e_L}, δ_{e_R}	left and right horizontal tail deflections, respectively; trailing edge down is positive, deg
δ_{rt}	rolling-tail deflection, defined by $\delta_{rt} = \delta_{e_L} - \delta_{e_R}$, deg
δ_a	aileron deflection, defined by $\delta_a = \delta_{a_L} - \delta_{a_R}$, deg
δ_f	symmetric aileron deflection, defined by $\delta_f = (\delta_{a_L} + \delta_{a_r})$ ('symmetric ailerons' and 'flaps' are synonymous in this report), deg
α	fuselage angle of attack, deg
Δ	incremental value in coefficient or surface deflection

APPARATUS AND TESTS

Model

The wind tunnel model was a .042-scale replica of the F-8C (F8U-2) airplane. Pertinent geometric characteristics of the model are given in Figure 1. It may be noted on the figure that the wind-tunnel model had a faired forebody; the full scale airplane configuration forebody contours are shown with broken lines. The wind tunnel model mounted on the sting is shown in Figure 2. Boundary layer transition was fixed by means of #180 carborundum strips. These transition strips were located one centimeter behind the leading edges of the wing, tail surfaces and ventral fins in a streamwise direction, and three centimeters aft on the fuselage nose. The only moveable controls of the model

were the left and right horizontal tail surfaces and the left and right ailerons. Symmetric displacement of the left and right aileron is sometimes referred to as a flap deflection. The latter is not to be confused with the small inboard flaps of the F-8C which remained faired into the wing throughout the present tests. Unlike the full-scale airplane, the model was not equipped with a wing leading edge droop.

Tests

The investigation was made in the Langley 8-foot transonic pressure tunnel. All configurations were tested at Mach numbers of .93, .9, .85, .8 and .7. The wind tunnel stagnation pressure was adjusted at each Mach number to provide for a test Reynolds number of 1.13 million based on the mean aerodynamic chord of the model. Horizontal tail deflections of 0, -5, -10 and -15 degrees were tested at symmetric ailerons or flap deflections of 0, 5, 10 and 15 degrees. Limited amount of testing was also performed on configurations having antisymmetric horizontal tail and flap deflections, since these conditions constitute a possible failure mode of the full-scale testbed airplane. The angle of attack for all configurations was varied from approximately -3 to 20 degrees.

Static aerodynamic force and moment data were obtained by a six-component, internally mounted, strain-guage balance. The values of the angles of attack presented herein were corrected for balance and sting deflection due to the aerodynamic loads and for a test-section flow angularity of .2 degrees. The drag data presented in the report contain the effects of the actual base pressures existing during the tests; consequently, the absolute magnitude of the drag coefficients should be used with caution. Increments in the drag coefficients due to configuration changes, however, are believed to be sufficiently accurate for purposes of flight simulation or preliminary performance calculations.

Presentation of Results

The results of the investigation are presented in the following figures.

Longitudinal aerodynamic characteristics:

Variation of lift, drag, and pitching moment coefficients with angle of attack at Mach numbers of .93, .90, .85, .80, .70:

$\delta_f = 0^\circ$ . . . . . Fig. 3

$\delta_f = 5^\circ$ . . . . . Fig. 4

$\delta_f = 10^\circ$ . . . . . Fig. 5

$\delta_f = 15^\circ$ . . . . . Fig. 6

The effect of flap deflections on lift, drag and pitching moment coefficients at Mach numbers of .93, .90, .85, .80, .70:

$\delta_e = 0^\circ$ . . . . . Fig. 8

$\delta_e = -5^\circ$ . . . . . Fig. 9

Variation of flap effectiveness parameters with angle of attack at Mach numbers of .98, .90, .85, and .6

. . . . . Fig. 10

Pictorial representation of curve fitting and extrapolation scheme

. . . . . Fig. 11

The ratio, $C_{m_{\delta_f}} / C_{m_{\delta_e}}$ as a function of angle of attack and Mach number

. . . . . Fig. 12

The effect of symmetric displacement of the ailerons on lateral control effectiveness. The effects of a 5° deflection of the ailerons and asymmetric horizontal tail are also compared in this figure

. . . . . Fig. 13

Comparison of the effects of a 10° deflection of the ailerons and asymmetric horizontal tail

. . . . . Fig. 14

DISCUSSION

The results presented in Figure 3 through 6 do not reveal any unusual longitudinal characteristics which might be attributed to flap deflections. At all Mach numbers and horizontal tail settings the condition $C_m = 0$ occurs at lower angles of attack whenever there is any positive flap deflection. Ideally, the lower angles of attack would result in reduced drag at the higher lift coefficients. The trimmed drag polars of Figure 7 demonstrate this effect, however, only at the highest test Mach number.

The next series of curves collected in Figures 8 and 9 can be used to establish the control derivatives $C_{L_{\delta_f}}$, $C_{D_{\delta_f}}$ and $C_{m_{\delta_f}}$ by considering the increments in the basic lift, drag and pitching moment coefficients due to

flap deflections. The latter data are presented in these figures for horizontal tail settings of 0 and -5 degrees. It can be seen from a comparison of corresponding figures at $\delta_e = 0^o$ and -5^o that horizontal tail setting had little or no effect on the effectiveness of the flaps. In generating additional lift, the flaps were most effective between 0 and 5 degrees with considerable effectiveness remaining between 5 and 15 degrees. This should be contrasted with the effect of flaps on the pitching moment. Beyond 10 degree flap deflection in most cases only small additional pitching moment is generated by the flaps.

The effect of the flaps on the static longitudinal characteristics is summarized in Figure 10. The data in this figure have been extrapolated to cover the Mach number range of .6 to .98, and thus be directly useable in the aerodynamic data package of several current simulators of the F-8C airplane. The extrapolation was carried out in the following manner:

1) At each of the test Mach numbers a cubic spline function was fitted through the coefficient data points at each angle of attack. A linear extrapolation was then made through the last valid data points to extend the α-range from -4^o to 20^o.

2) At each angle of attack a spline function was fitted in the Mach number direction and an extrapolation was made to cover the Mach number range of interest. The procedure is shown schematically in Figure 11.

Figure 12 shows the ratio $C_{m_{\delta_f}} \Big/ C_{m_{\delta_e}}$ at the test Mach numbers over a range of angles of attack. Accurate knowledge of this ratio is important in the design of a direct lift control system. Undesirable pitching moment changes produced by deflecting the flaps can be cancelled for steady-state flight by including in the design a flap-to-elevator linkage having a gearing ratio numerically equal to $C_{m_{\delta_f}} \Big/ C_{m_{\delta_e}}$.

Since direct lift is controlled by the ailerons deflected symmetrically, it is important to examine the effect of symmetrically displaced aileron surfaces on the lateral and directional characteristics. Figure 13 shows that except at the higher test Mach numbers, the roll control effectiveness of the ailerons does not change significantly when the symmetric component of the deflection is increased from 2.5 to 7.5 degrees. The reason for the large rolling moment increment, ΔC_l, at M = .7 at high angles of attack is not understood. Figure 13 also presents data obtained when the horizontal tail was deflected differentially 5 degrees about a mean or symmetric displacement of -7.5 degrees. The data show that at high angles of attack and high Mach numbers the roll control effectiveness, ΔC_l, of the ailerons and of horizontal tail is about the same. However, the asymmetrically deflected horizontal tail surfaces result in large incremental yawing moment,

ΔC_n at all test conditions. The large positive value of the parameter

$\frac{\Delta C_n}{\Delta C_l}$ would be detrimental from the standpoint of good handling qualities.

Figure 14 also shows the effects of identical angular displacements, 10 degrees, of the ailerons and of the horizontal tail surfaces on the lateral-directional characteristics. The mean or symmetric component of the aileron and horizontal tail displacement was 0 and -10 degrees, respectively. Because of the large incidence, one of the horizontal tail surfaces was stalled at the lower values of fuselage angle of attack. This resulted in smaller incremental rolling and yawing moments than those shown in the previous figure for the 5-degree differential tail displacement.

CONCLUDING REMARKS

A short wind tunnel investigation of the effects of symmetrically deflected ailerons and asymmetrically deflected horizontal tail surfaces indicates the following:

1) At all test Mach numbers the trim angle of attack decreases with positive flap settings.

2) In generating additional lift, the flaps were most effective between 0 and 5 degrees with considerable effectiveness remaining between 5 and 15 degrees. Beyond 5 degree deflection the flaps generated no significant additional pitching moments.

3) The roll control effectiveness of the ailerons is reduced with positive flap settings only at Mach numbers beyond .9.

4) The lateral control effectivess of asymmetric horizontal tail is significant only at high angles of attack. Asymmetric tail deflections generate large proverse yawing moments.

REFERENCES

1. Boisseau, Peter C.: Low-Speed Roll Effectiveness of a Differentially Deflected Horizontal-Tail Surface on a 42° Swept-Wing Model. NACA RM L56E03, 1956.

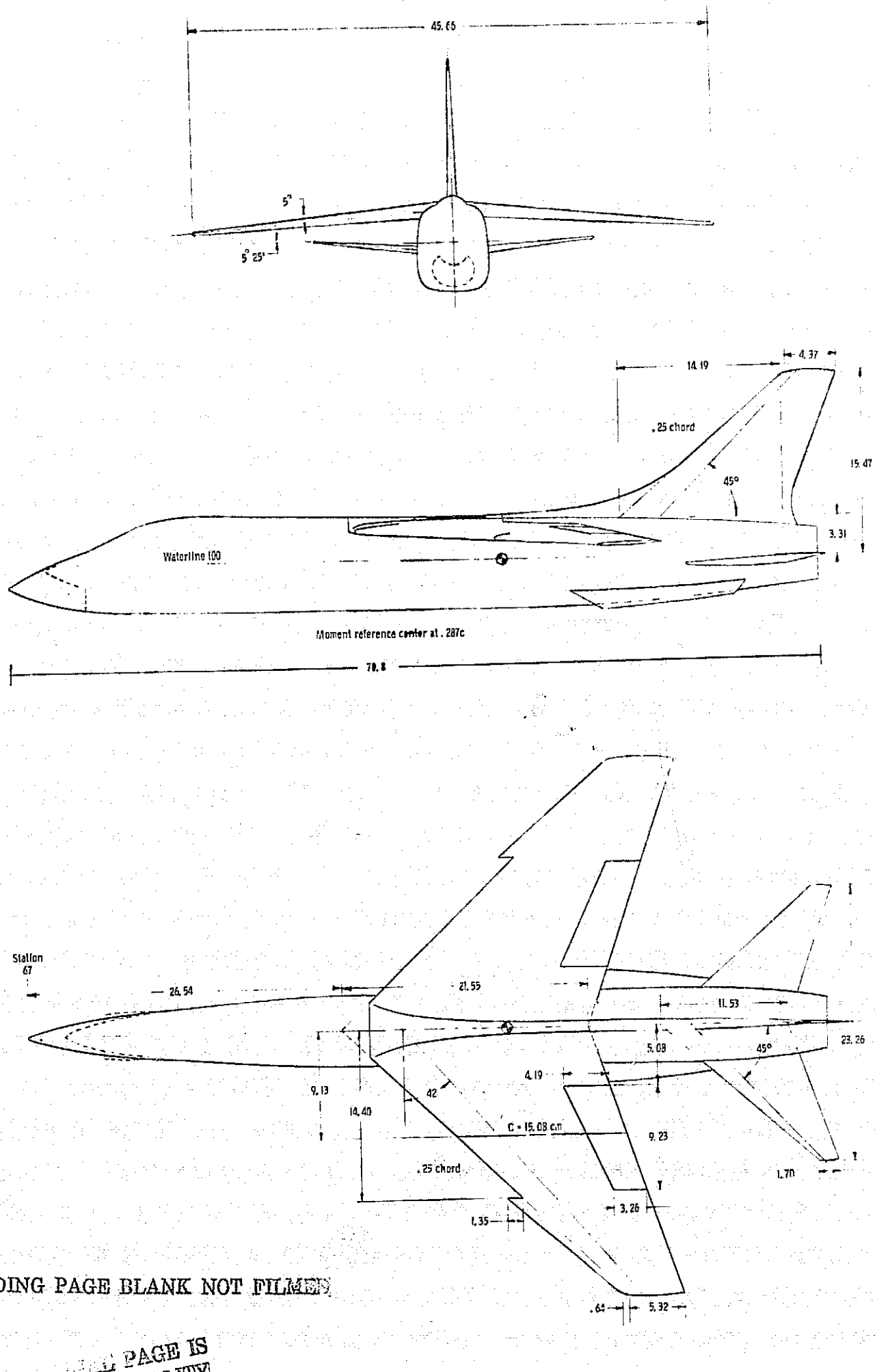

PRECEDING PAGE BLANK NOT FILMED

Figure 1. Geometric characteristics of .042-scale wind tunnel model. All dimensions are in centimeters.

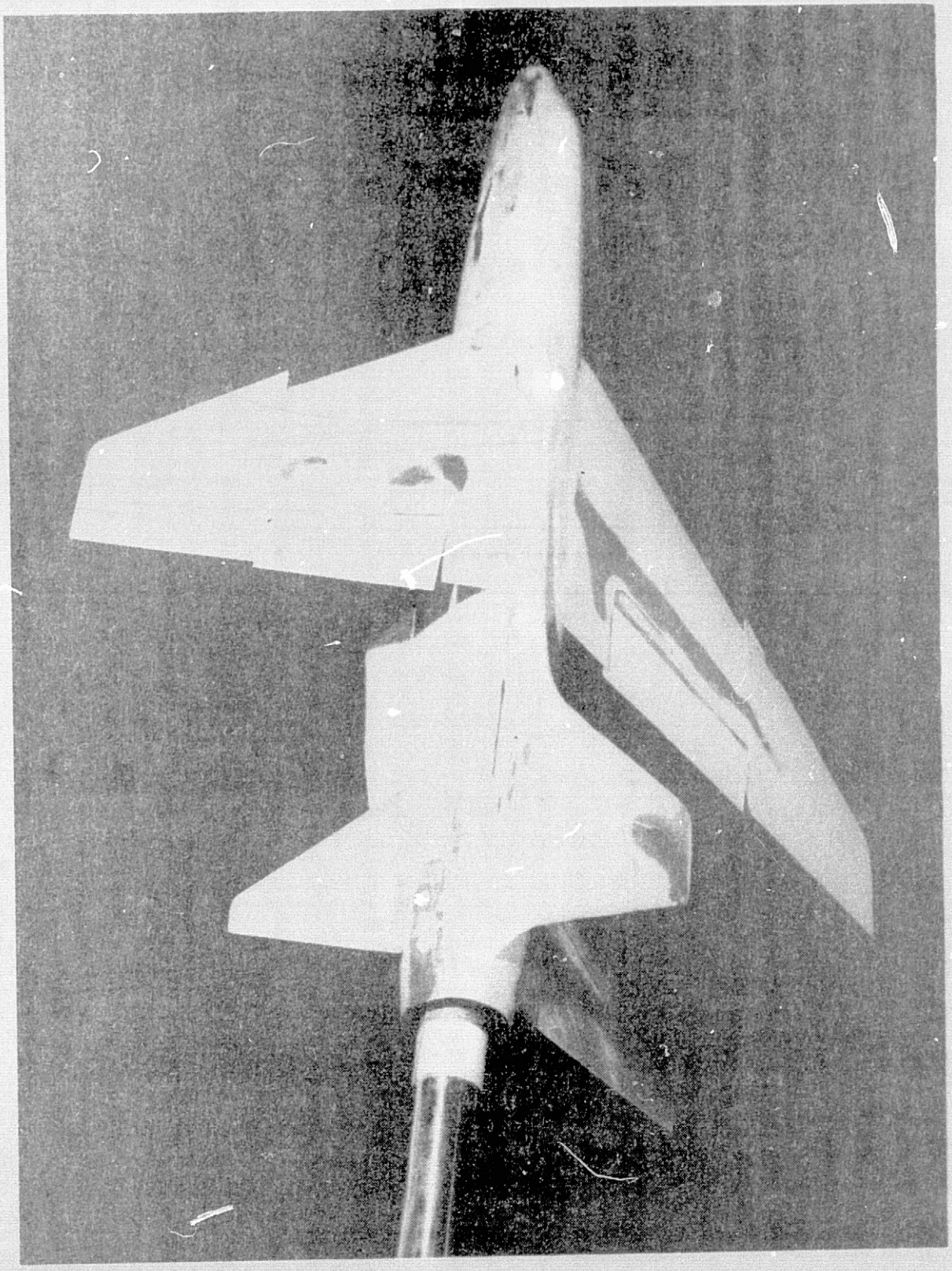

Figure 2.- Photograph of the model installed on wind tunnel sting.

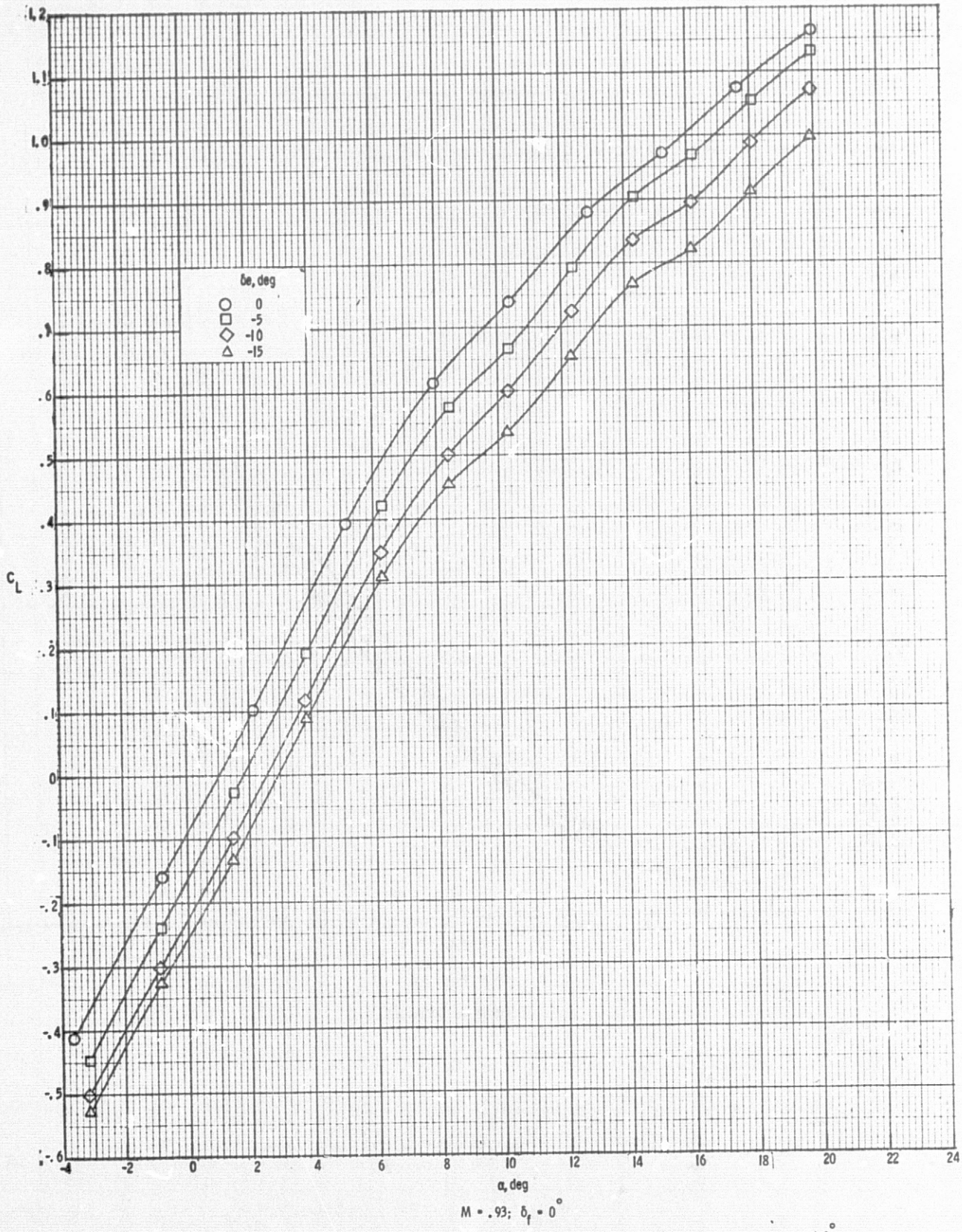

M = .93; $\delta_f = 0^\circ$

Figure 3. Variation of lift, drag and pitching moment coefficients with angle of attack at flap setting of 0°.

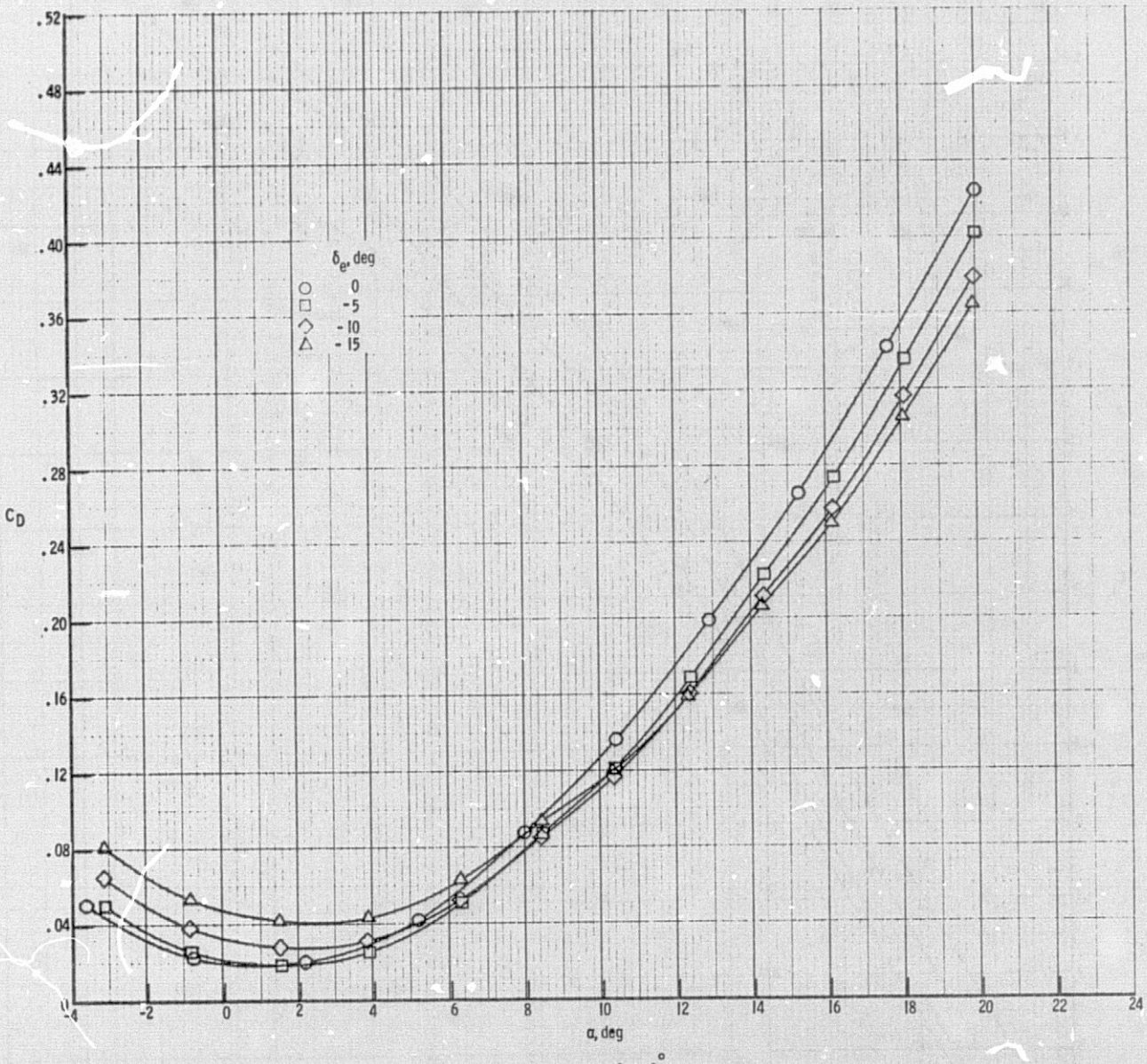

M = .93; δ_f = 0°

Figure 3. Continued.

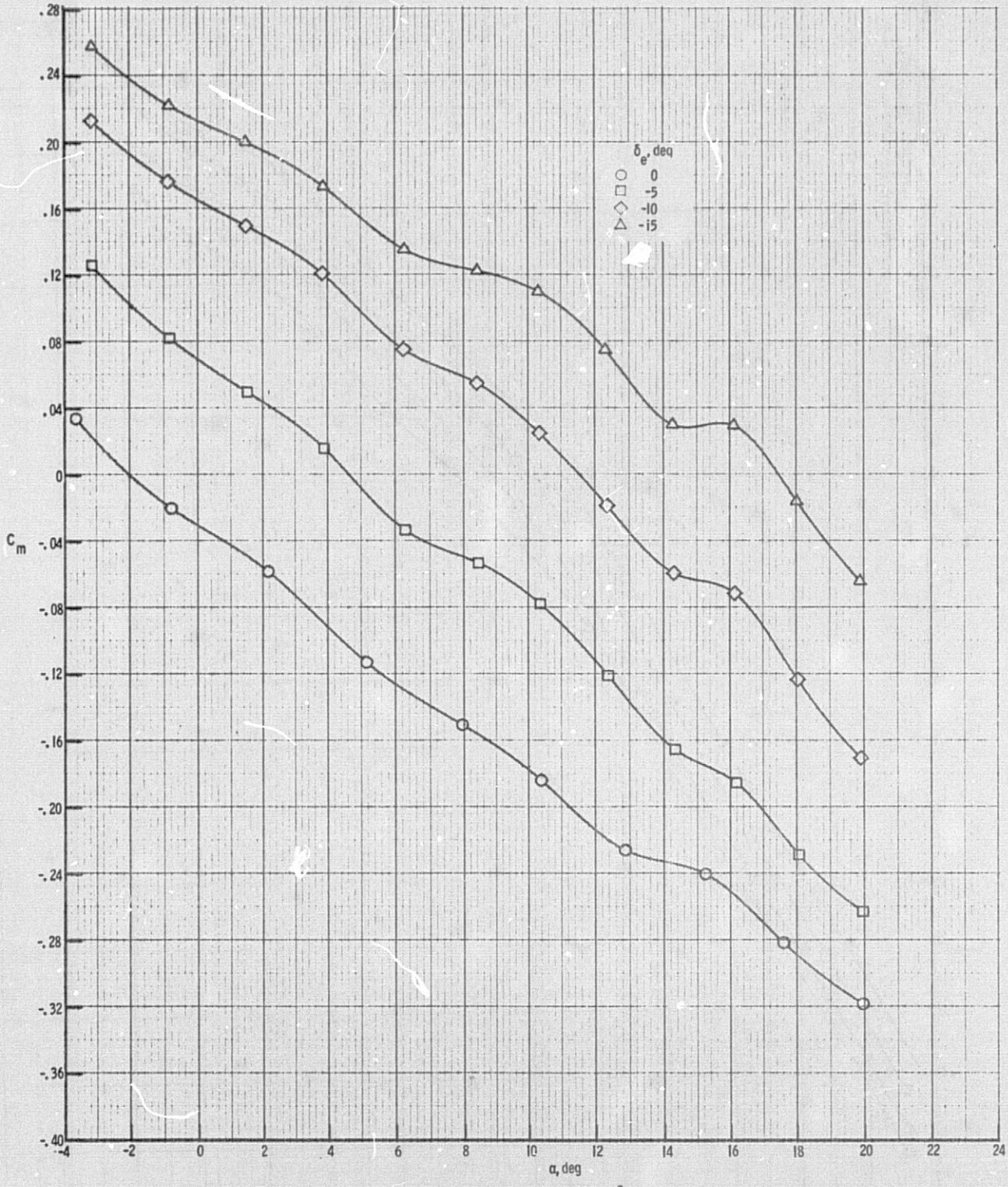

M = .93; $\delta_f = 0^\circ$

Figure 3. Continued.

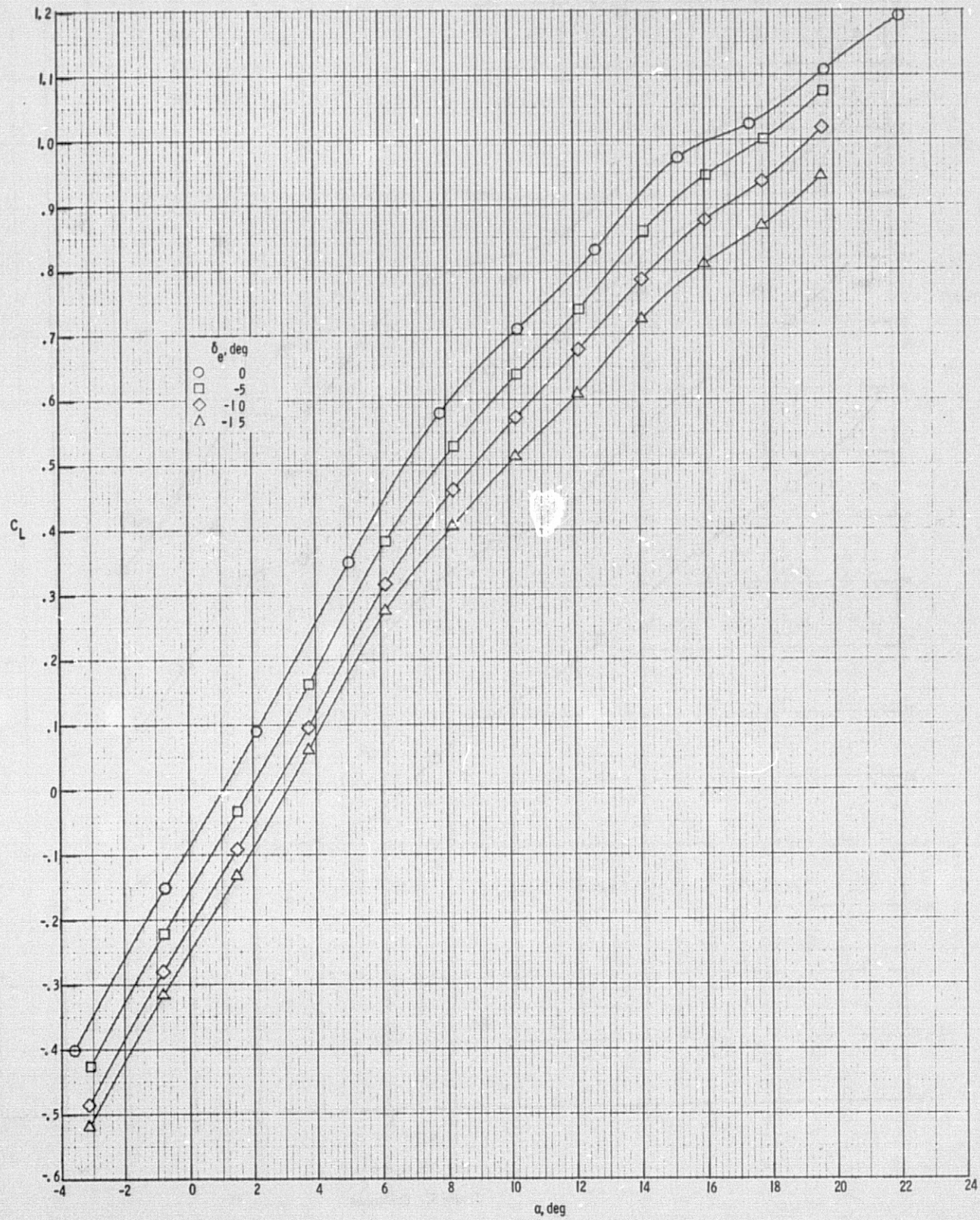

M = .90; $\delta_f = 0^\circ$

Figure 3. Continued.

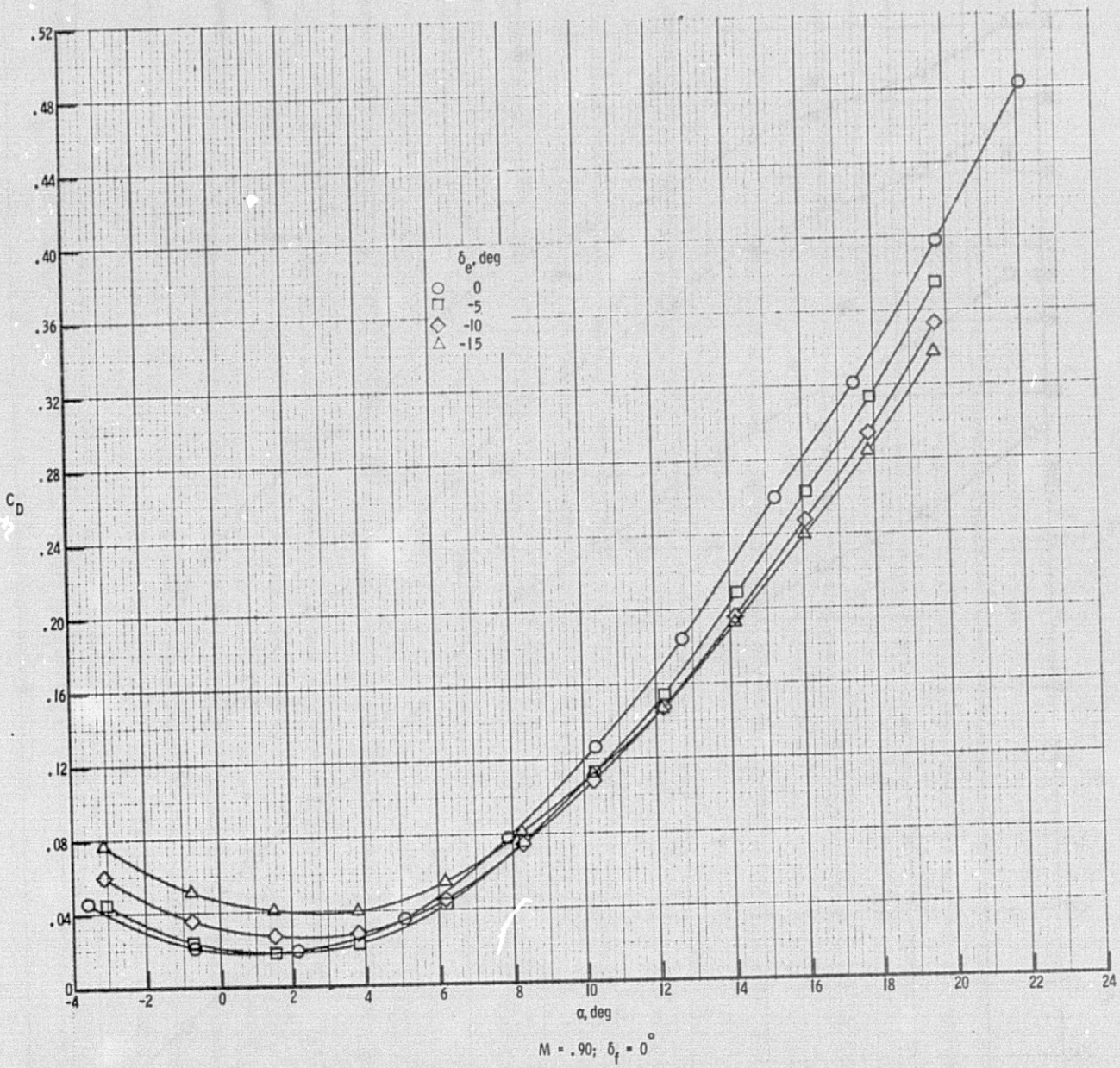

M = .90; $\delta_f = 0°$

Figure 3. Continued.

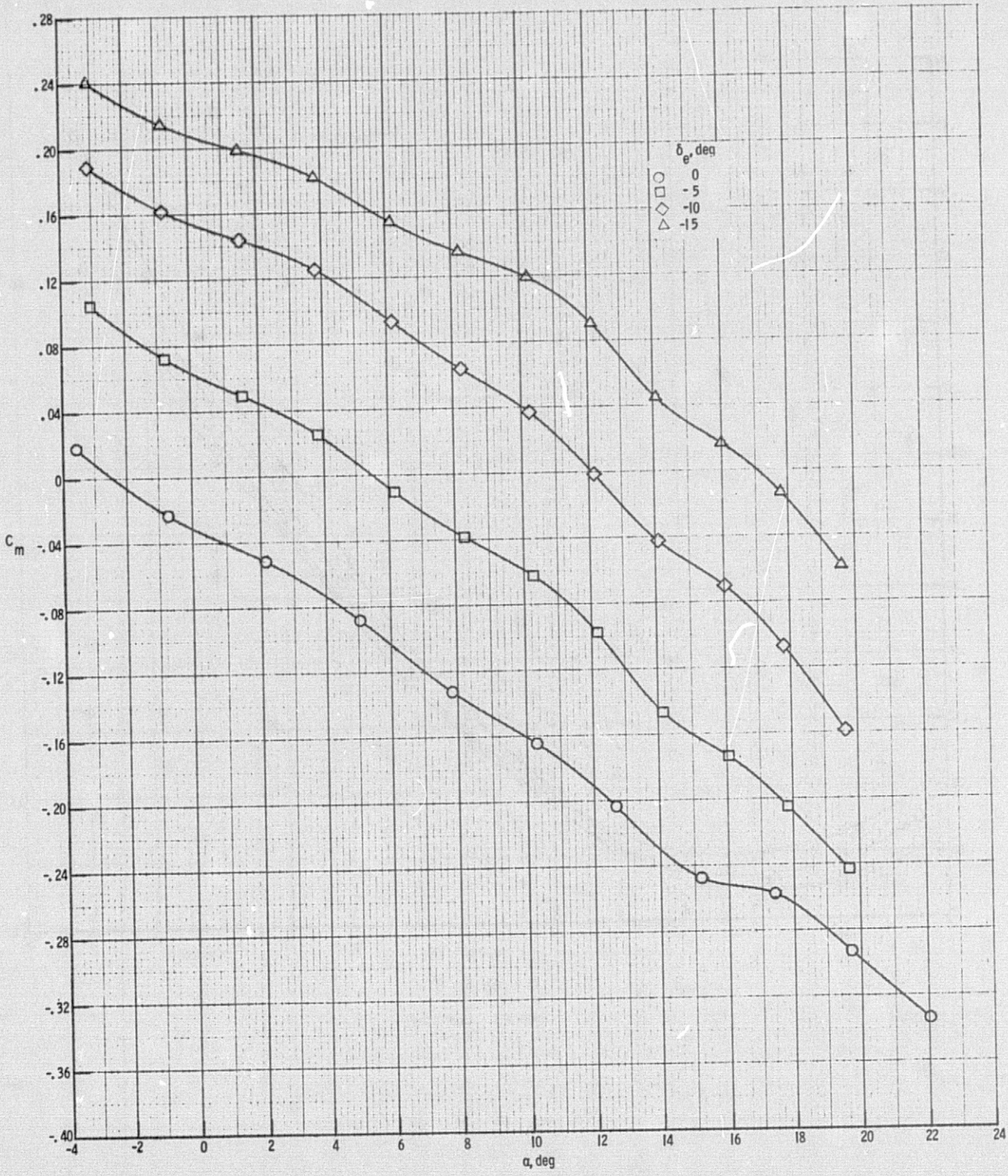

M = .90; $\delta_f = 0^\circ$

Figure 3. Continued.

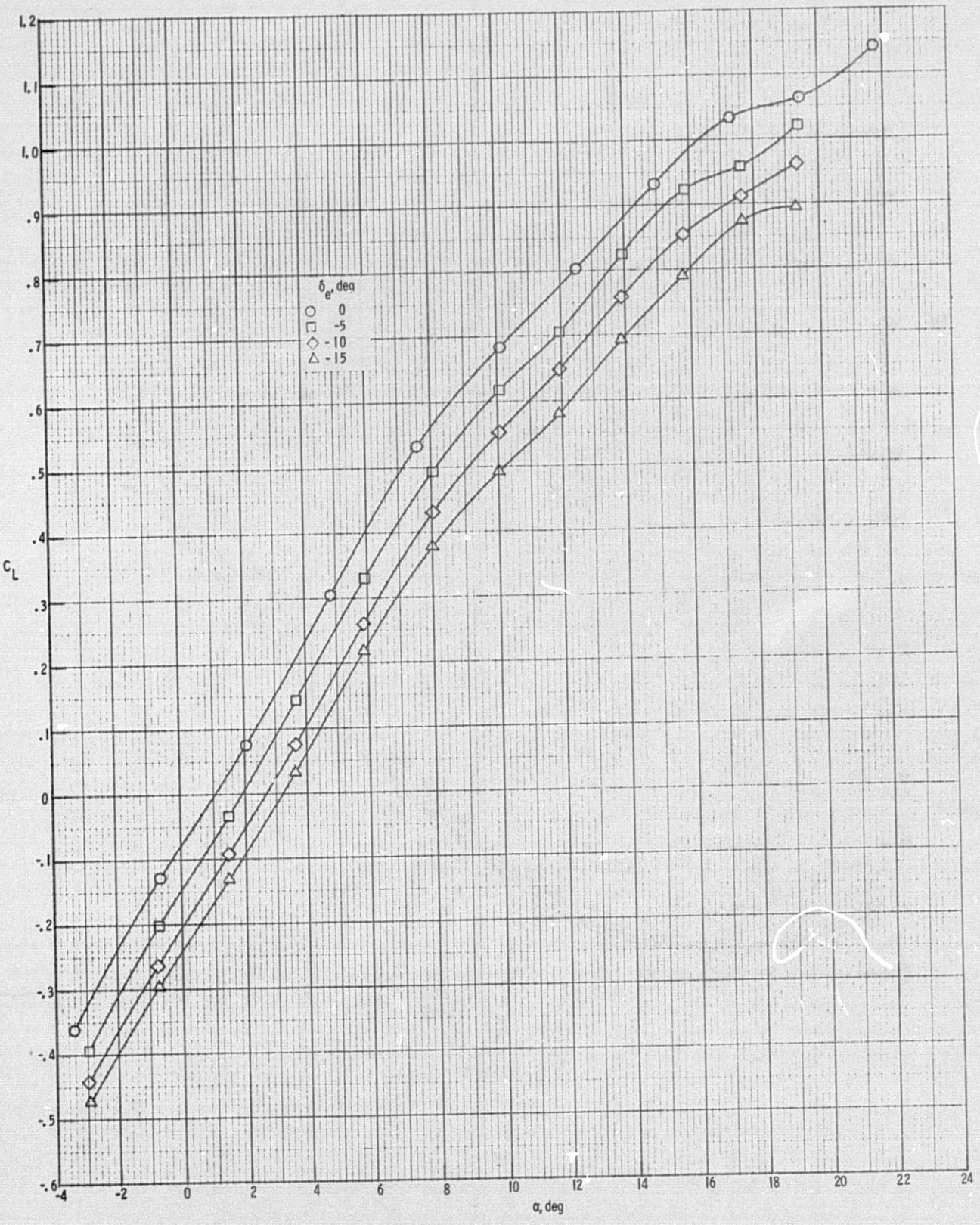

M = .85; δ_f = 0°

Figure 3. Continued.

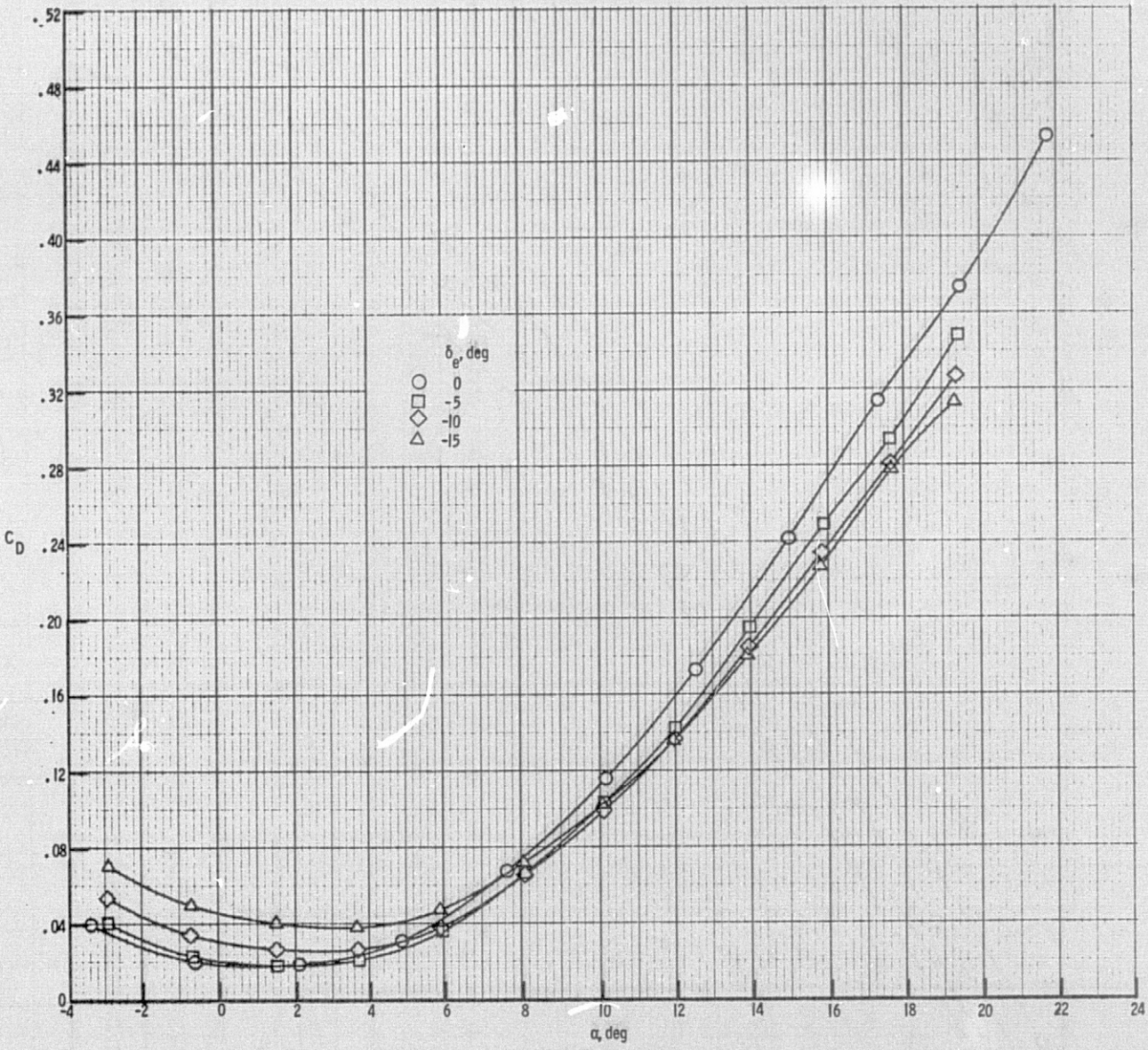

M = .85; δ_f = 0°

Figure 3. Continued.

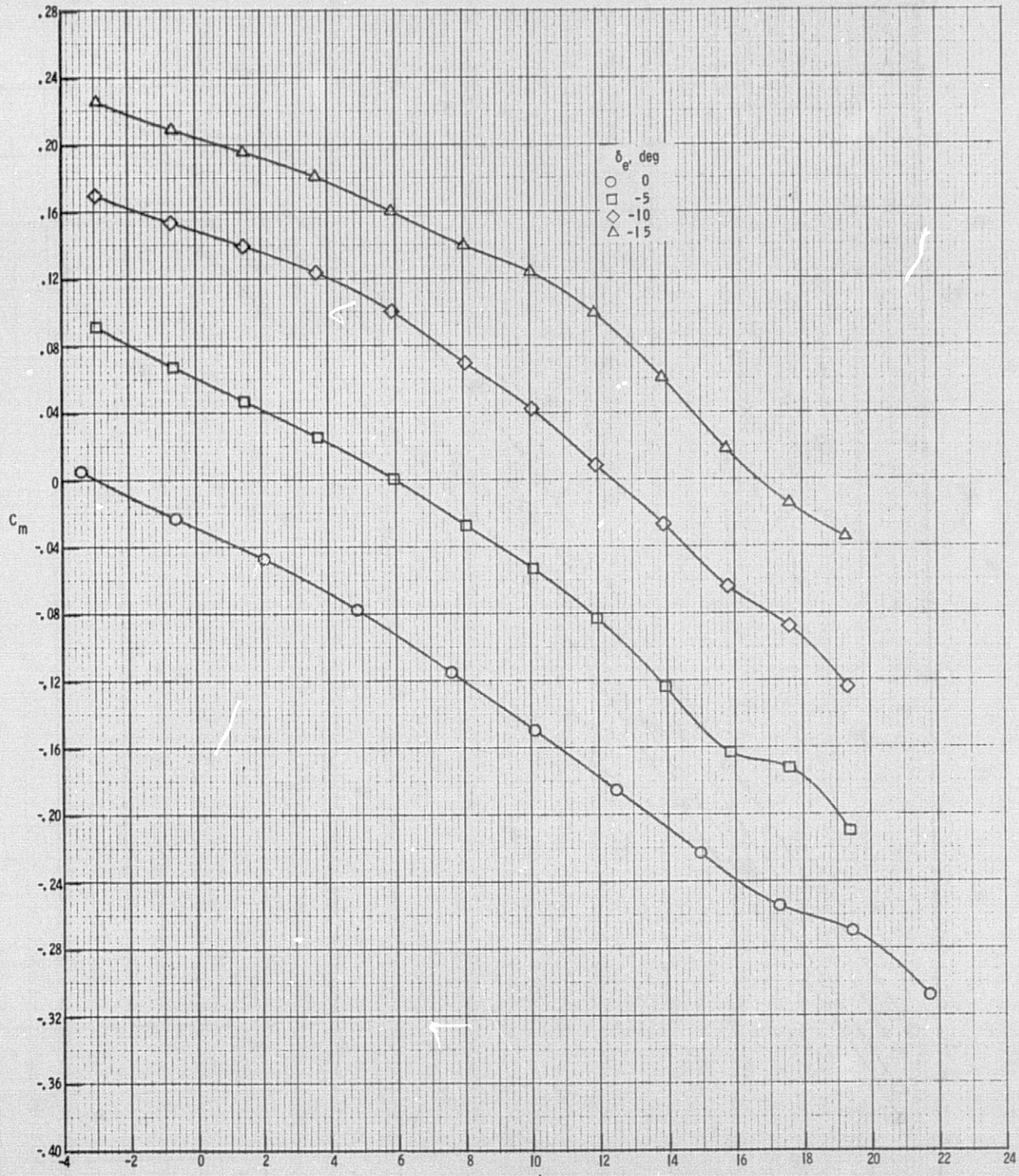

M = .85; δ_f = 0°

Figure 3. Continued.

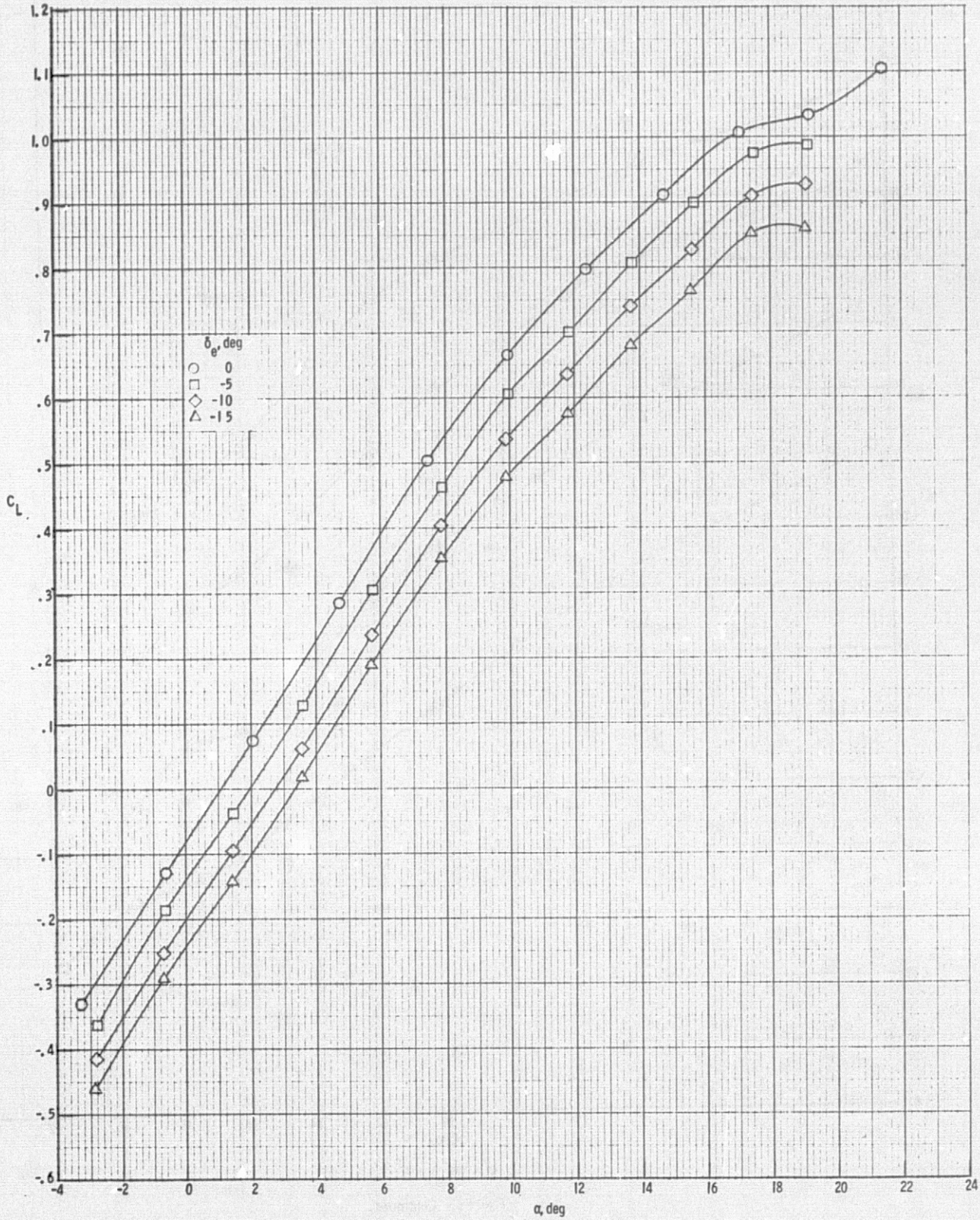

M = .80; $\delta_f = 0^\circ$

Figure 3. Continued.

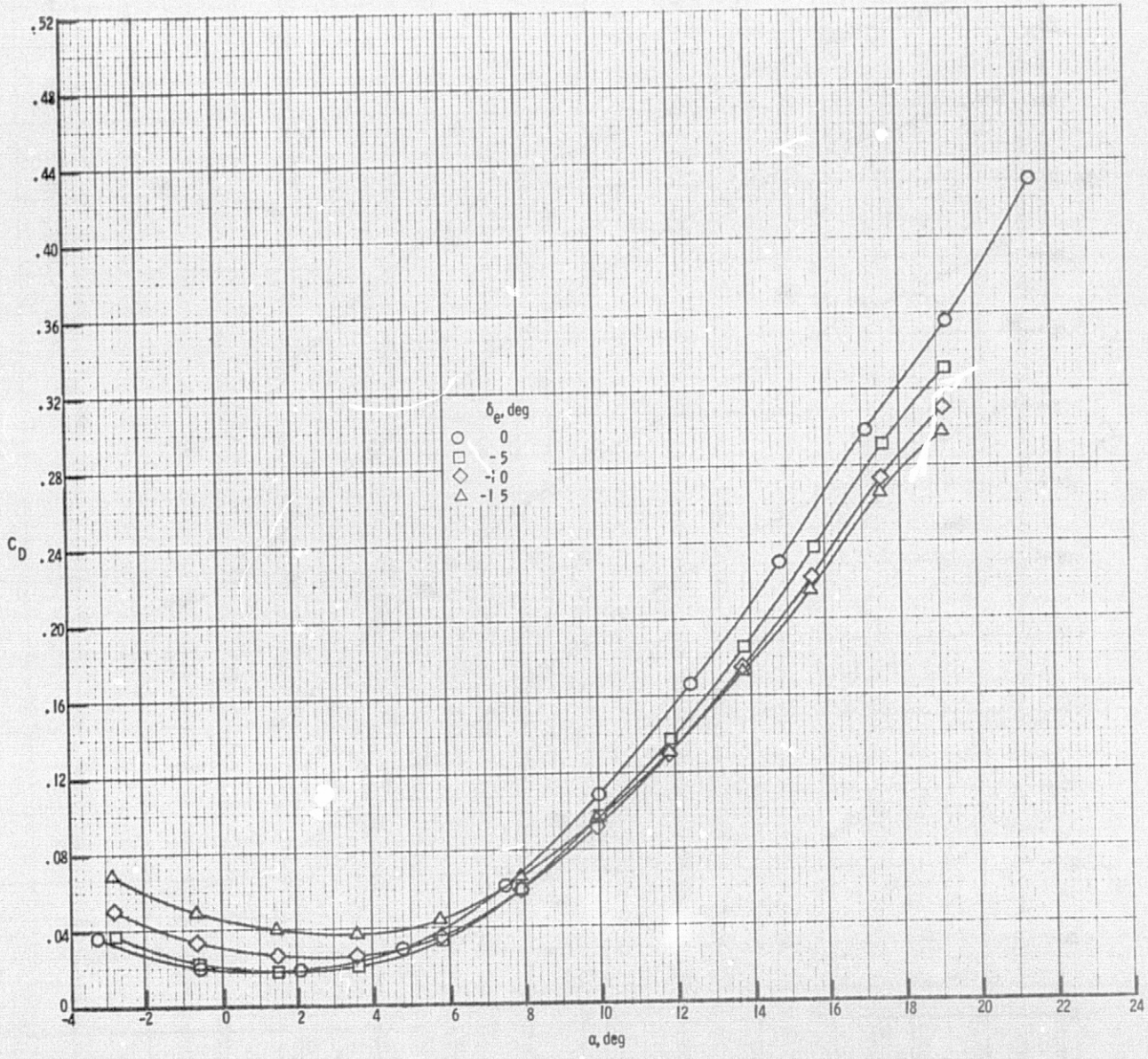

M = .80; $\delta_f = 0°$

Figure 3. Continued.

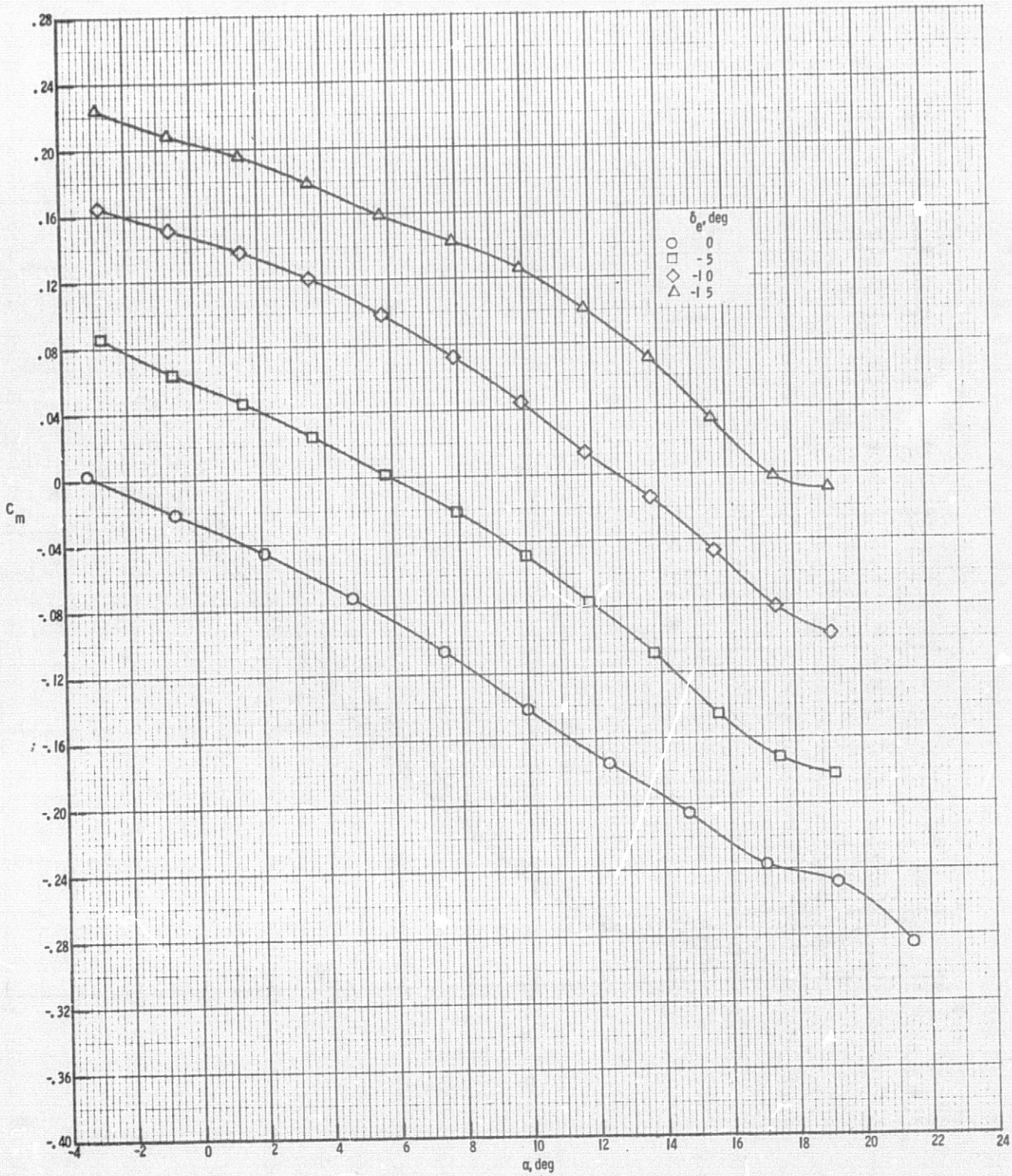

M = .80; δ_f = 0°

Figure 3. Continued.

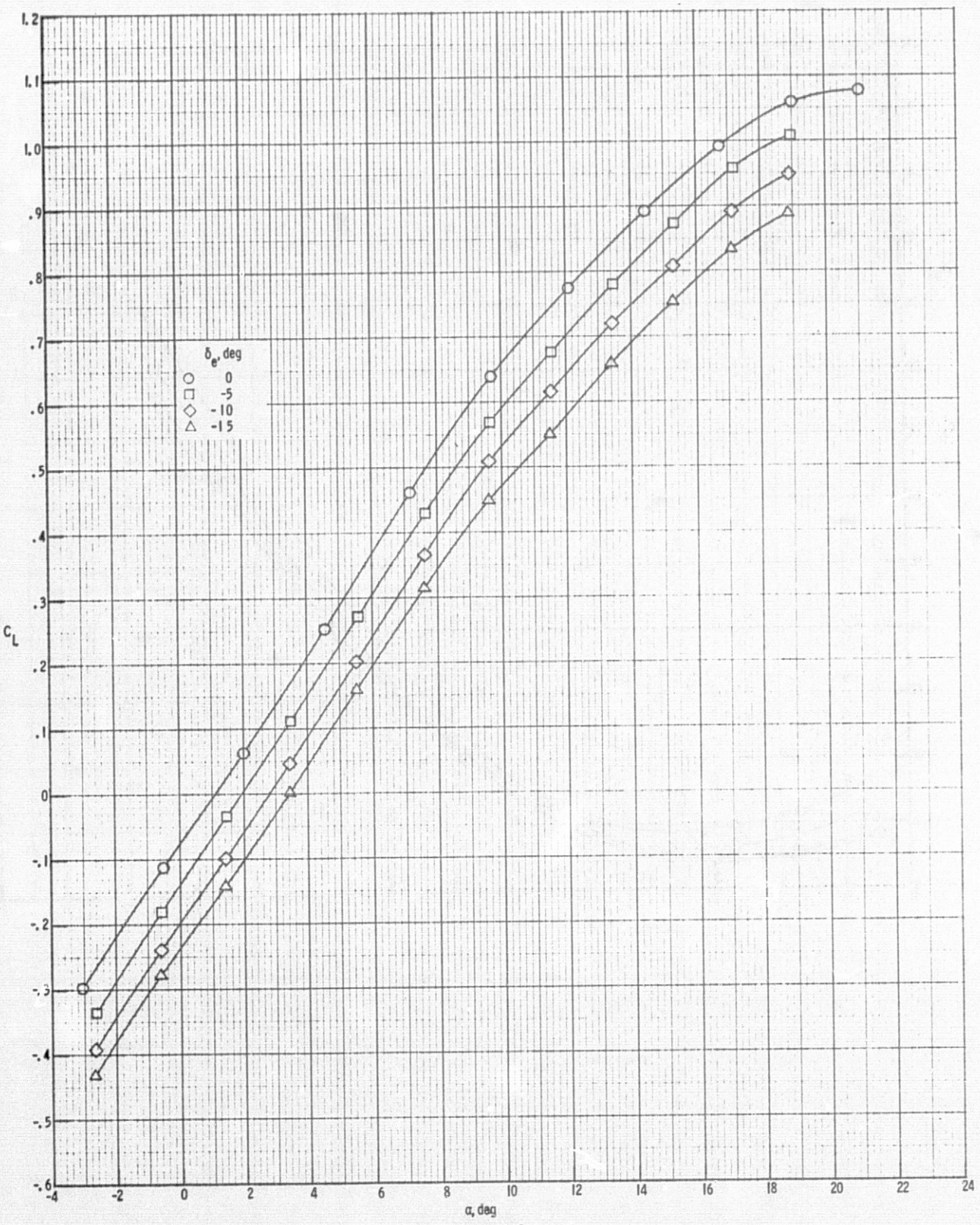

M = .70; $\delta_f = 0^\circ$

Figure 3. Continued.

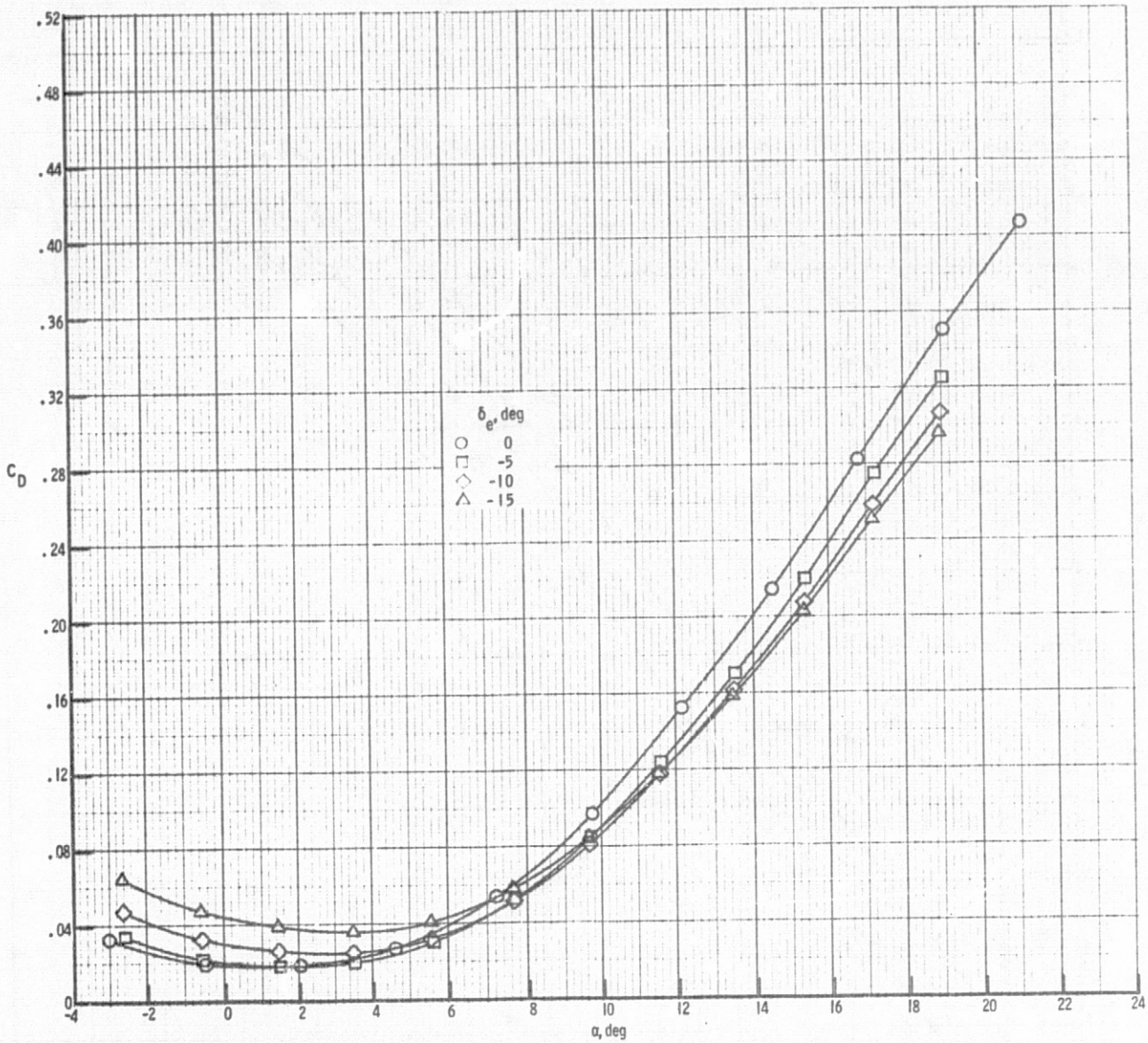

M = .70; $\delta_f = 0^\circ$

Figure 3. Continued.

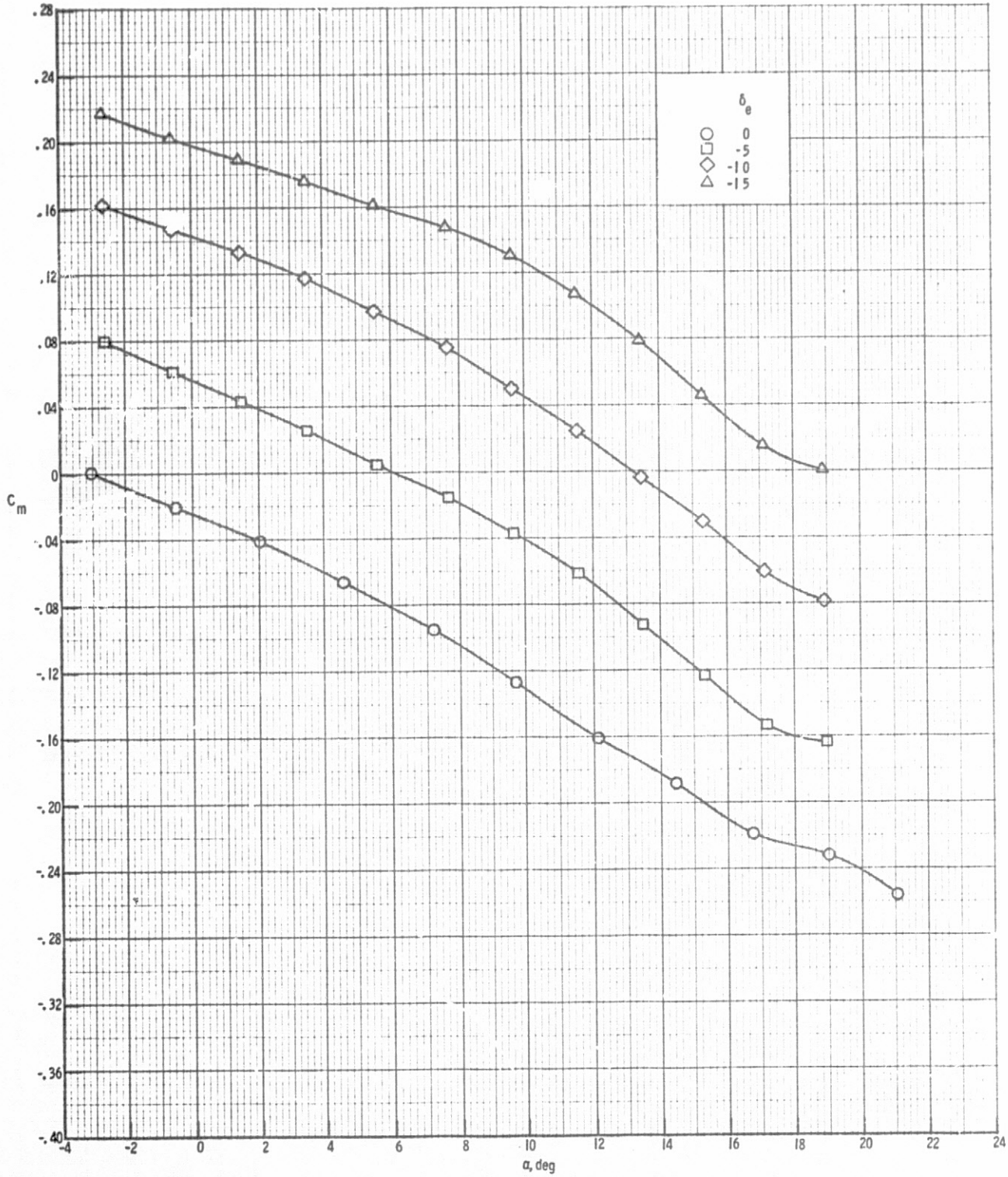

$M = .70$; $\delta_f = 0^\circ$

Figure 3. Concluded.

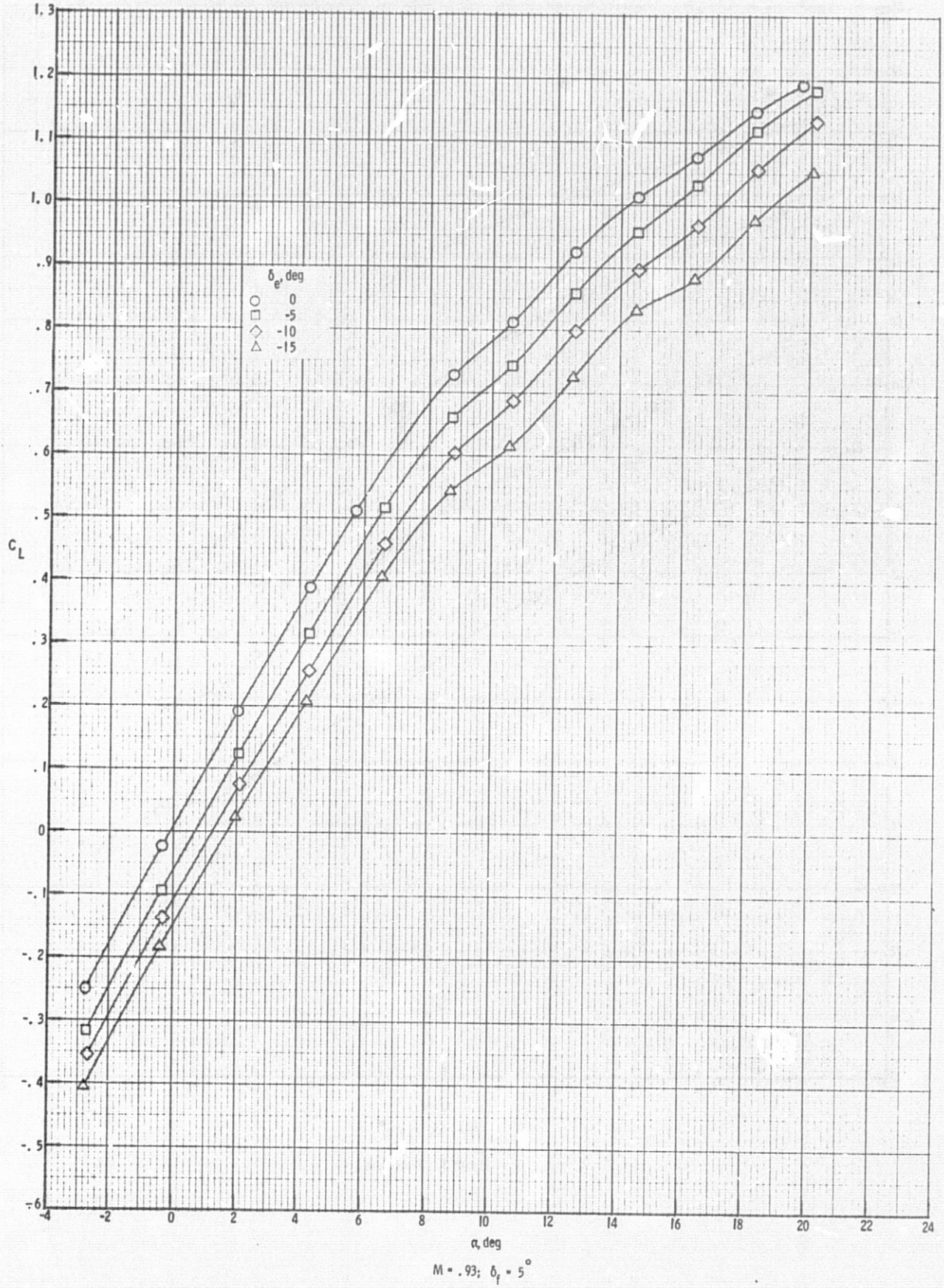

Figure 4. Variation of lift, drag and pitching moment coefficients with angle of attack at flap setting of 5°.

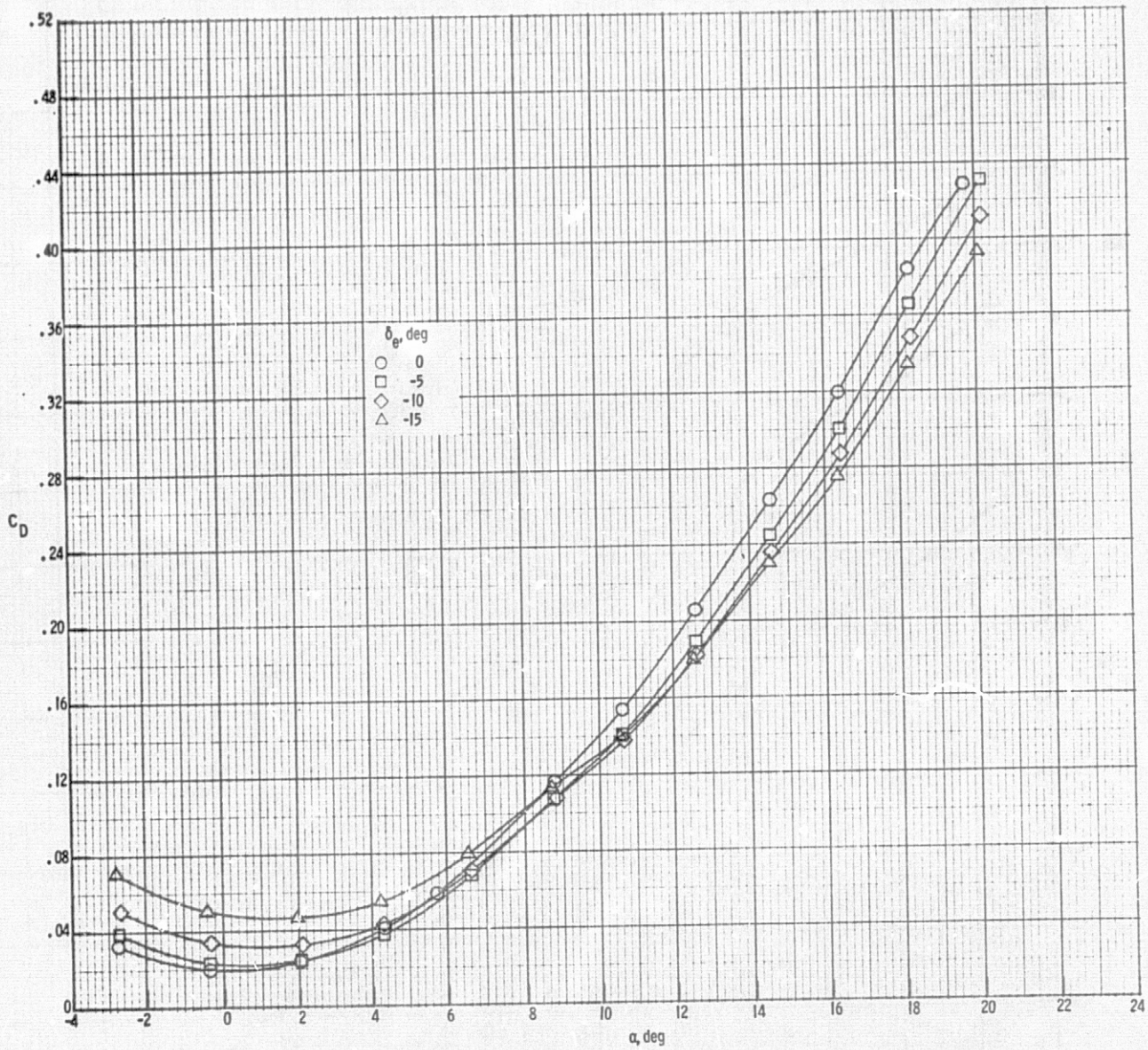

M = .93; δ_f = 5°

Figure 4. Continued.

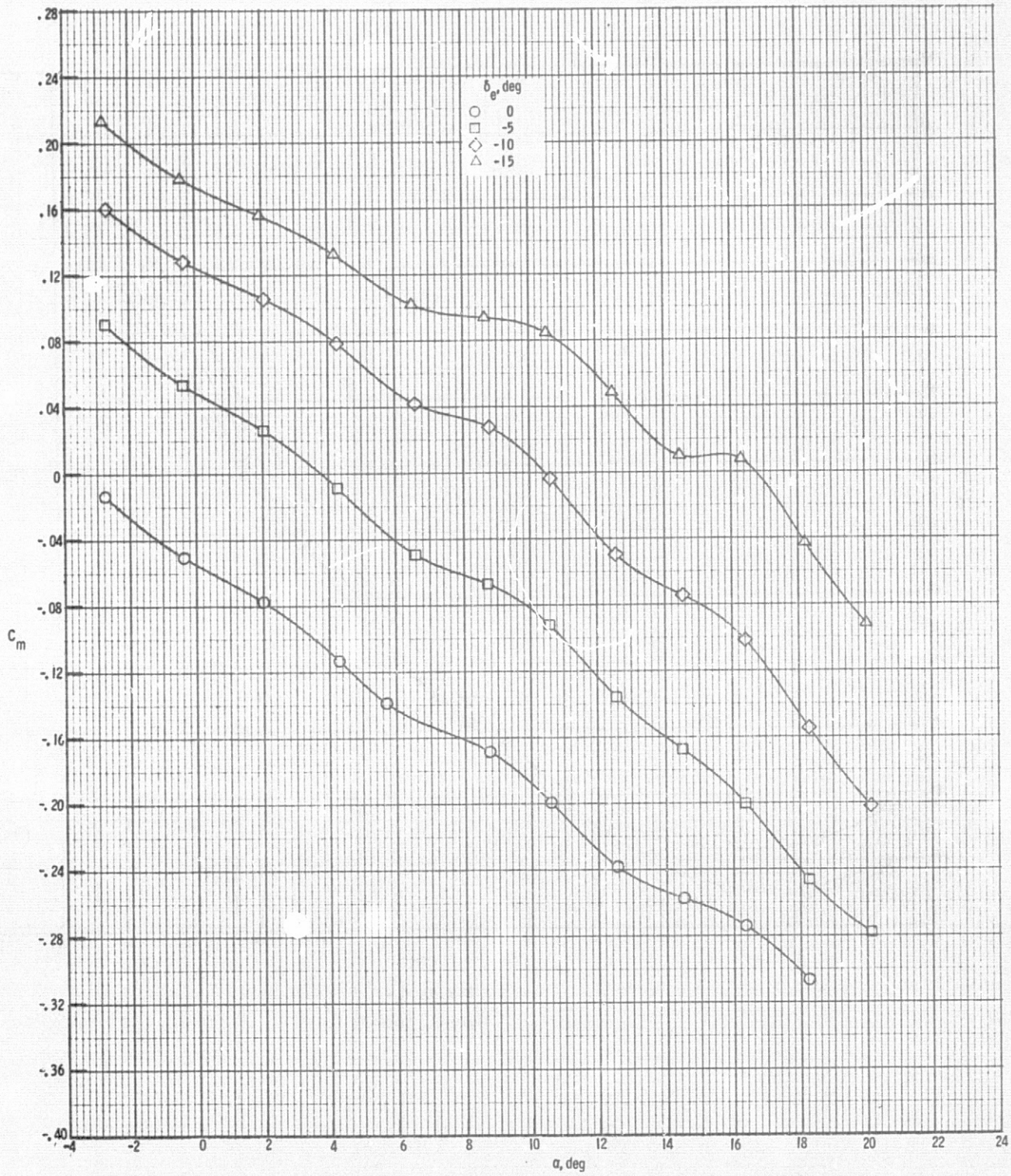

M = .93; δ_f = 5°

Figure 4. Continued.

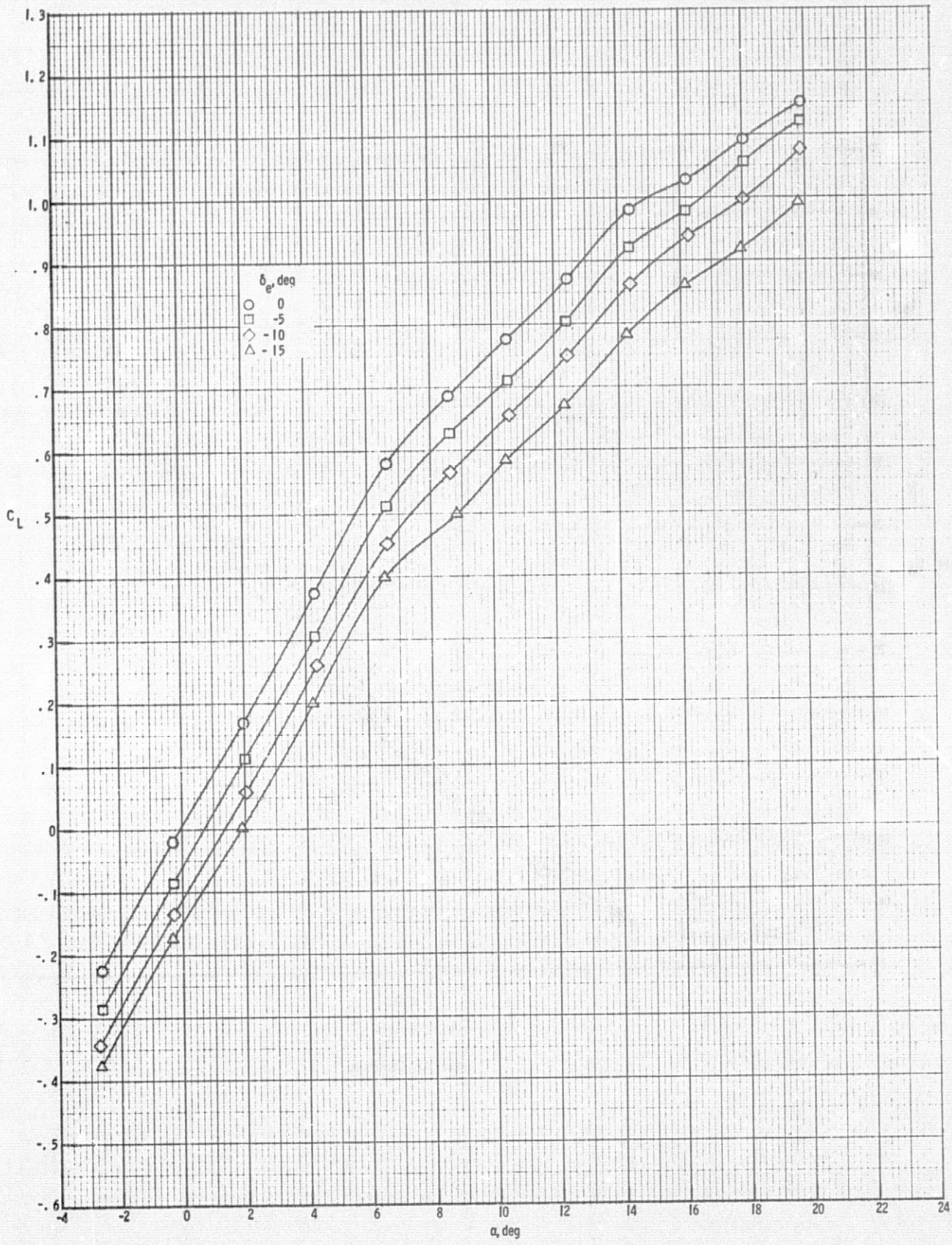

M = .90; δ_f = 5°

Figure 4. Continued.

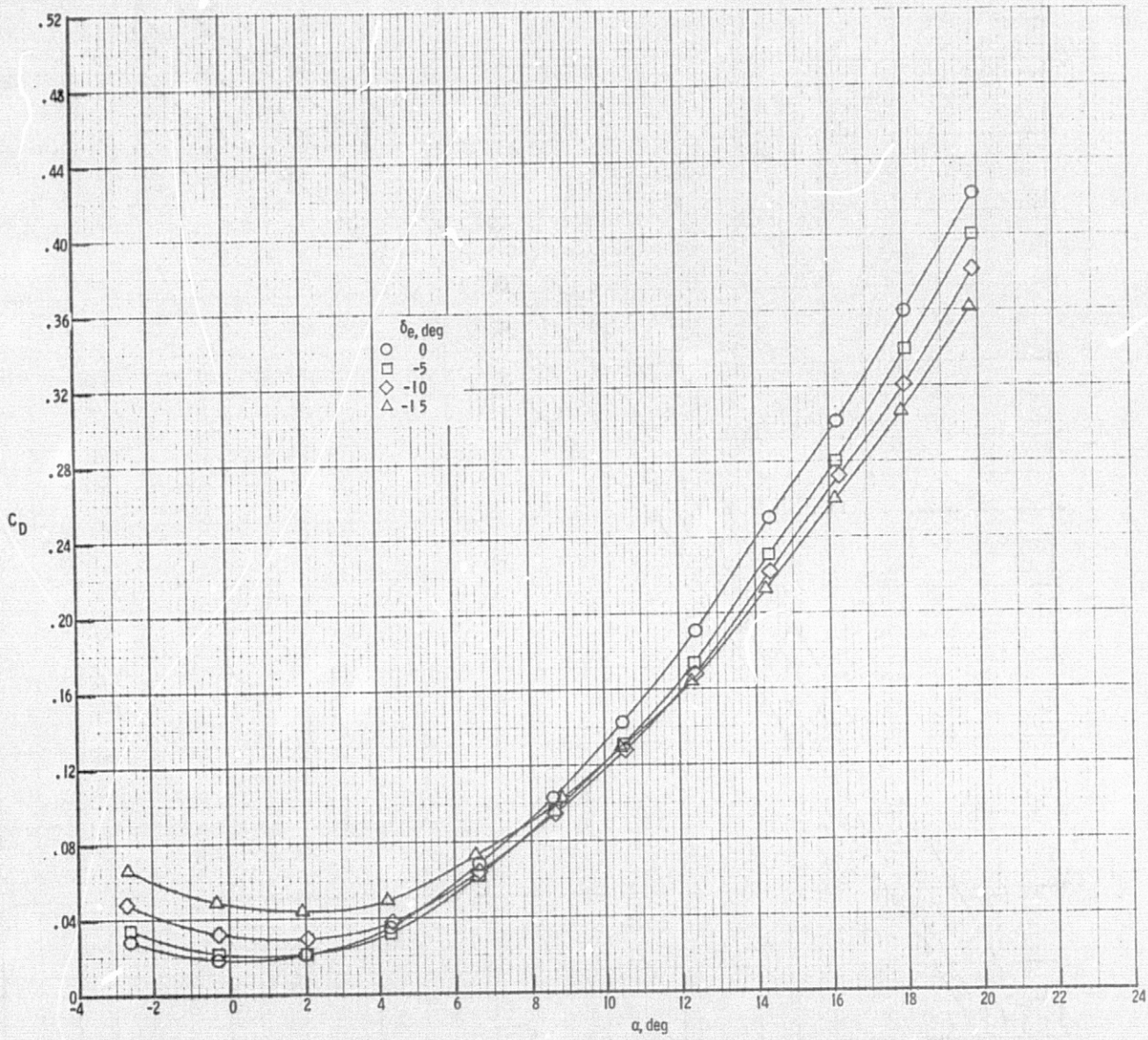

M = .90; δ_f = 5°

Figure 4. Continued.

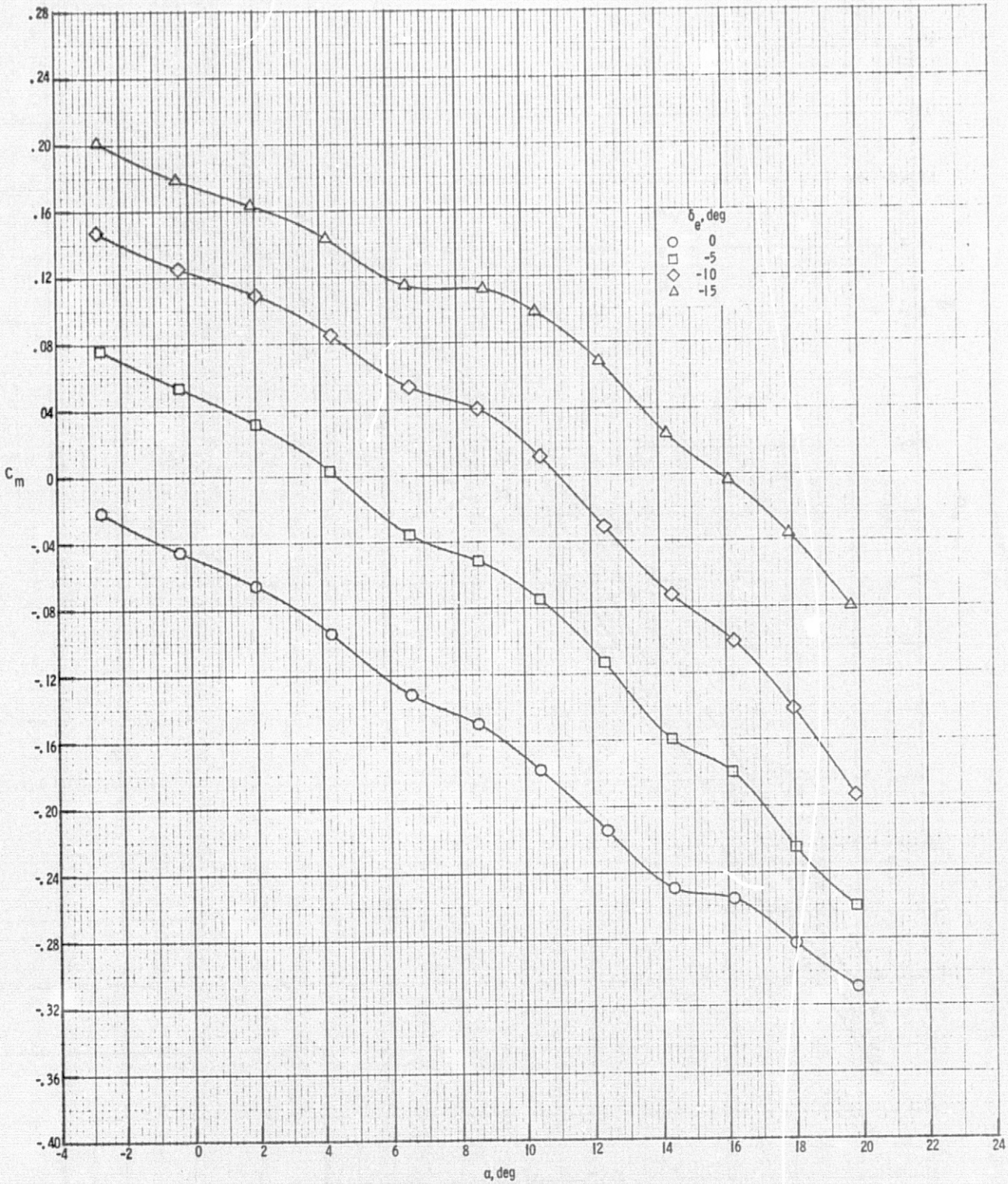

M = .90; δ_f = 5°

Figure 4. Continued.

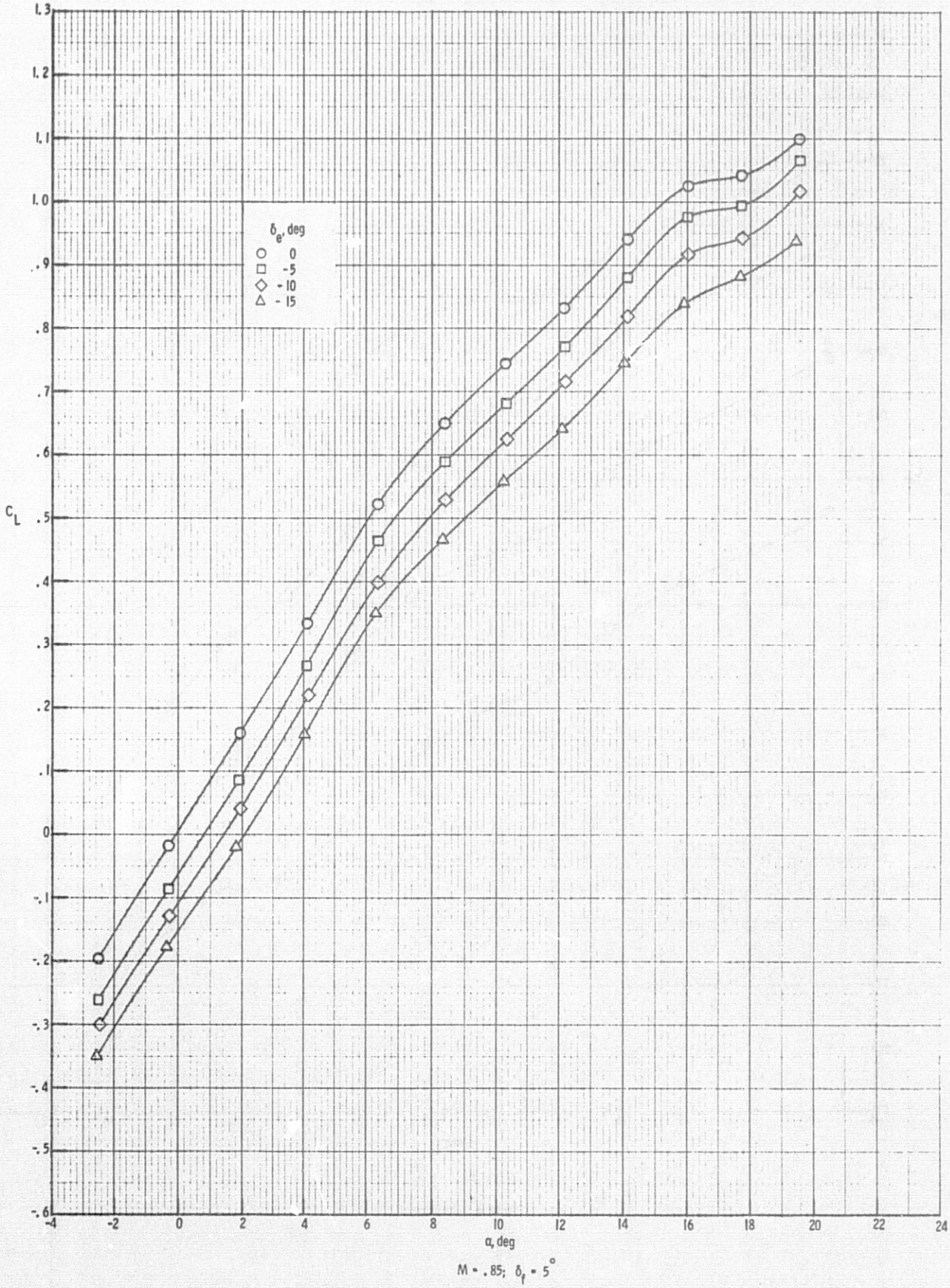

M = .85; δ_f = 5°

Figure 4. Continued.

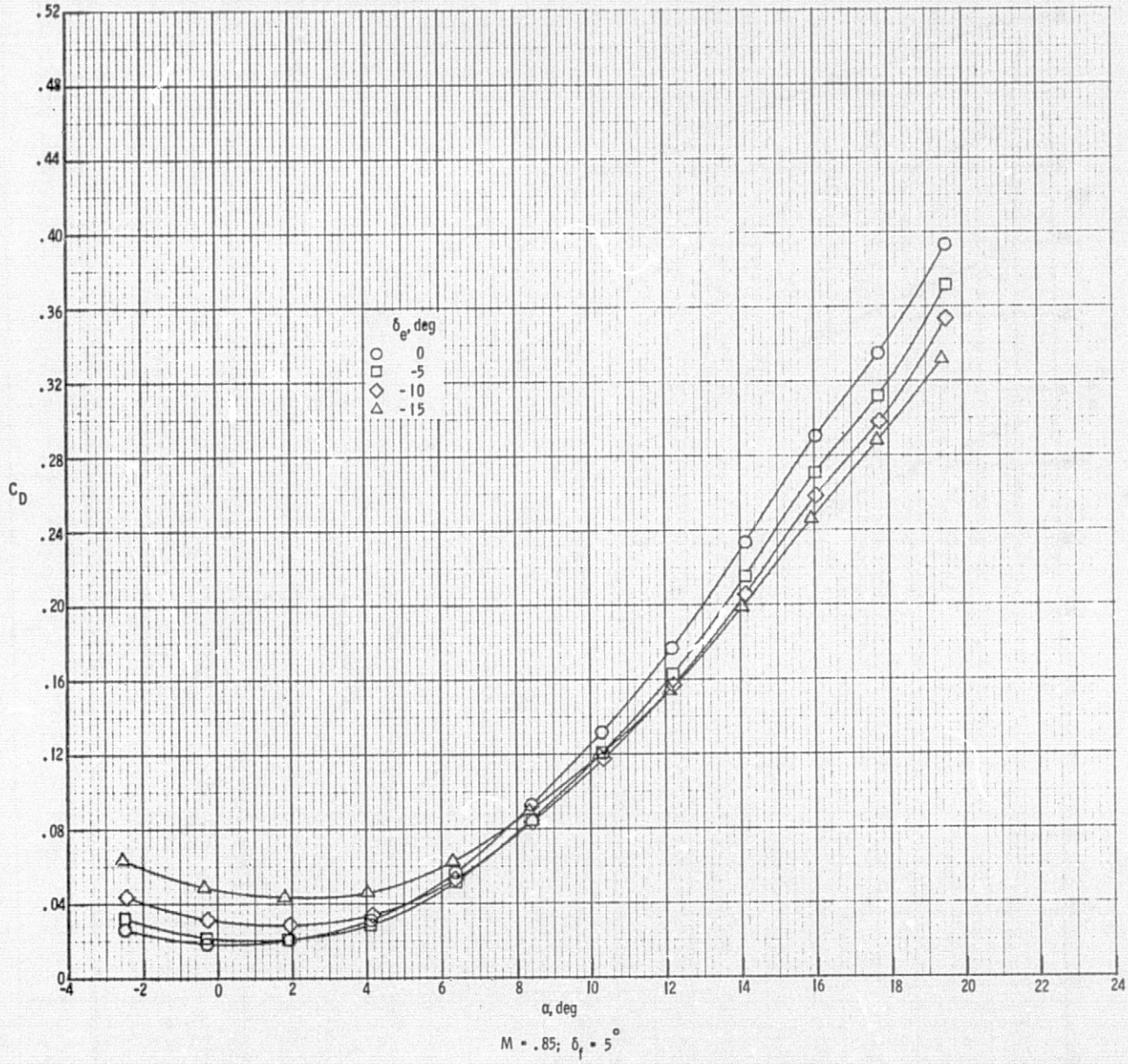

M = .85; δ_f = 5°

Figure 4. Continued.

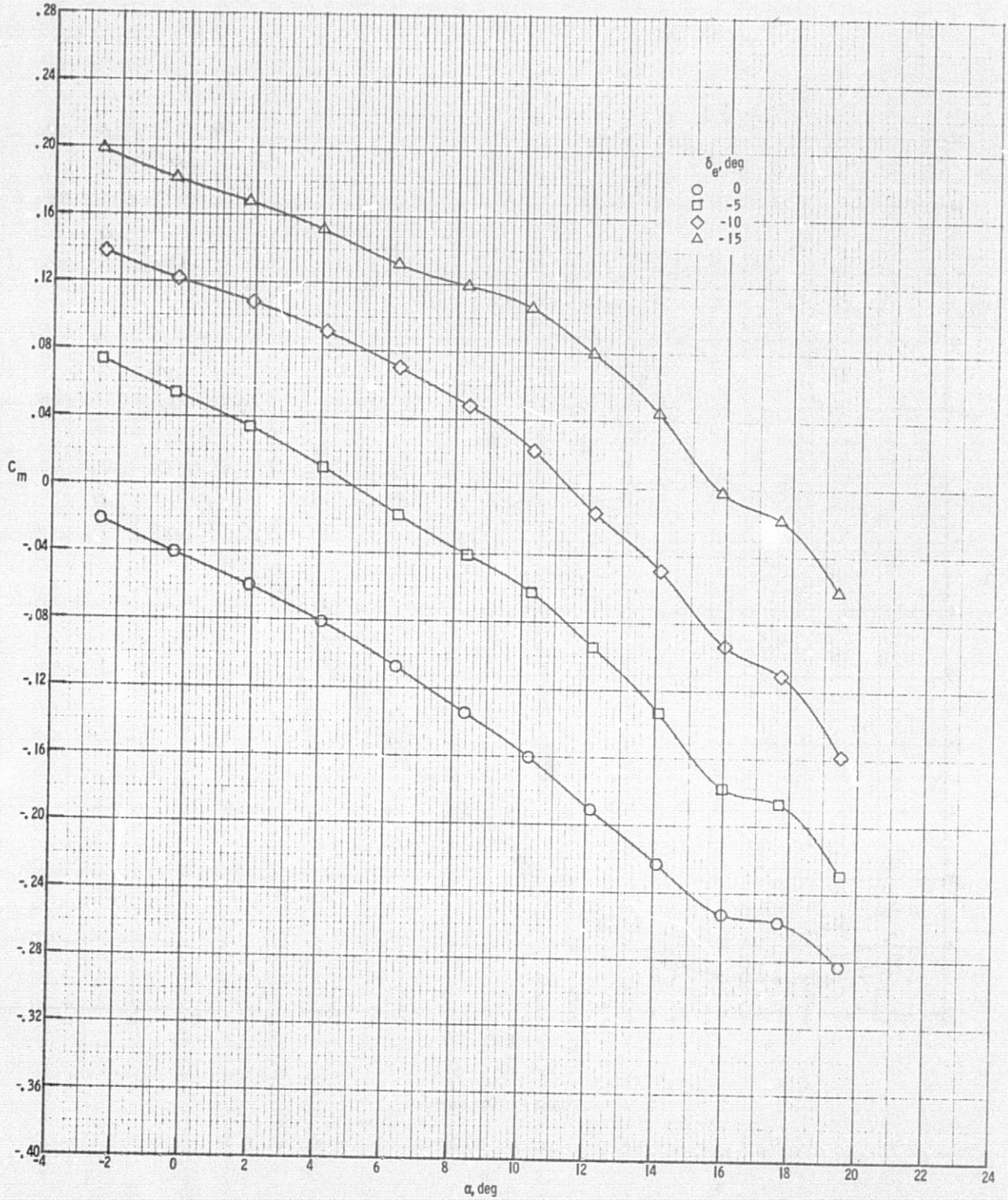

M = .85; δ_f = 5°

Figure 4. Continued.

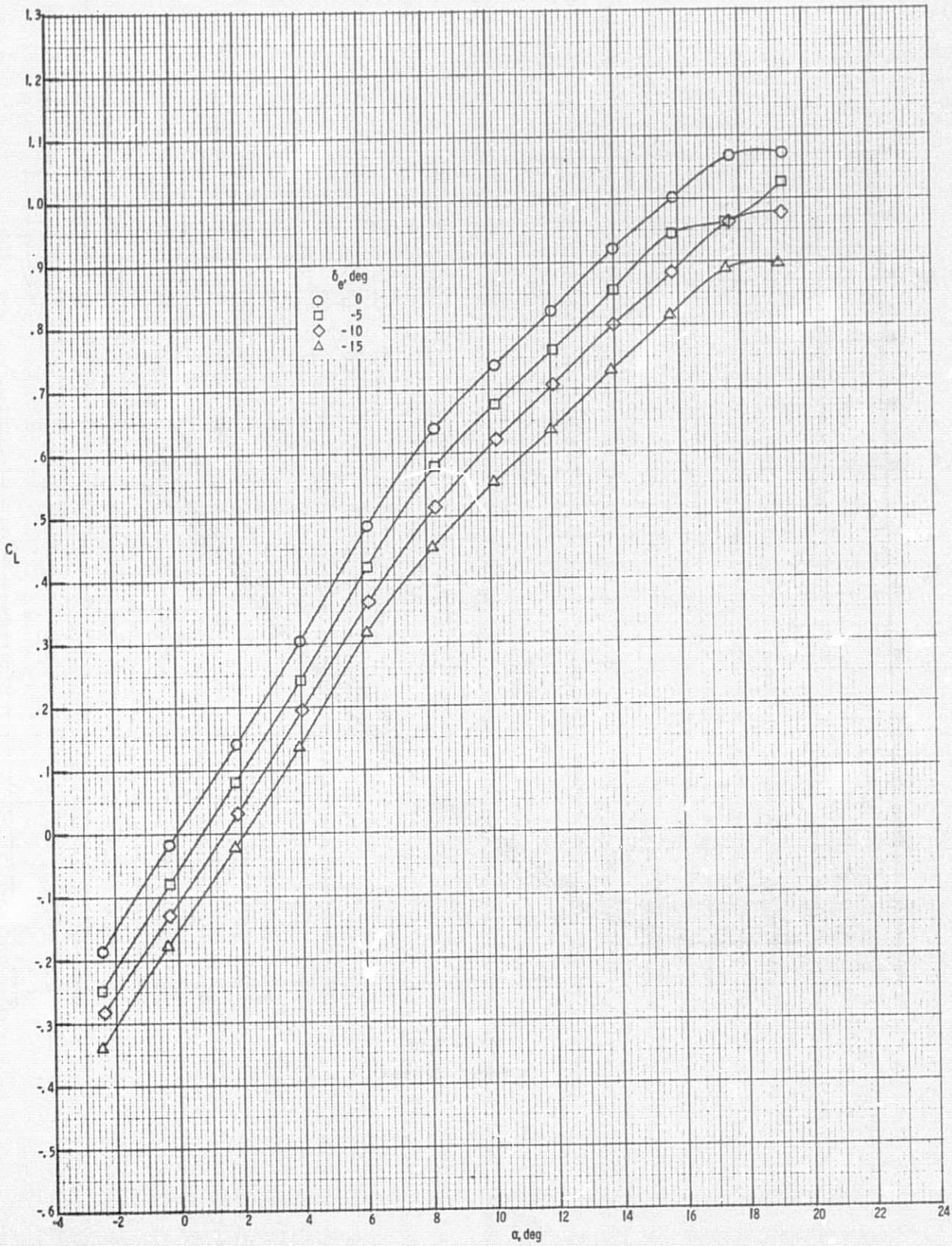

M = .80; δ_f = 5°

Figure 4. Continued.

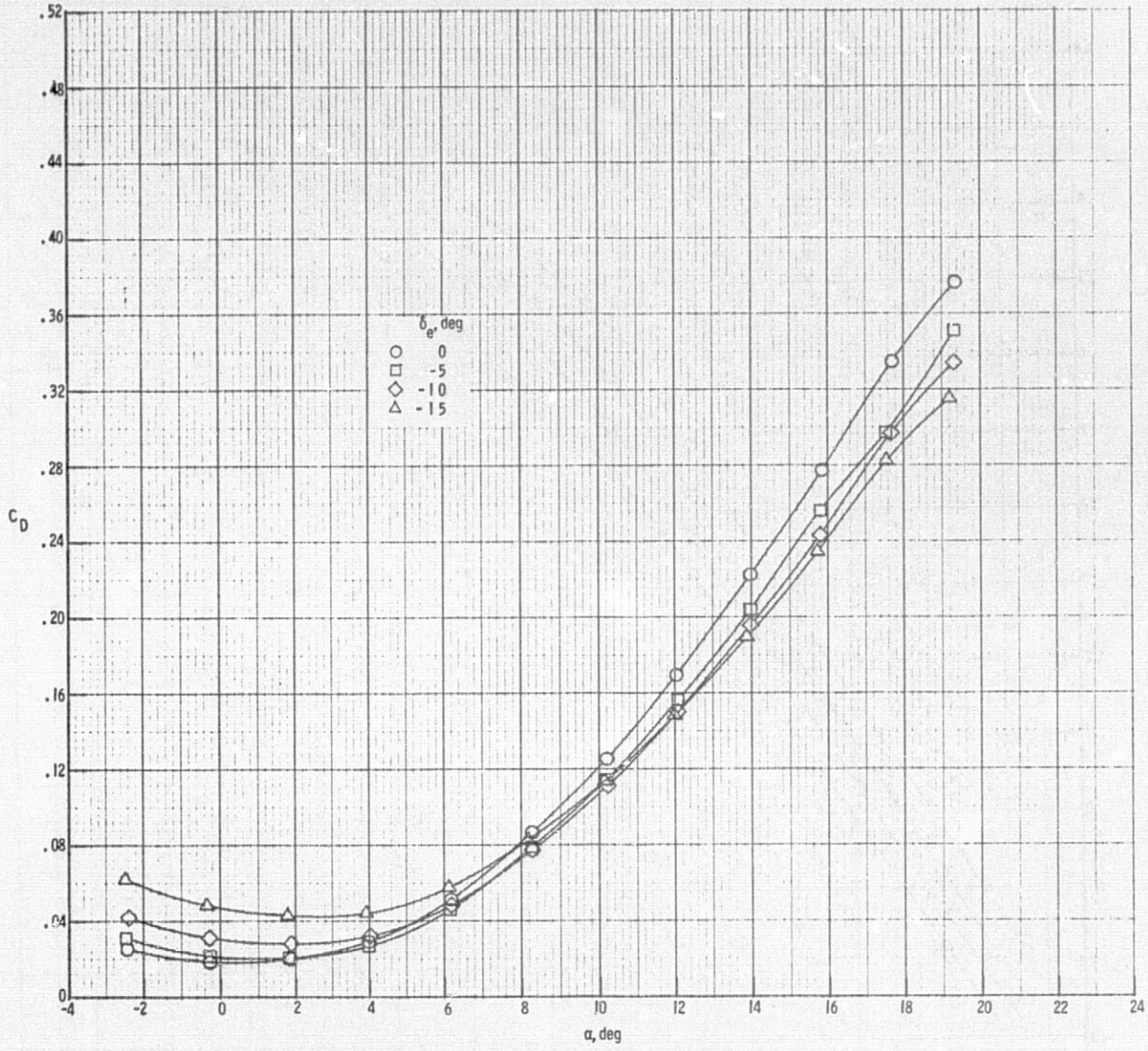

M = .80; δ_f = 5°

Figure 4. Continued.

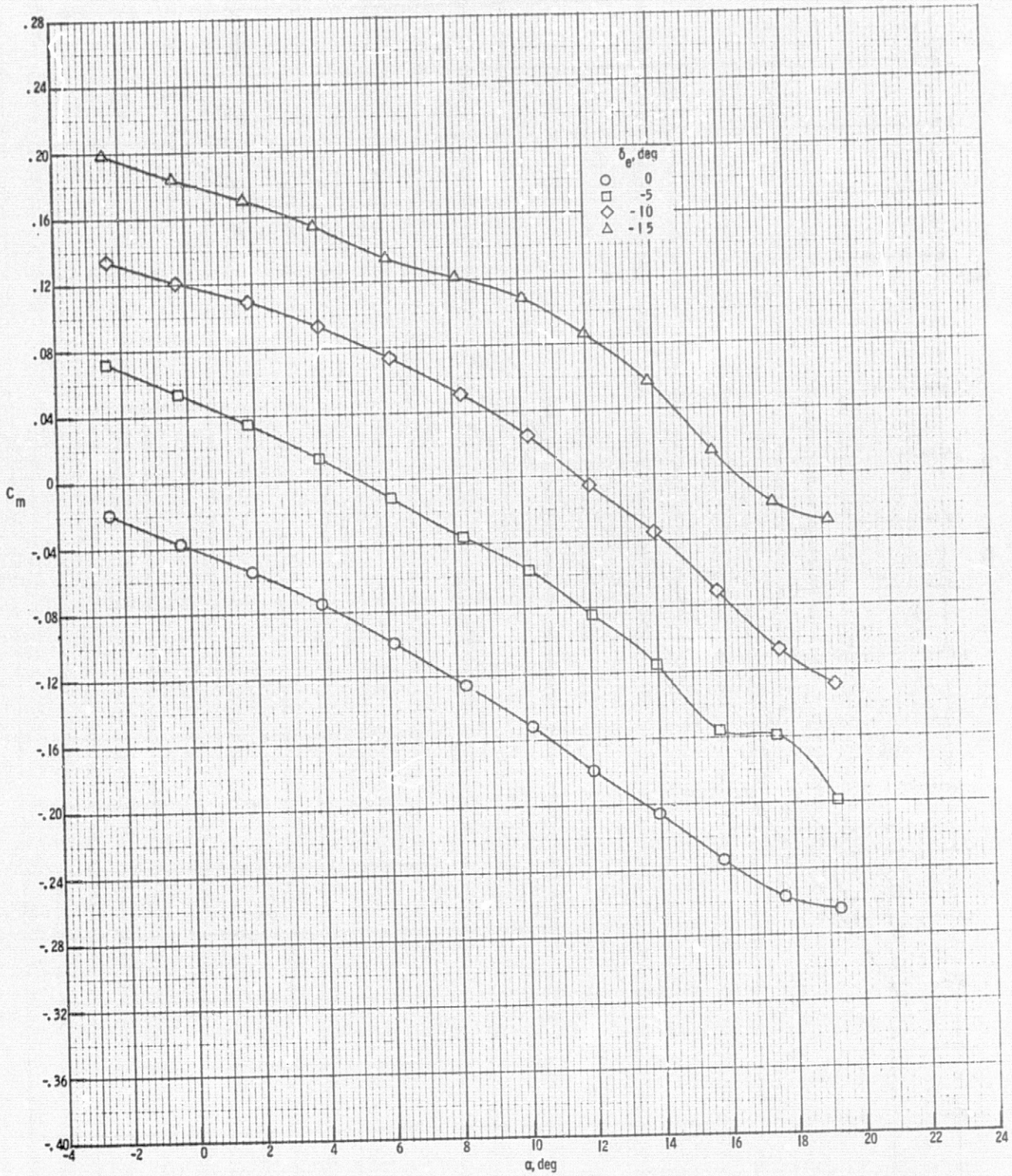

M = .80; δ_f = 5°

Figure 4. Continued.

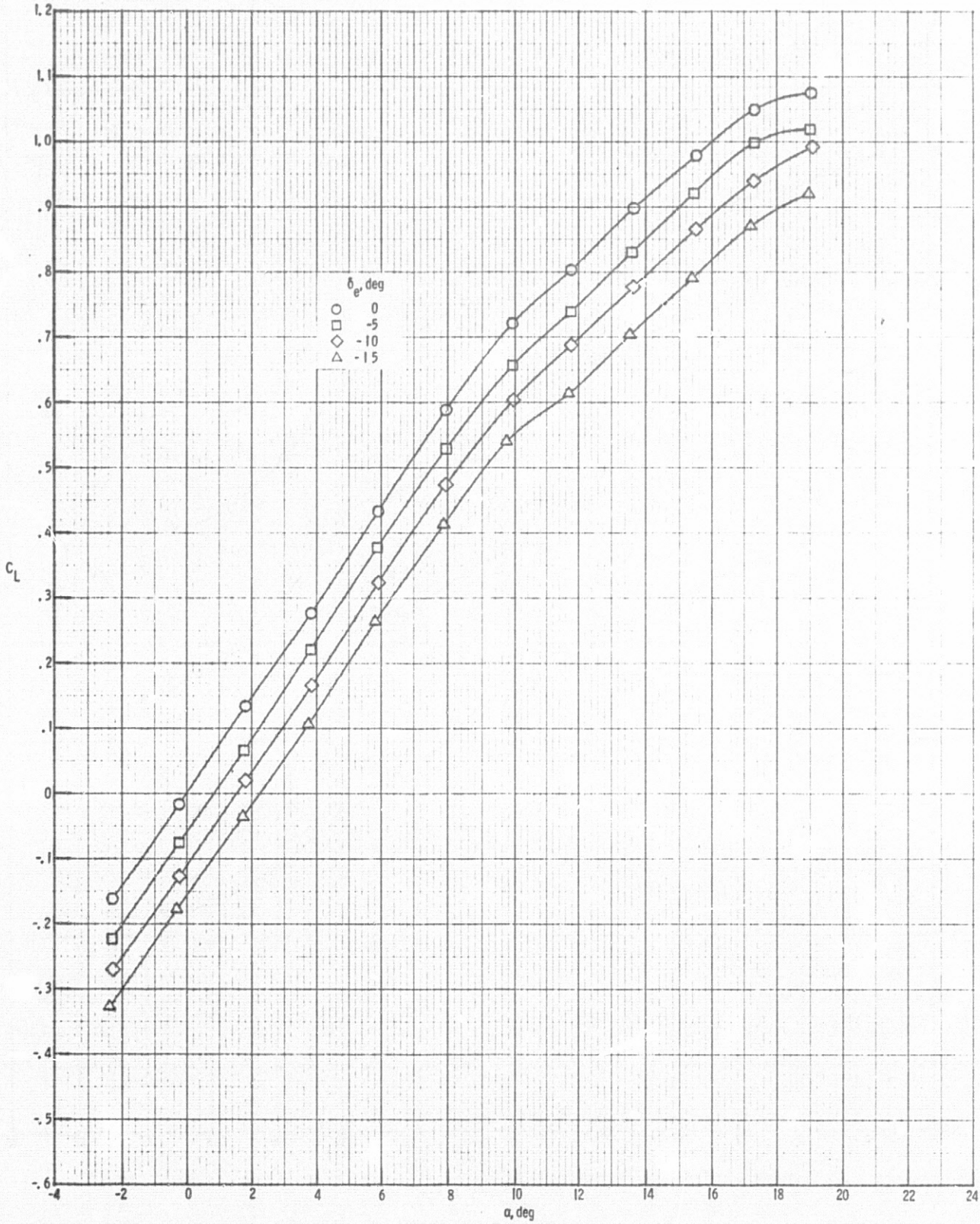

M = .70; $\delta_f = 5^\circ$

Figure 4. Continued.

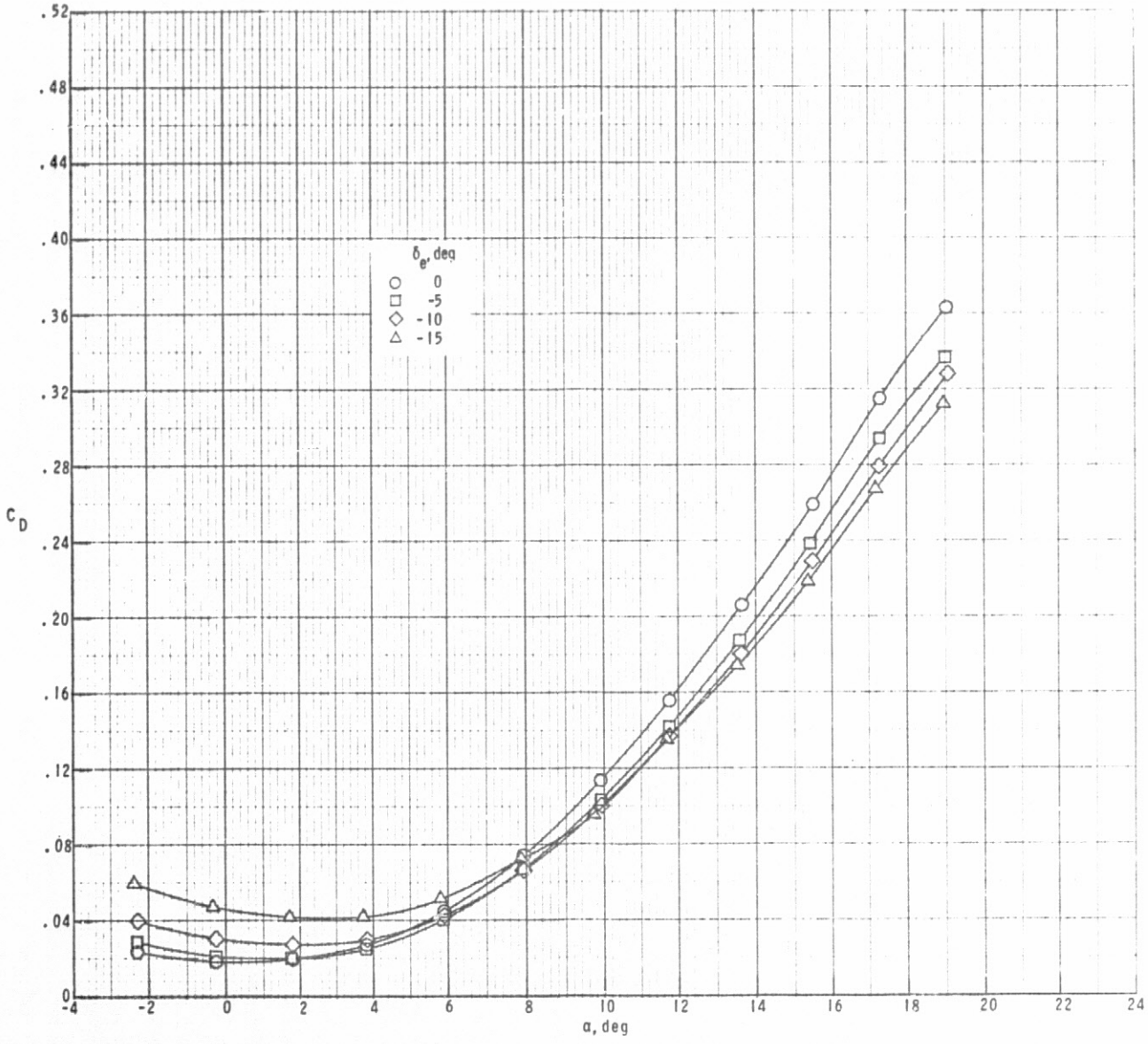

M = .70; δ_f = 5°

Figure 4. Continued.

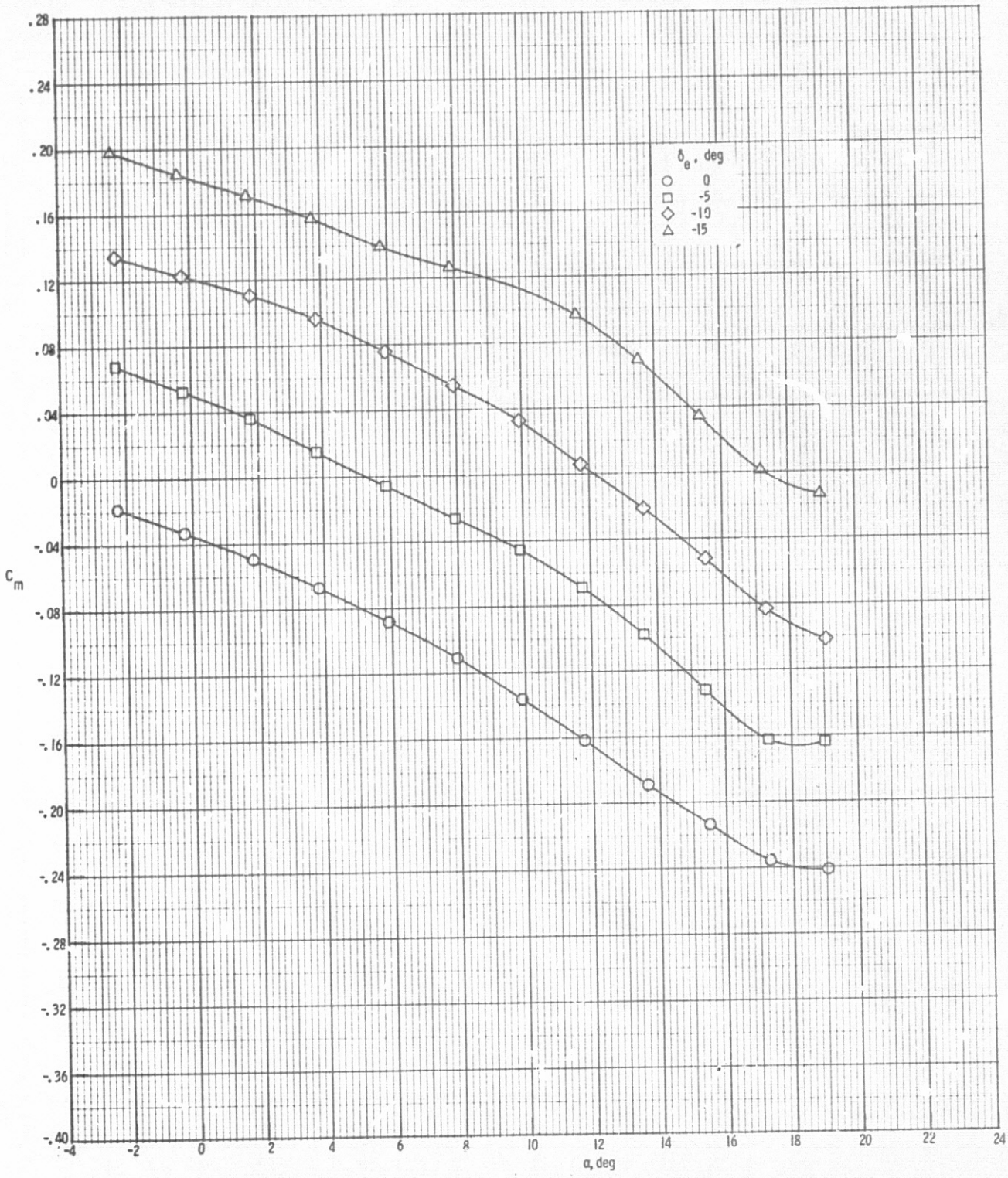

M = .70; δ_f = 5°

Figure 4. Concluded.

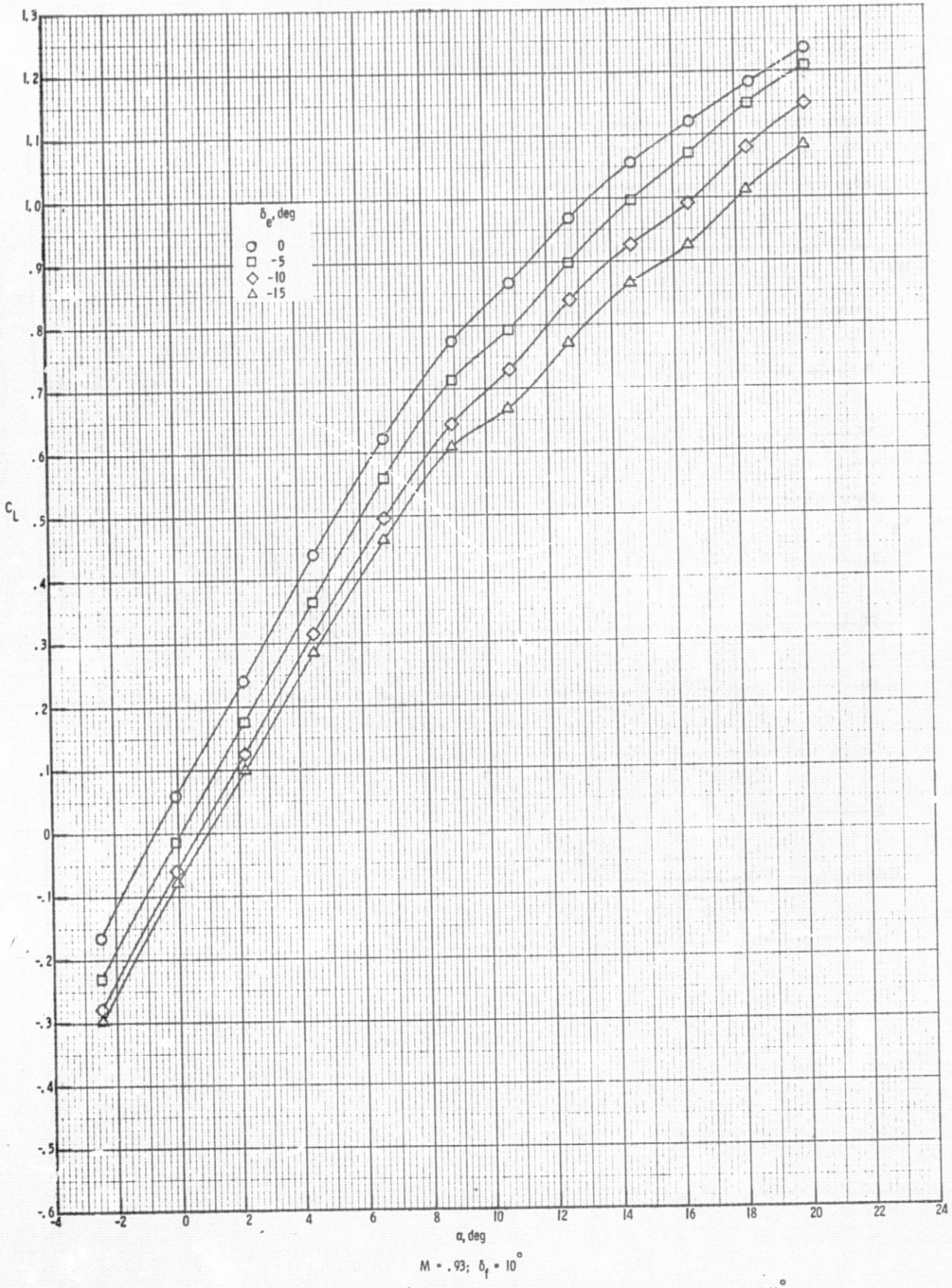

Figure 5 . Variation of lift, drag and pitching moment coefficients with angle of attack at flap setting of 10°.

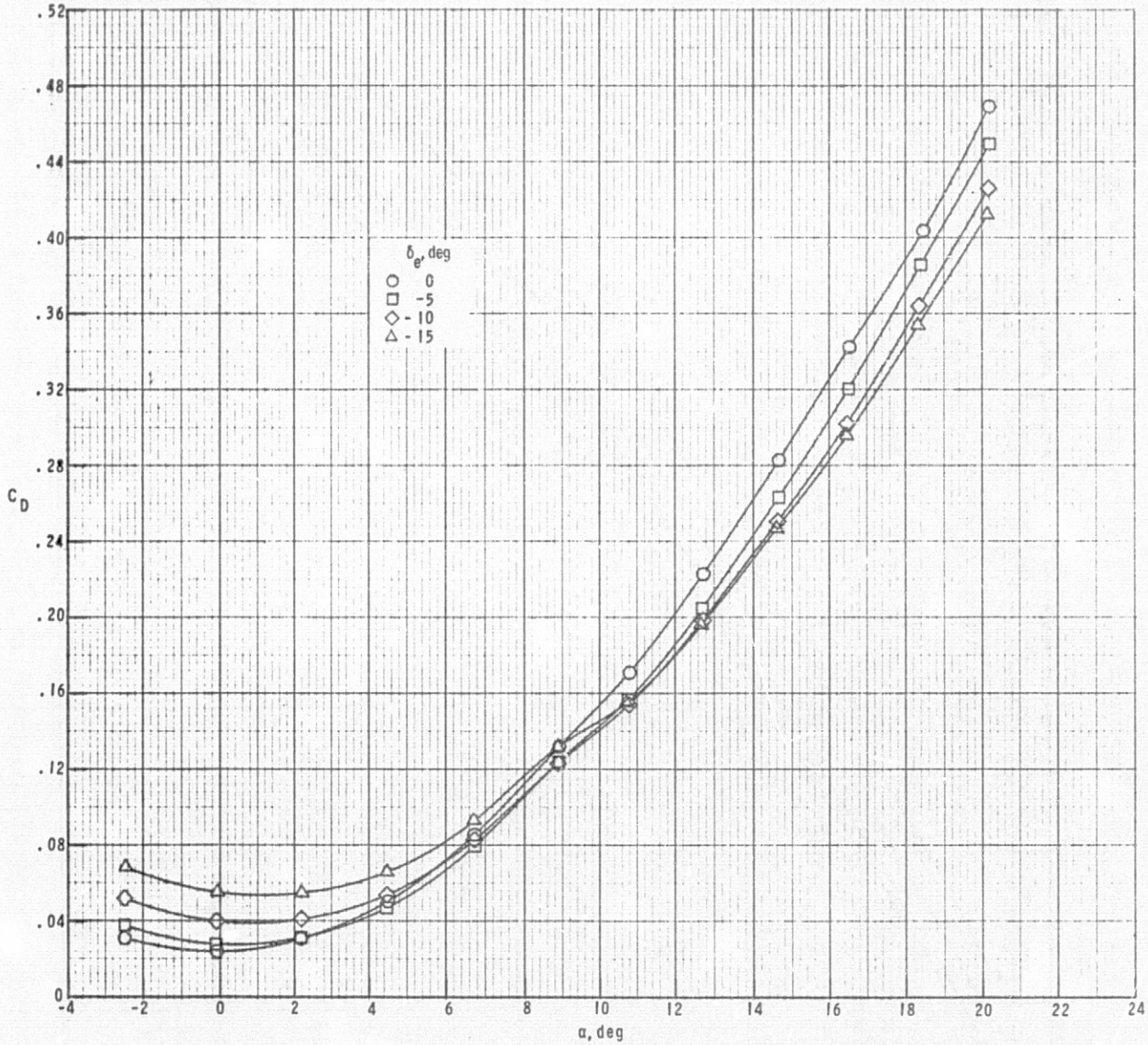

M = .93; δ_f = 10°

Figure 5. Continued.

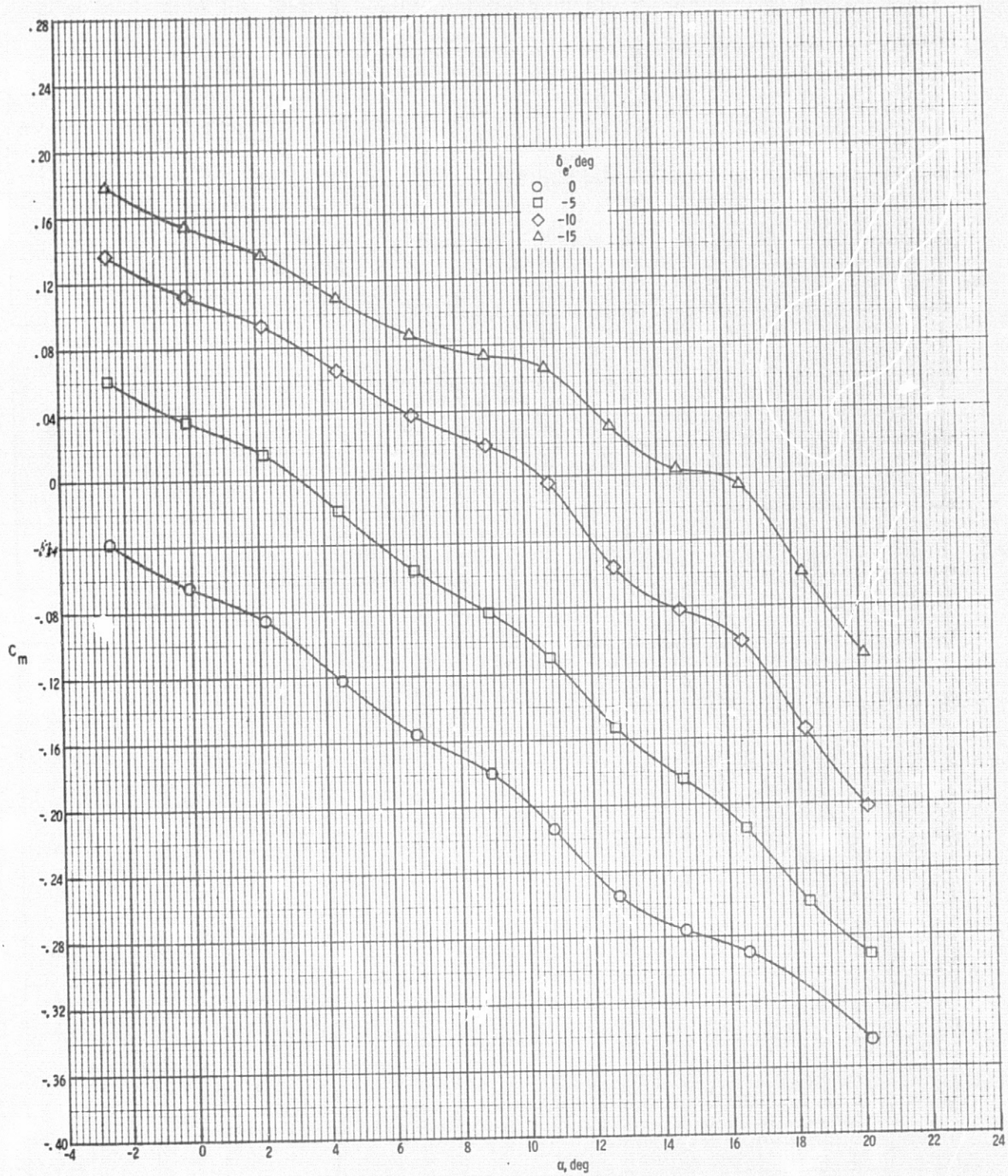

M = .93; δ_f = 10°

Figure 5. Continued.

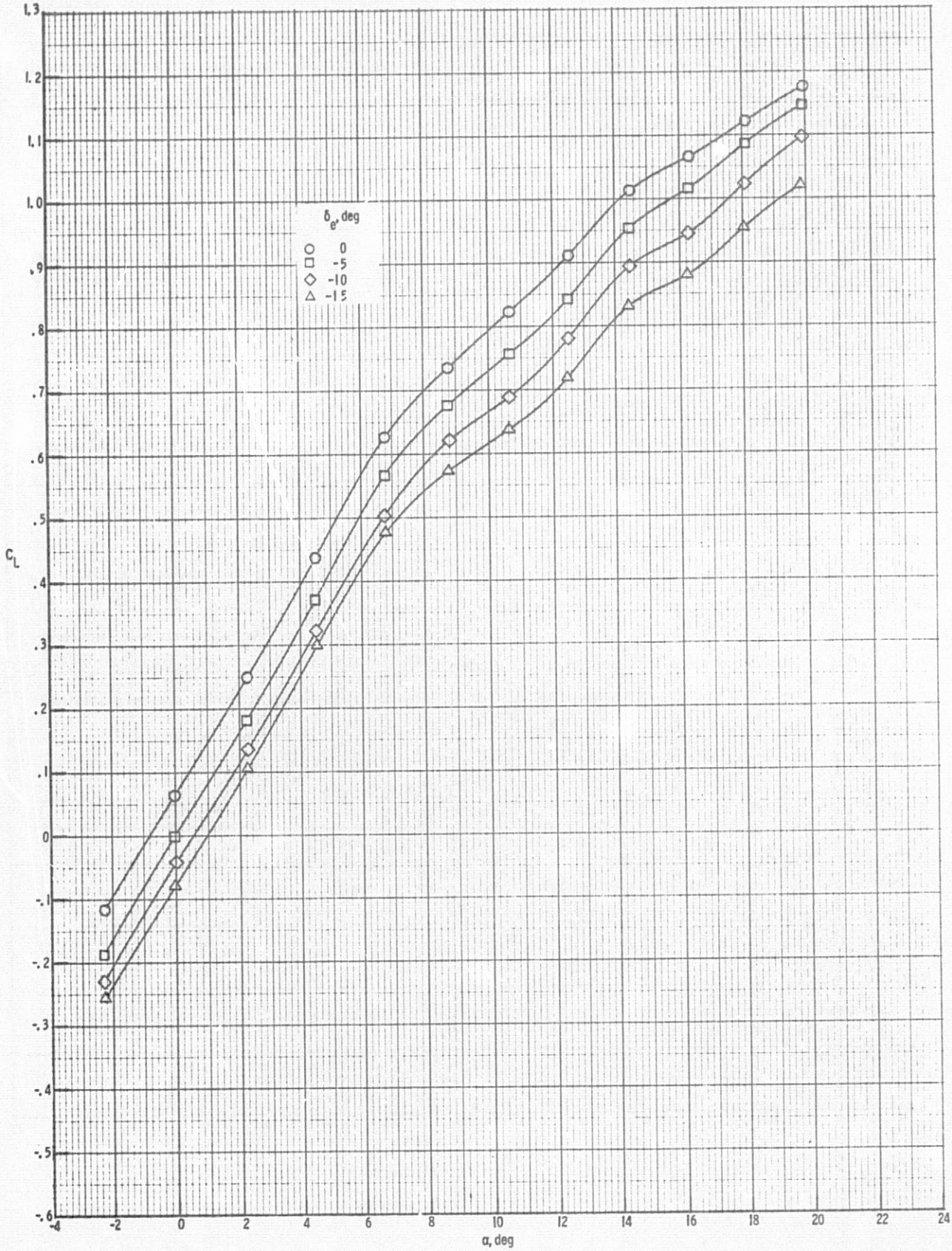

M = .90; δ_f = 10°

Figure 5. Continued.

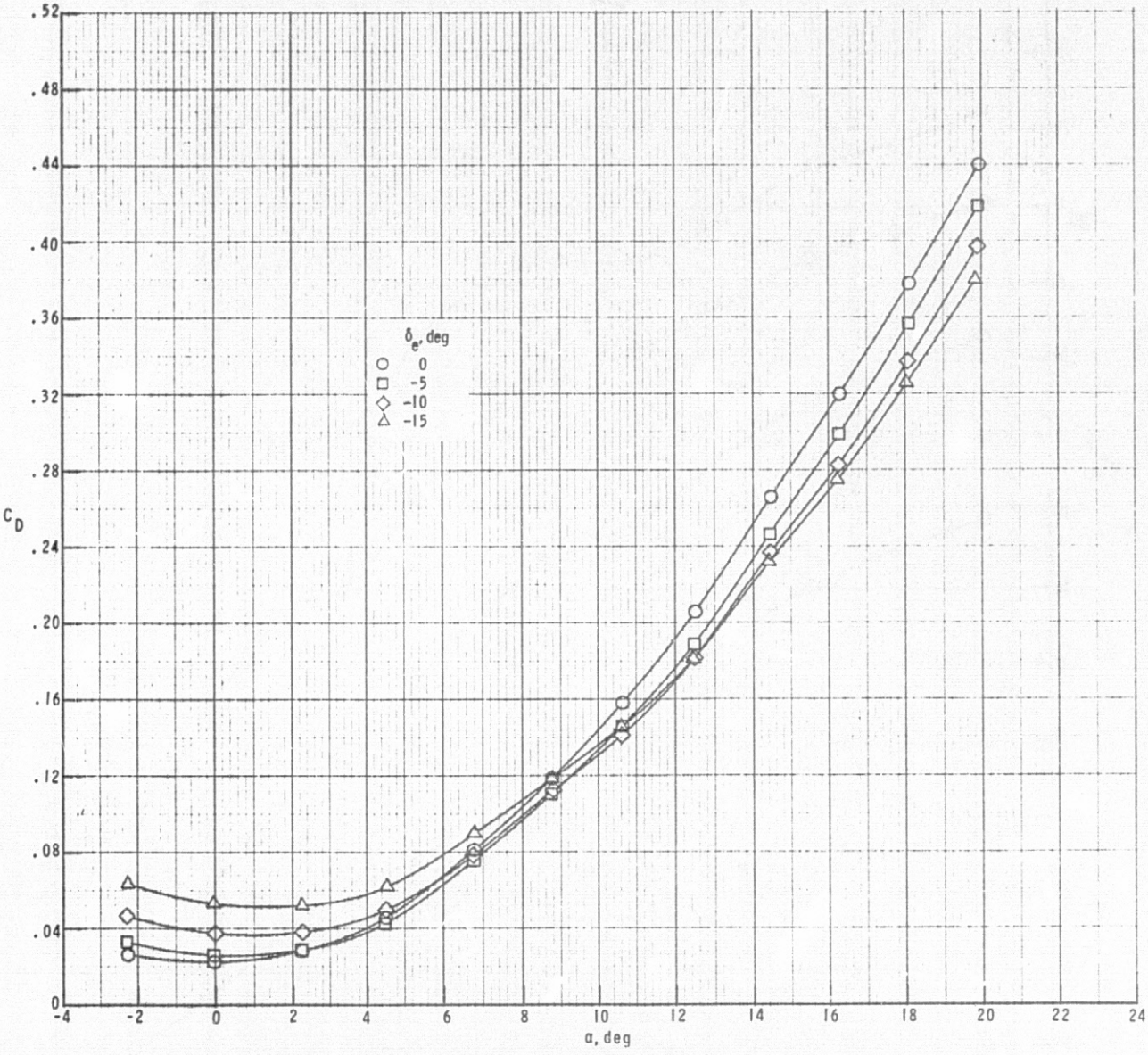

M = .90; δ_f = 10°

Figure 5. Continued.

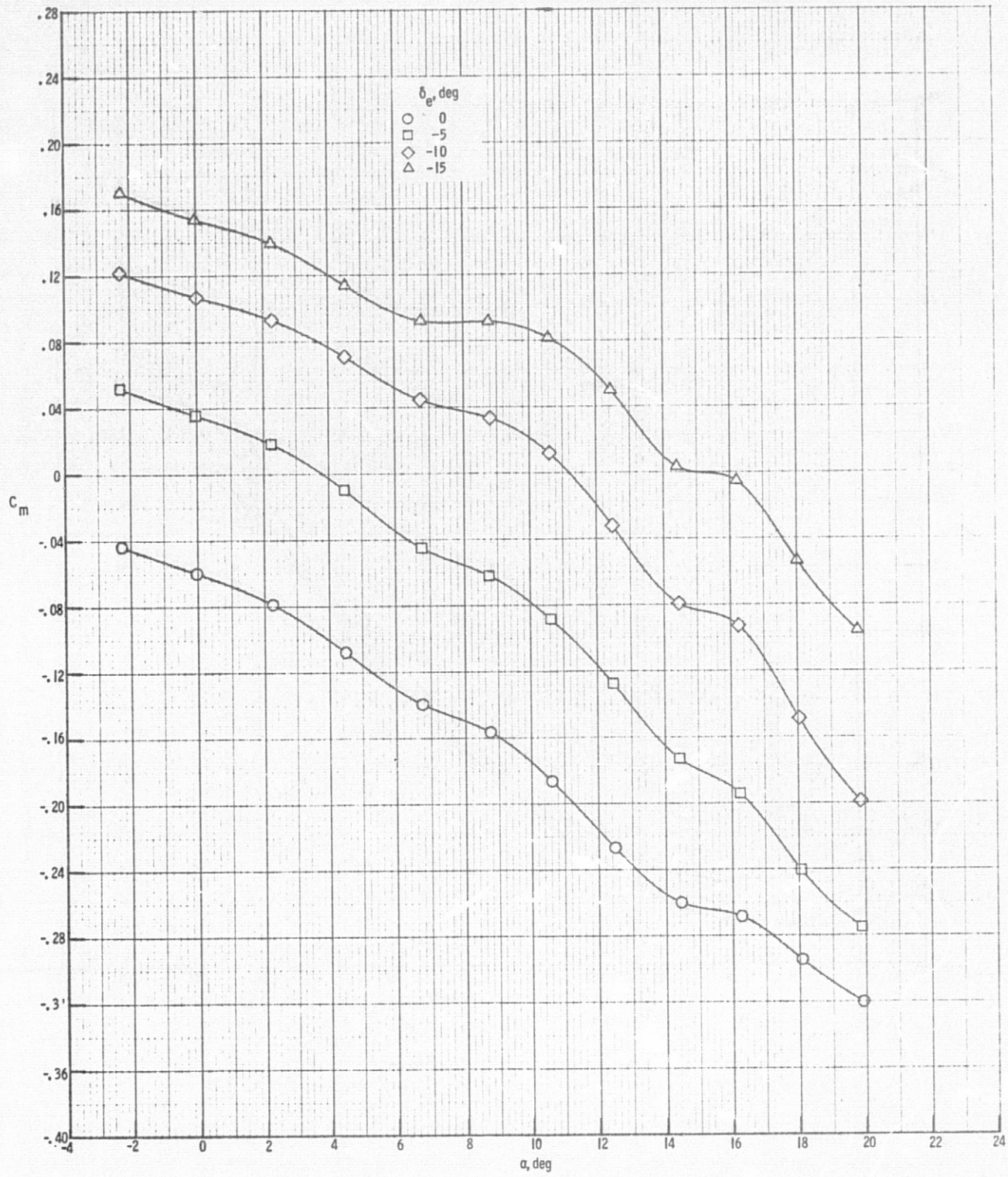

M = .90; δ_f = 10°

Figure 5. Continued.

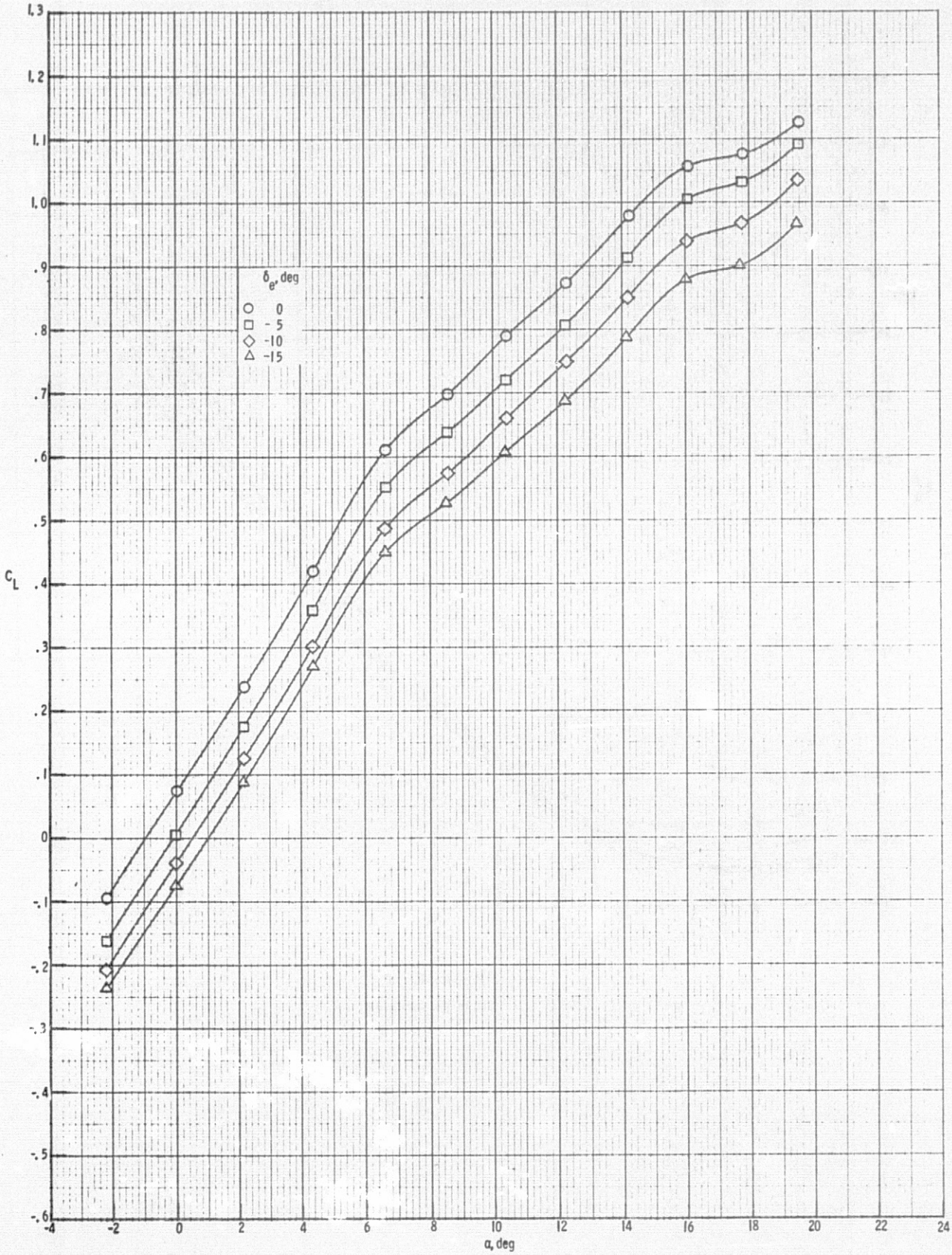

M = .85; δ_f = 10°

Figure 5. Continued.

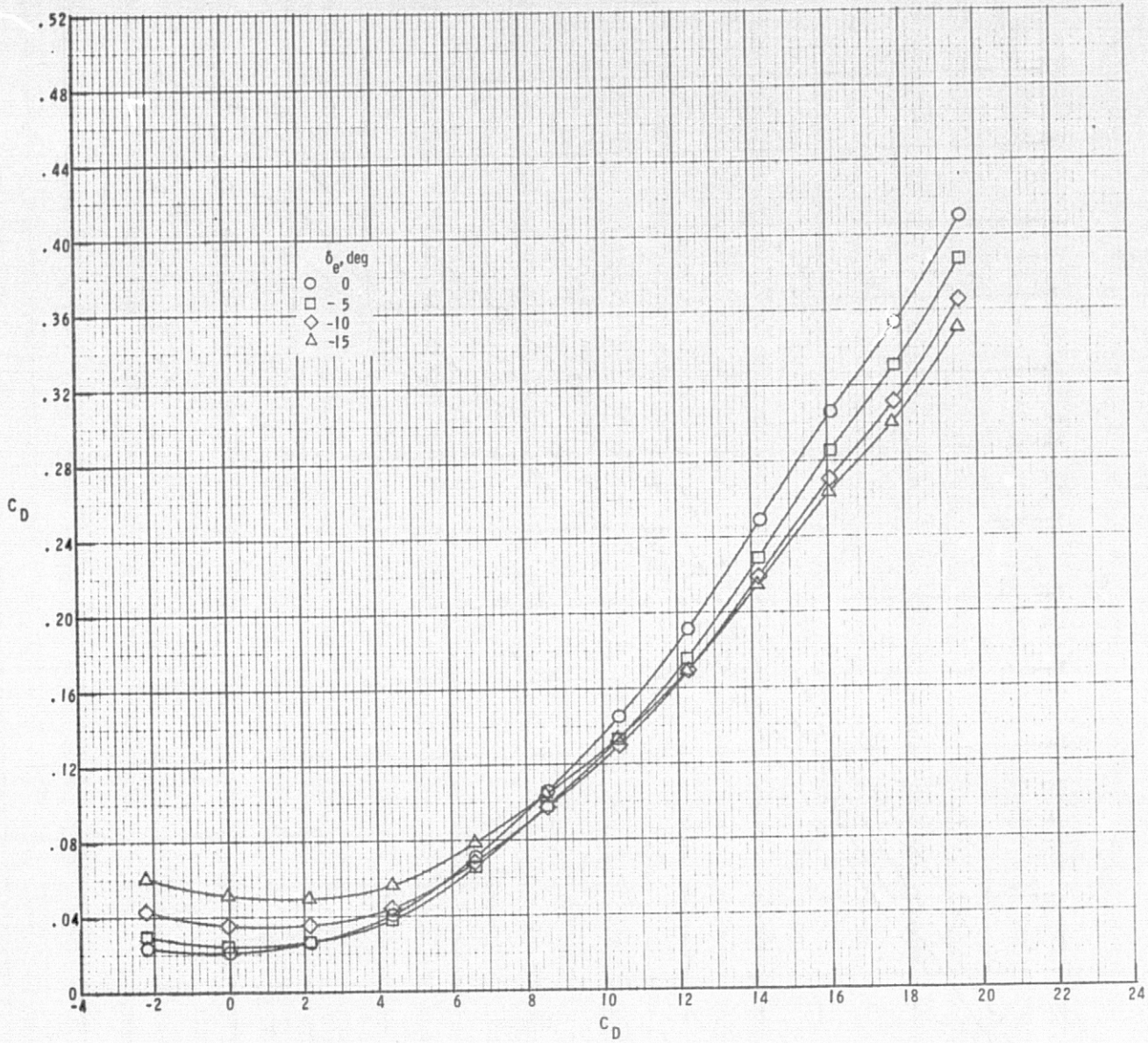

$M = .85$; $\delta_f = 10^\circ$

Figure 5. Continued.

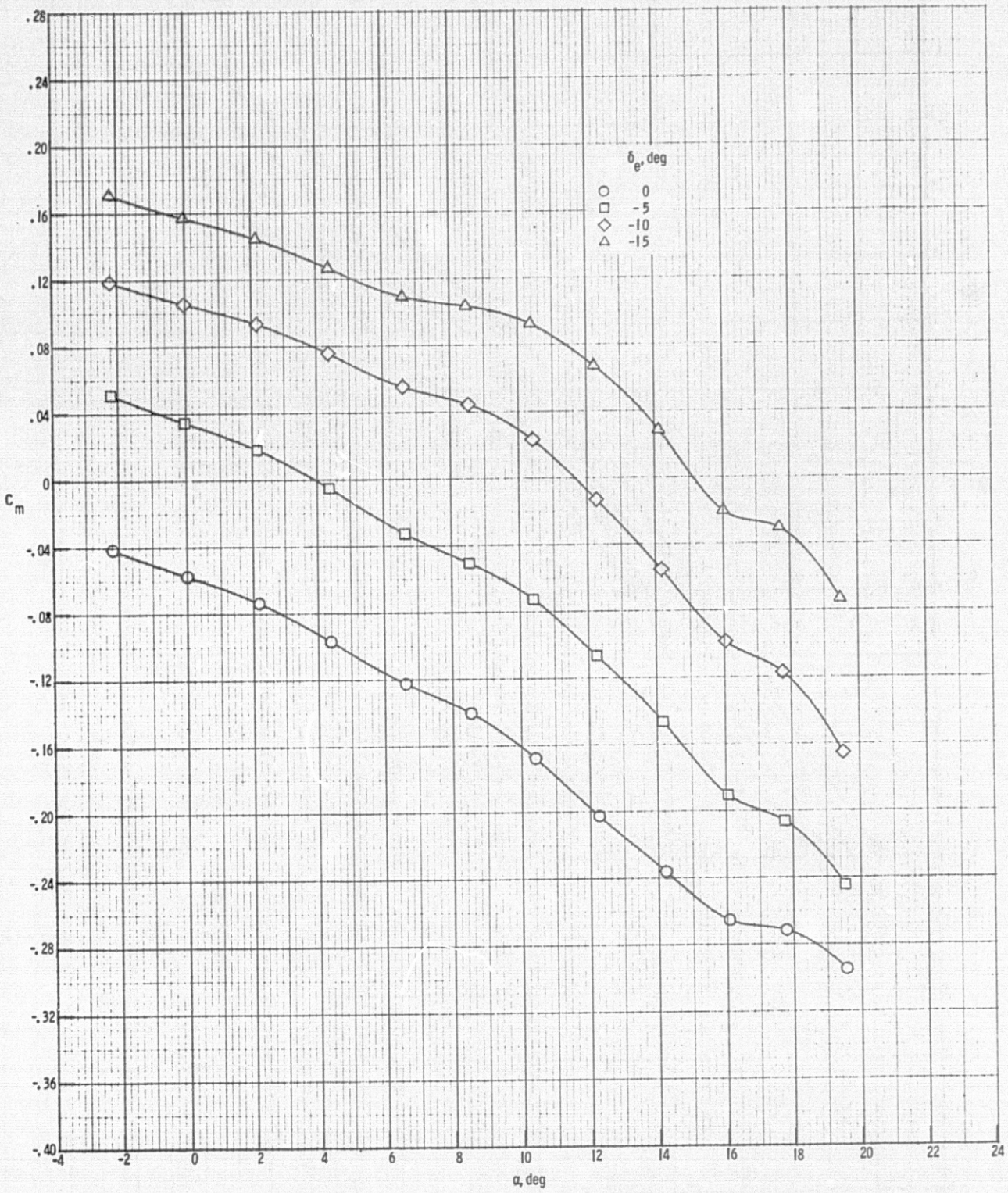

M = .85; δ_f = 10°

Figure 5. Continued.

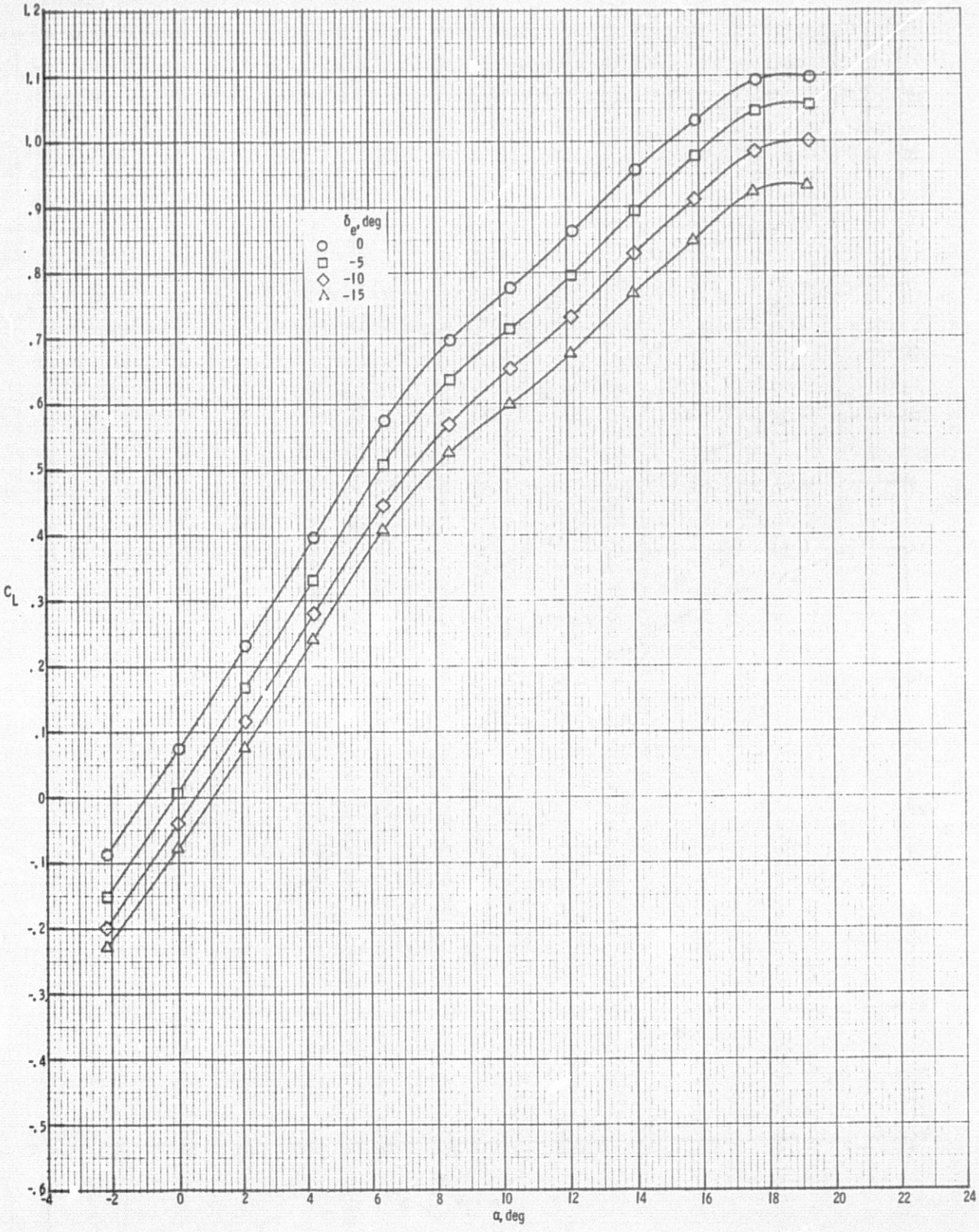

M = .80; δ_f = 10°

Figure 5. Continued.

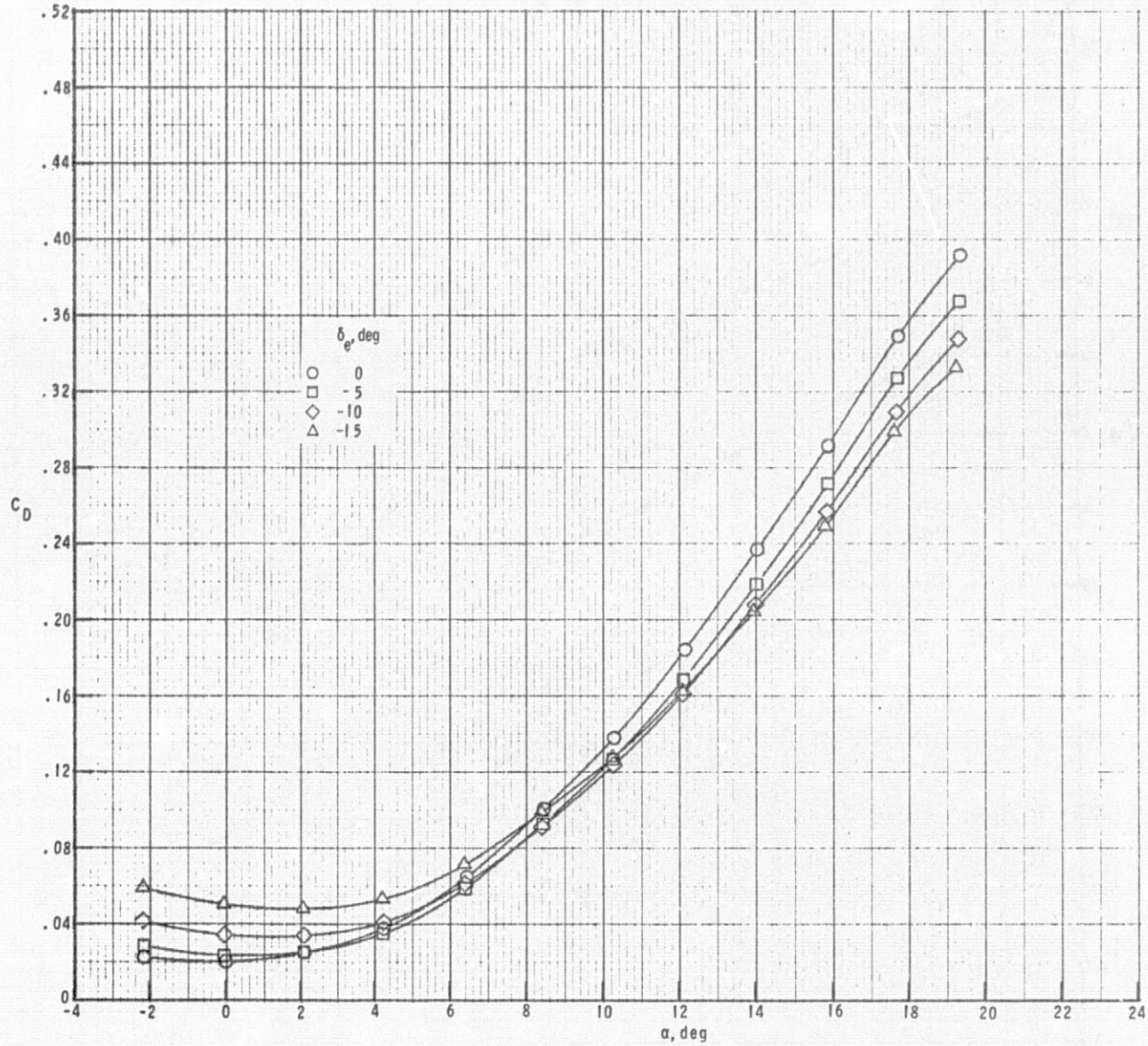

M = .80; δ_f = 10°

Figure 5. Continued.

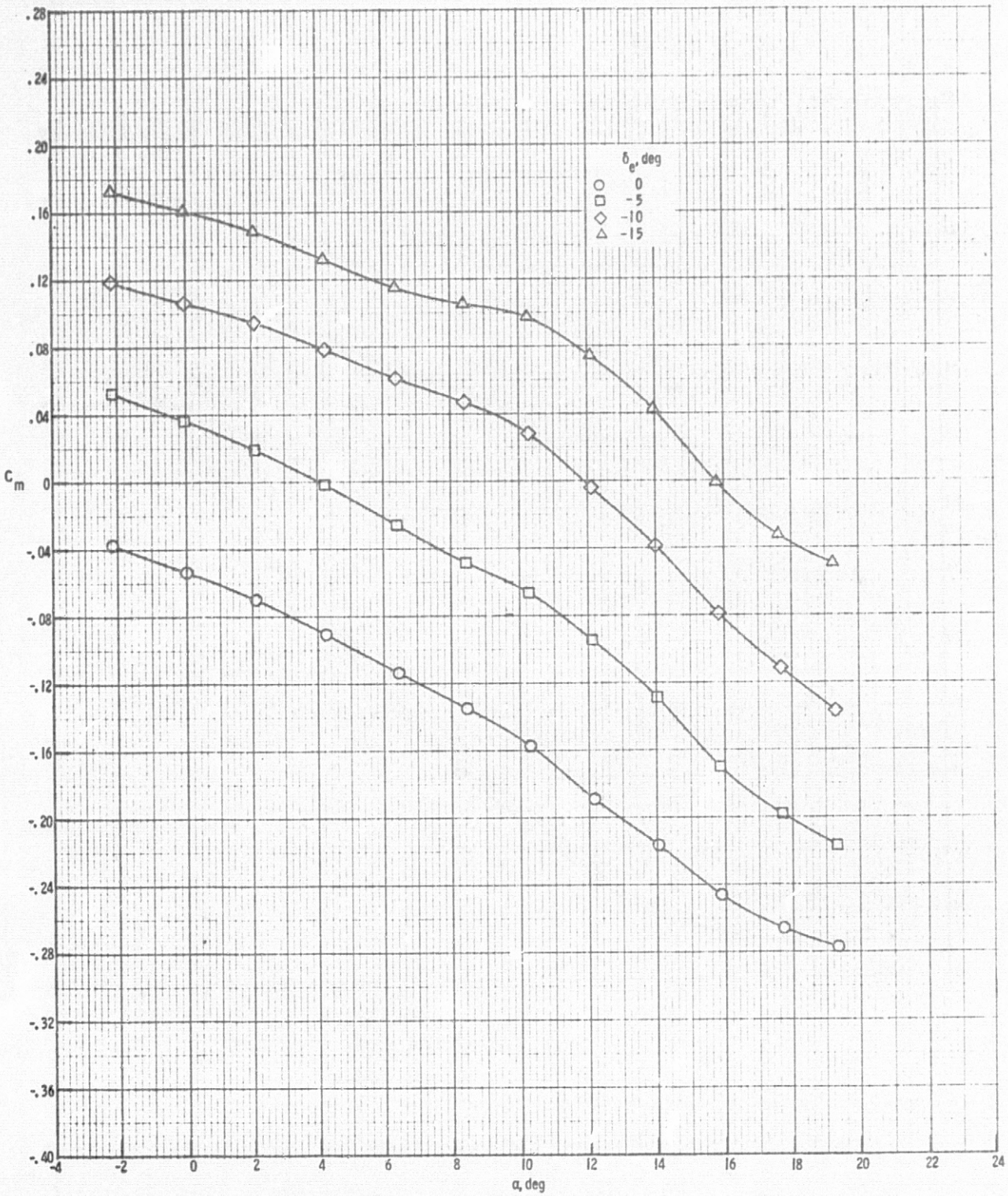

M = .80; δ_f = 10°

Figure 5. Continued.

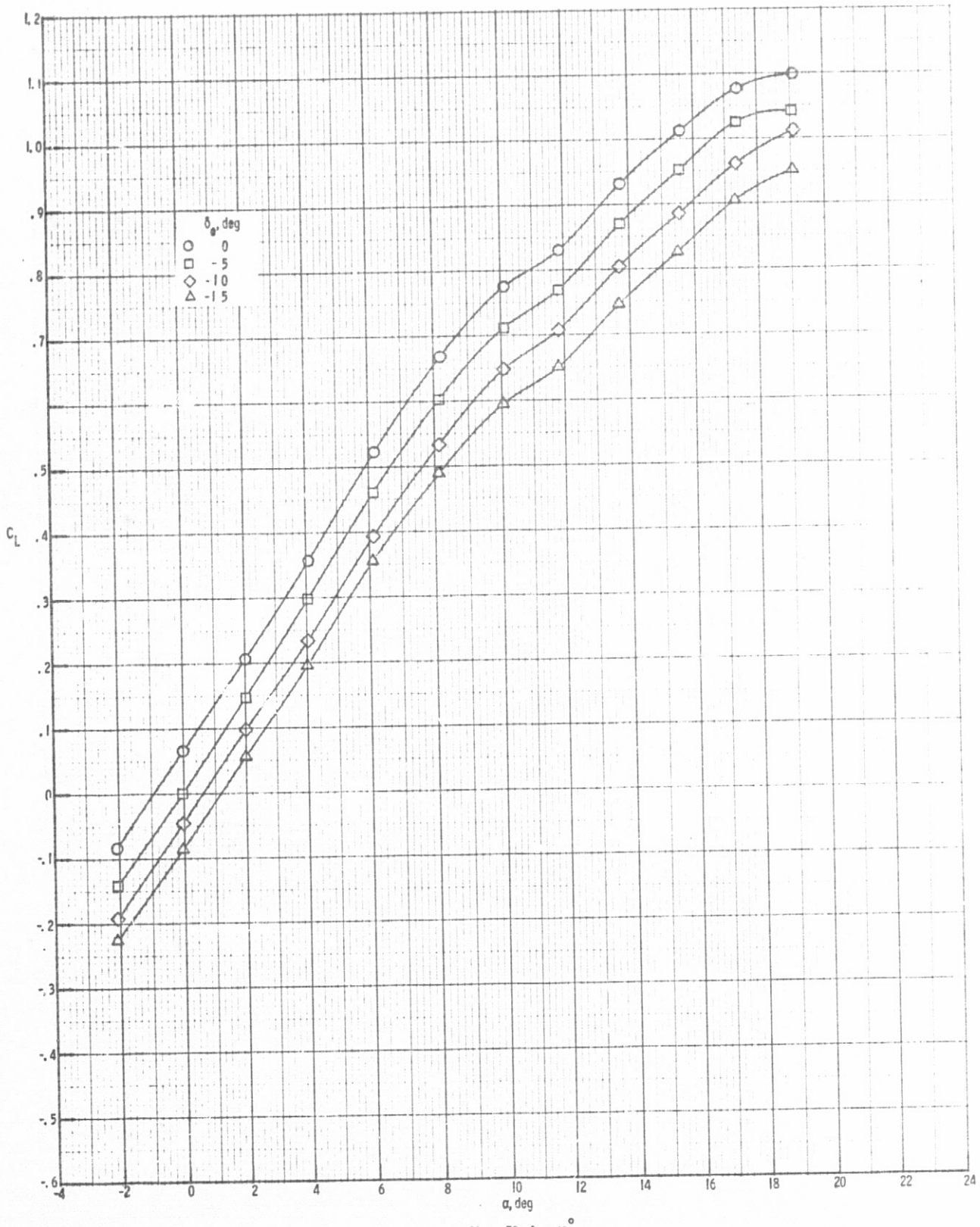

M = .70; δ_f = 10°

Figure 5. Continued.

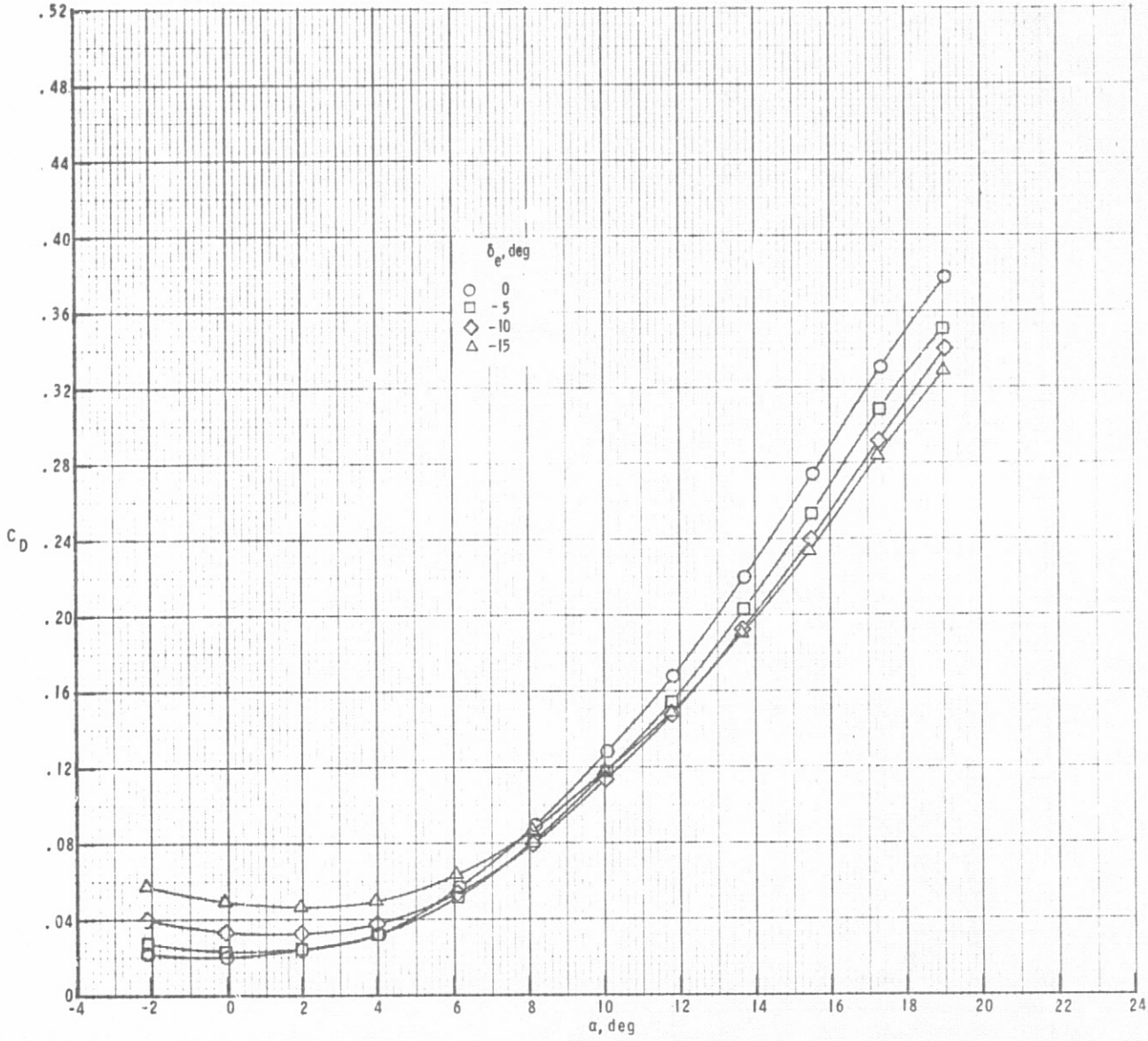

M = .70; δ_f = 10°

Figure 5. Continued.

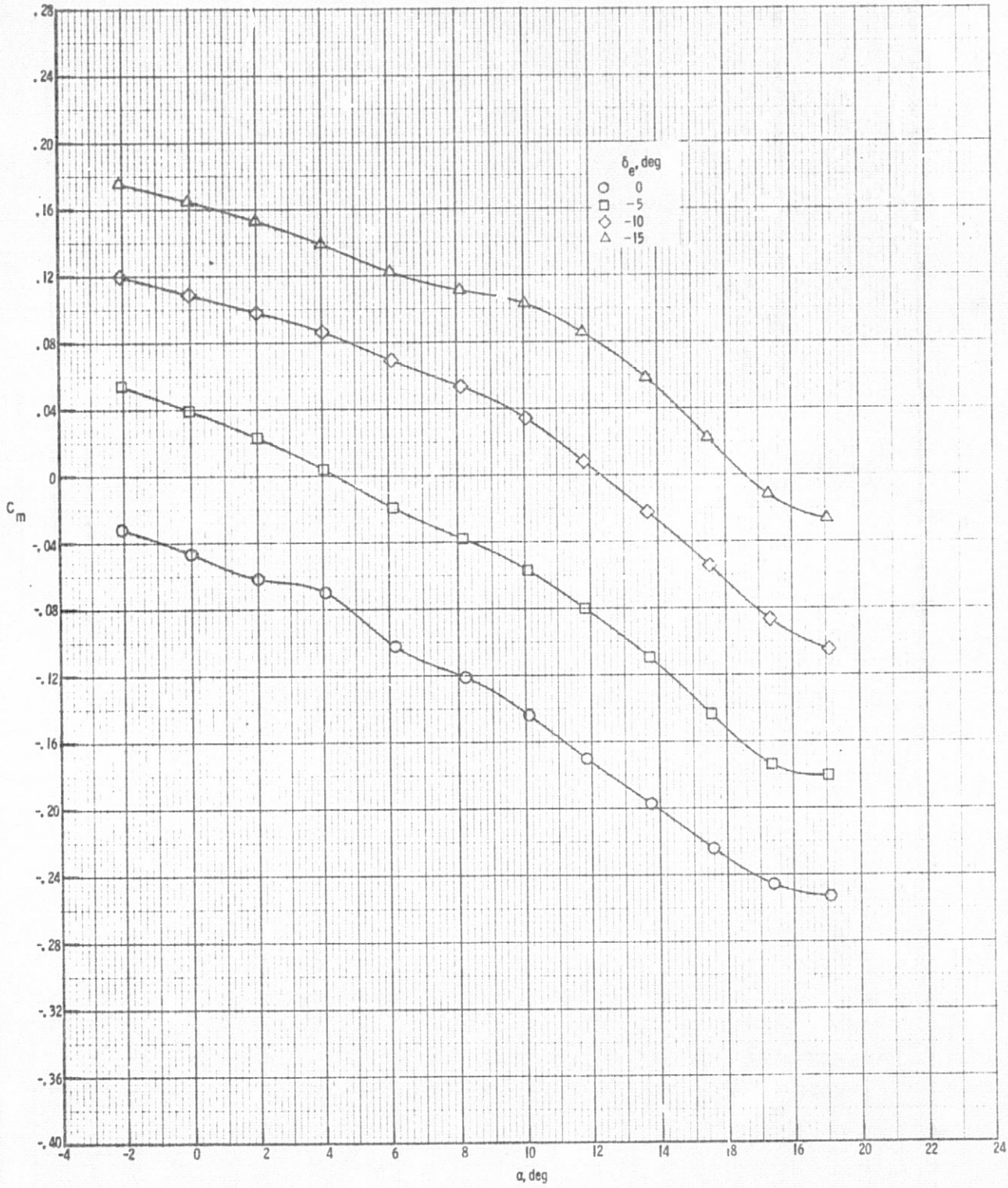

$M = .70$; $\delta_f = 10^\circ$

Figure 5. Concluded.

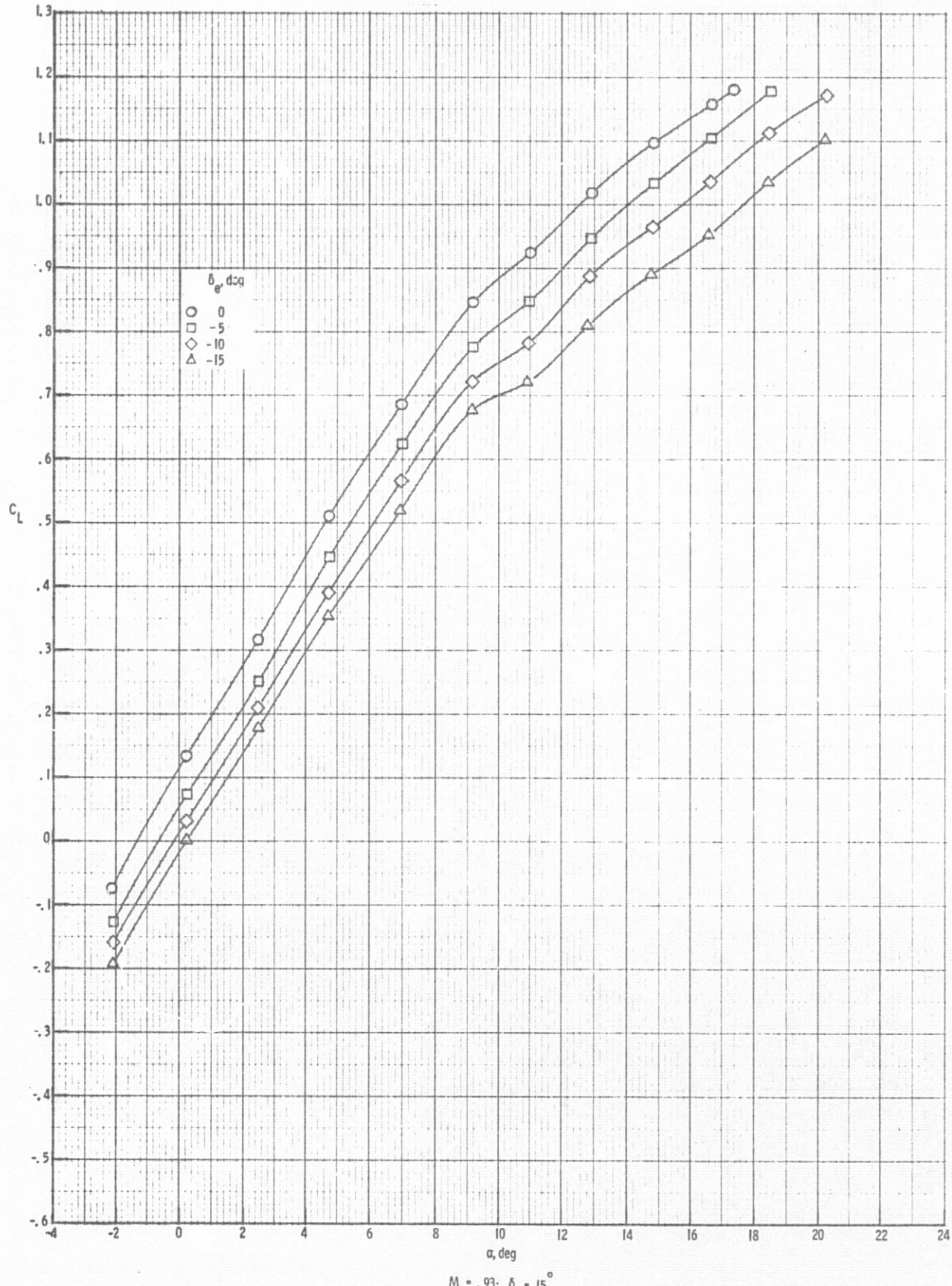

M = .93; δ_f = 15°

Figure 6. Variation of lift, drag and pitching moment coefficients with angle of attack at flap setting of 15°.

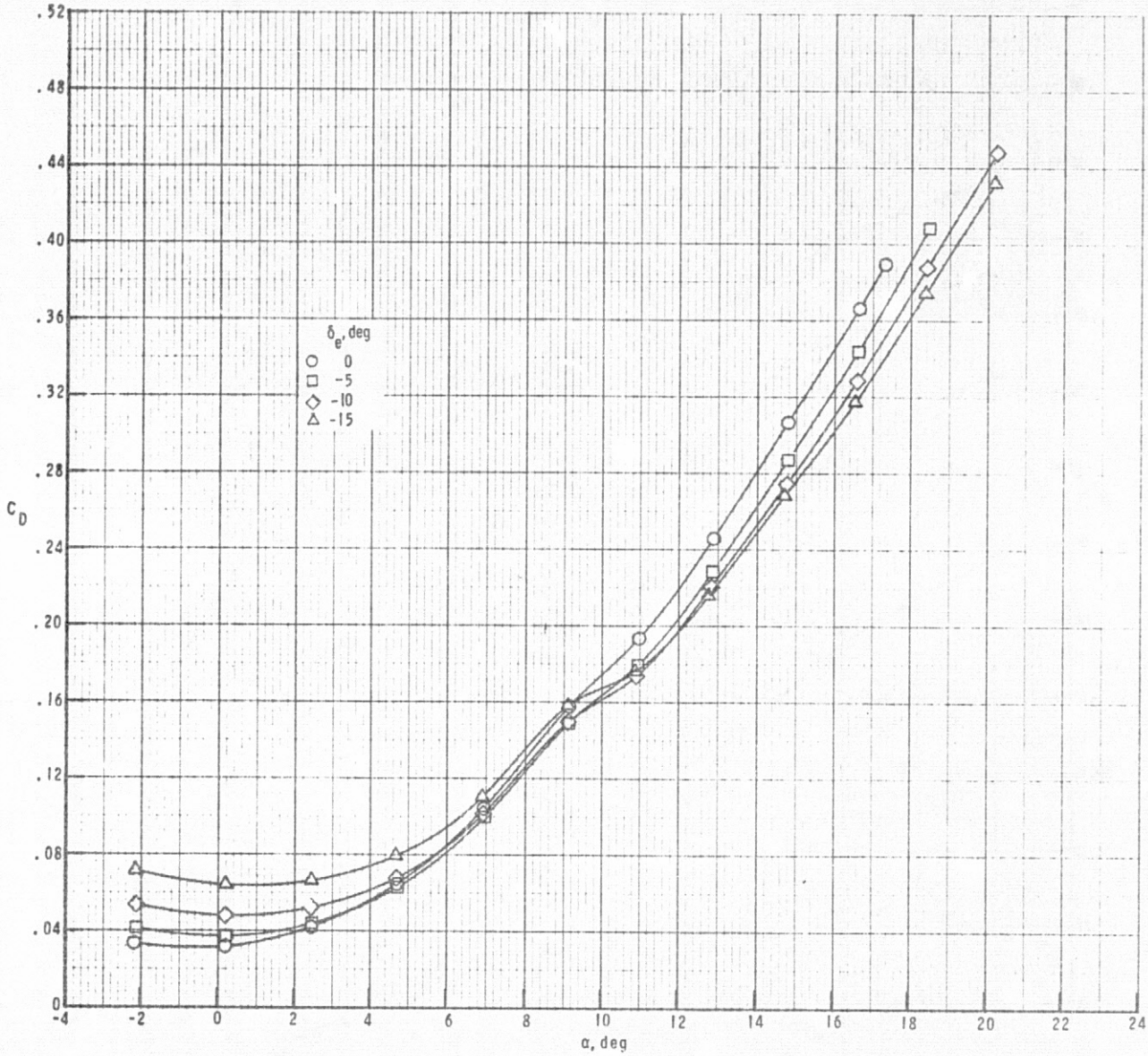

M = .93; δ_f = 15°

Figure 6. Continued.

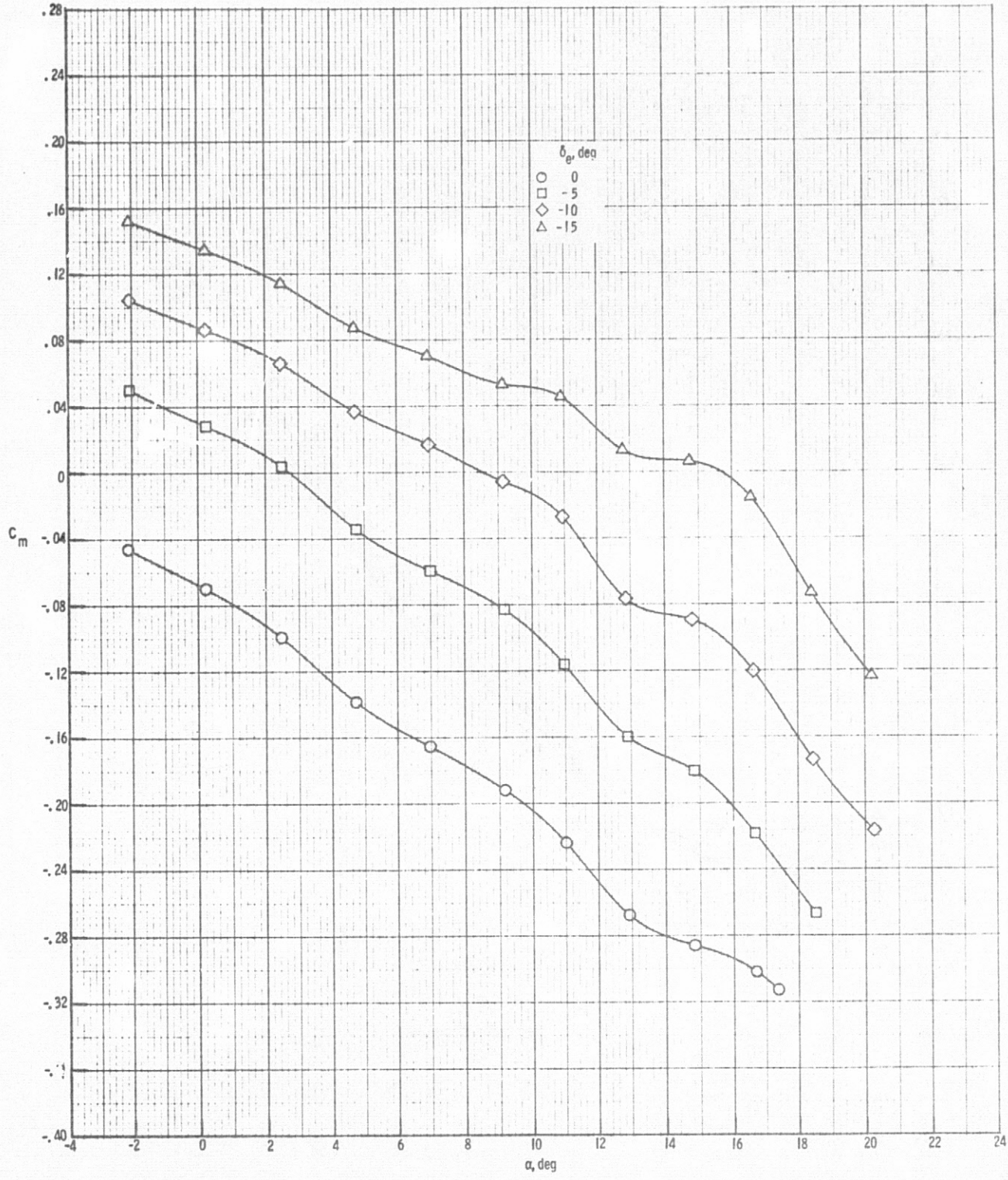

M = .93; δ_f = 15°

Figure 6. Continued.

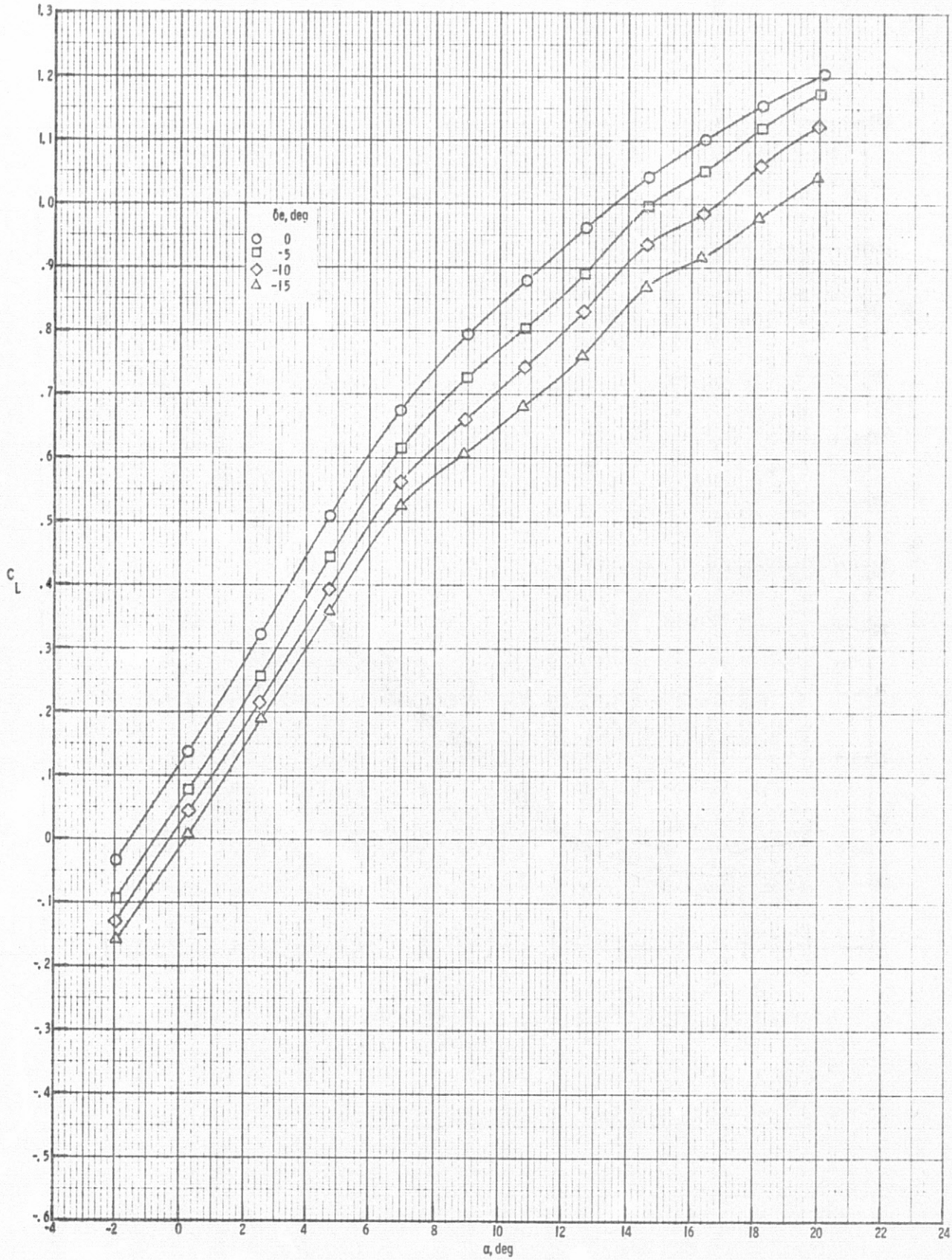

M = .90; δ_f = 15°

Figure 6. Continued.

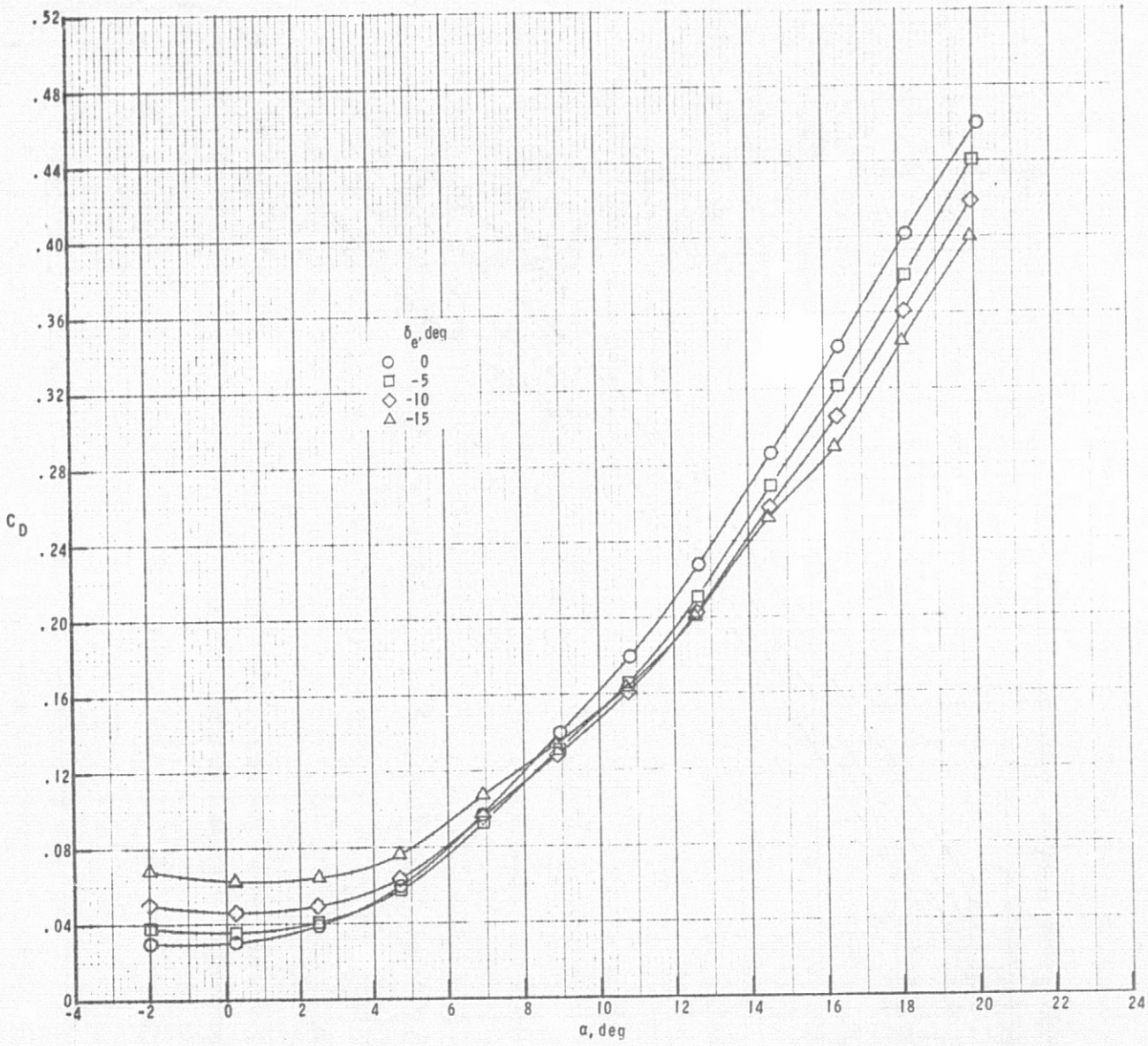

M = .90; δ_f = 15°

Figure 6. Continued.

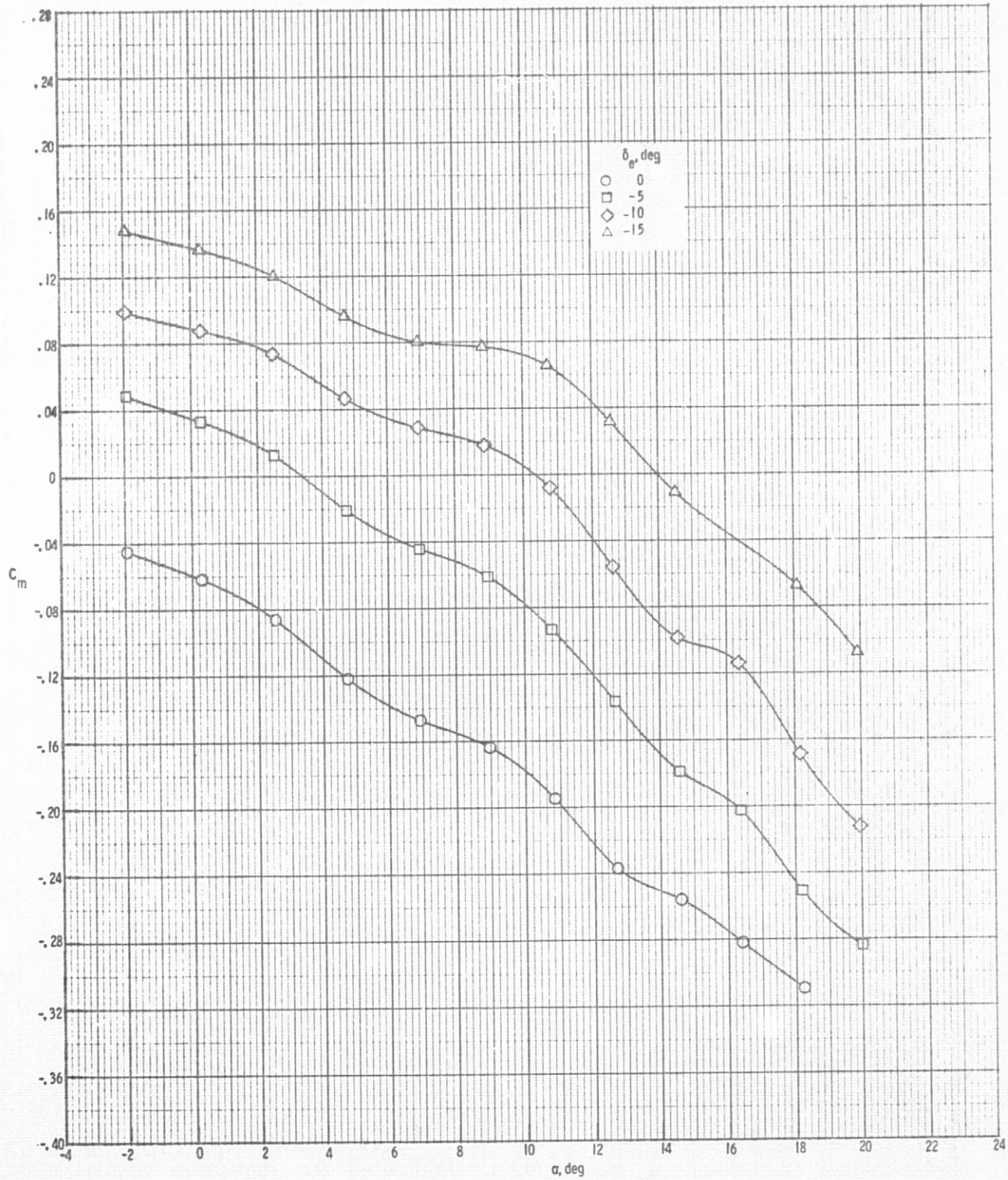

M = .90; δ_f = 15°

Figure 6. Continued.

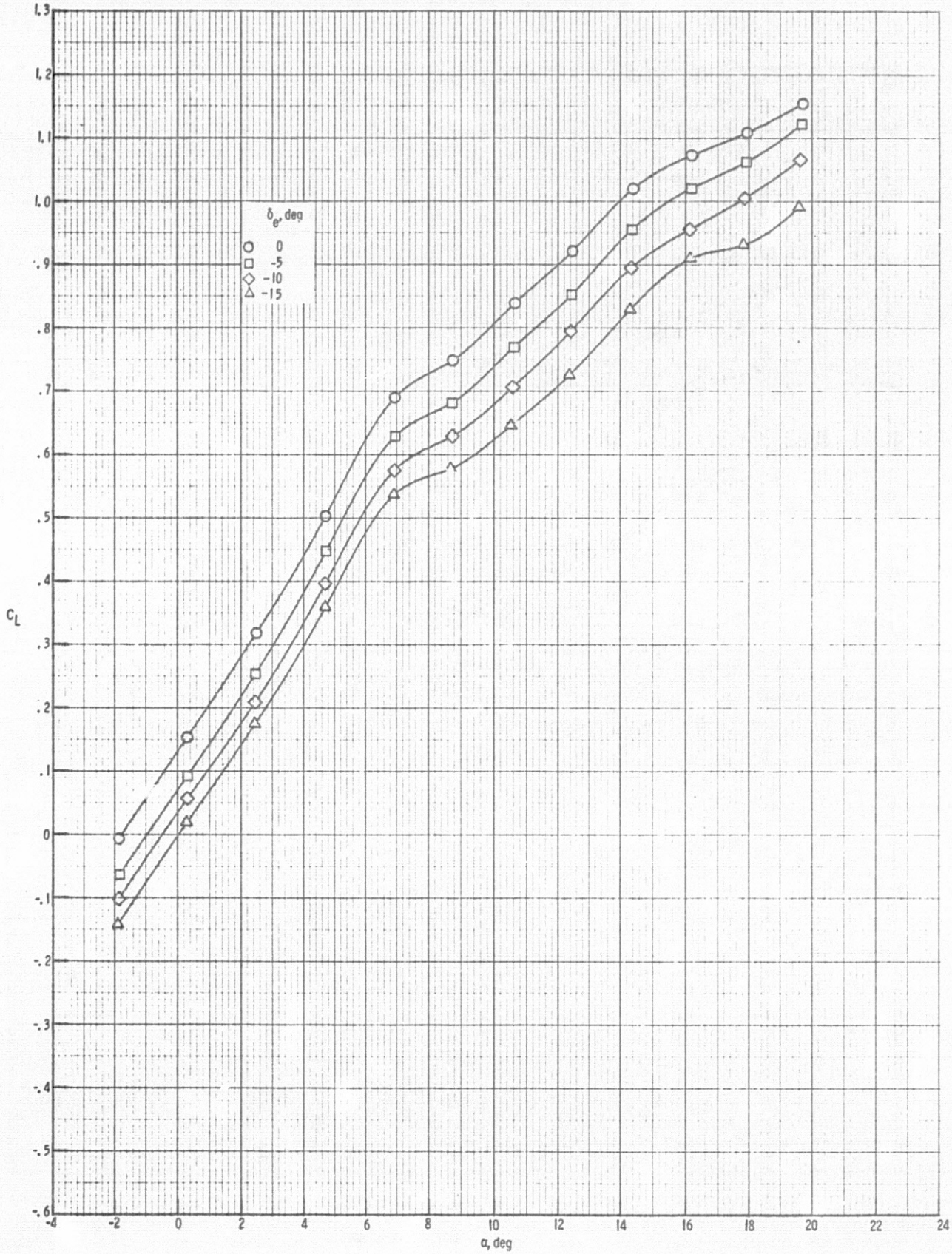

M = .85; δ_f = 15°

Figure 6. Continued.

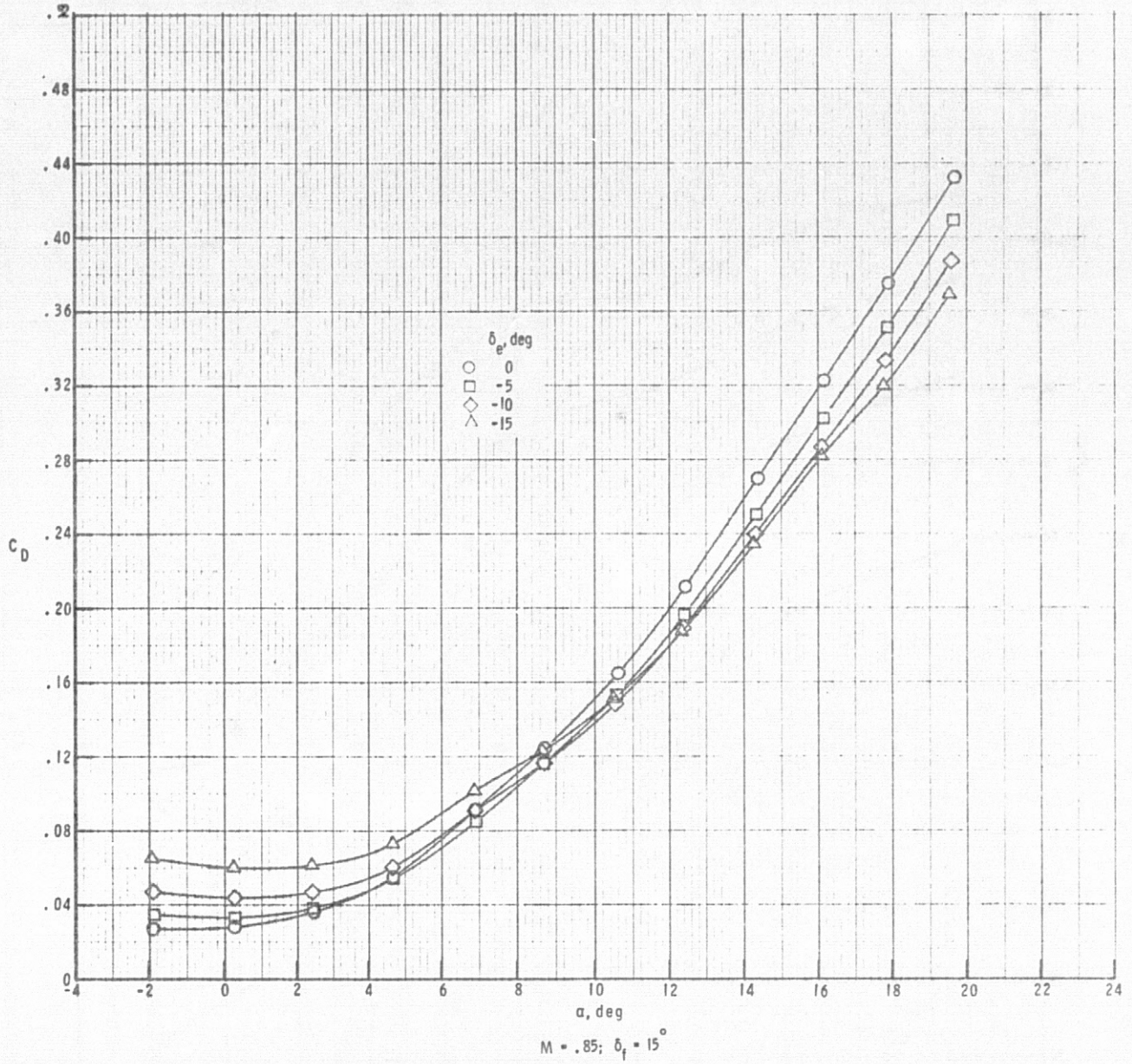

M = .85; δ_f = 15°

Figure 6. Continued.

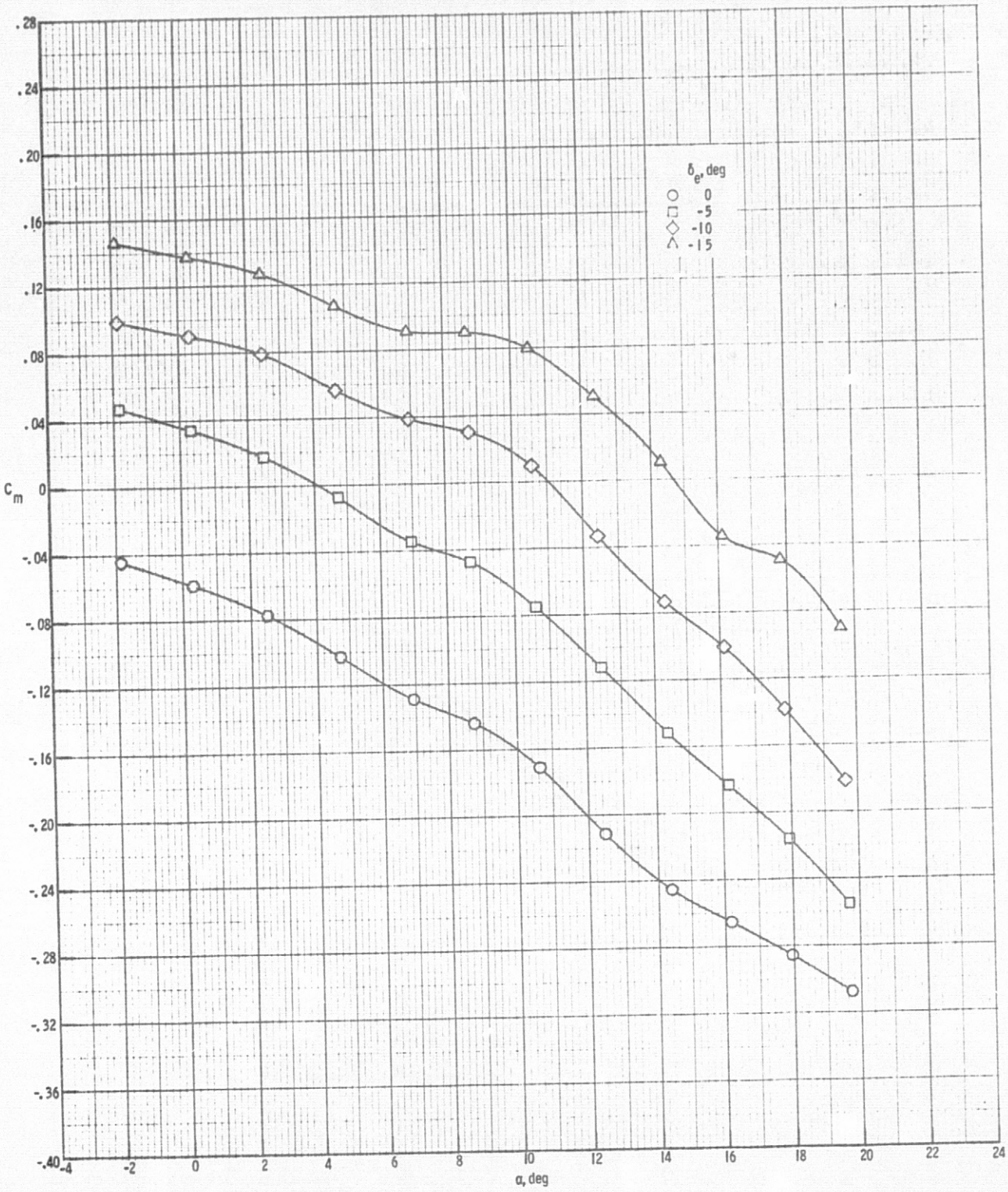

M = .85; δ_f = 15°

Figure 6. Continued.

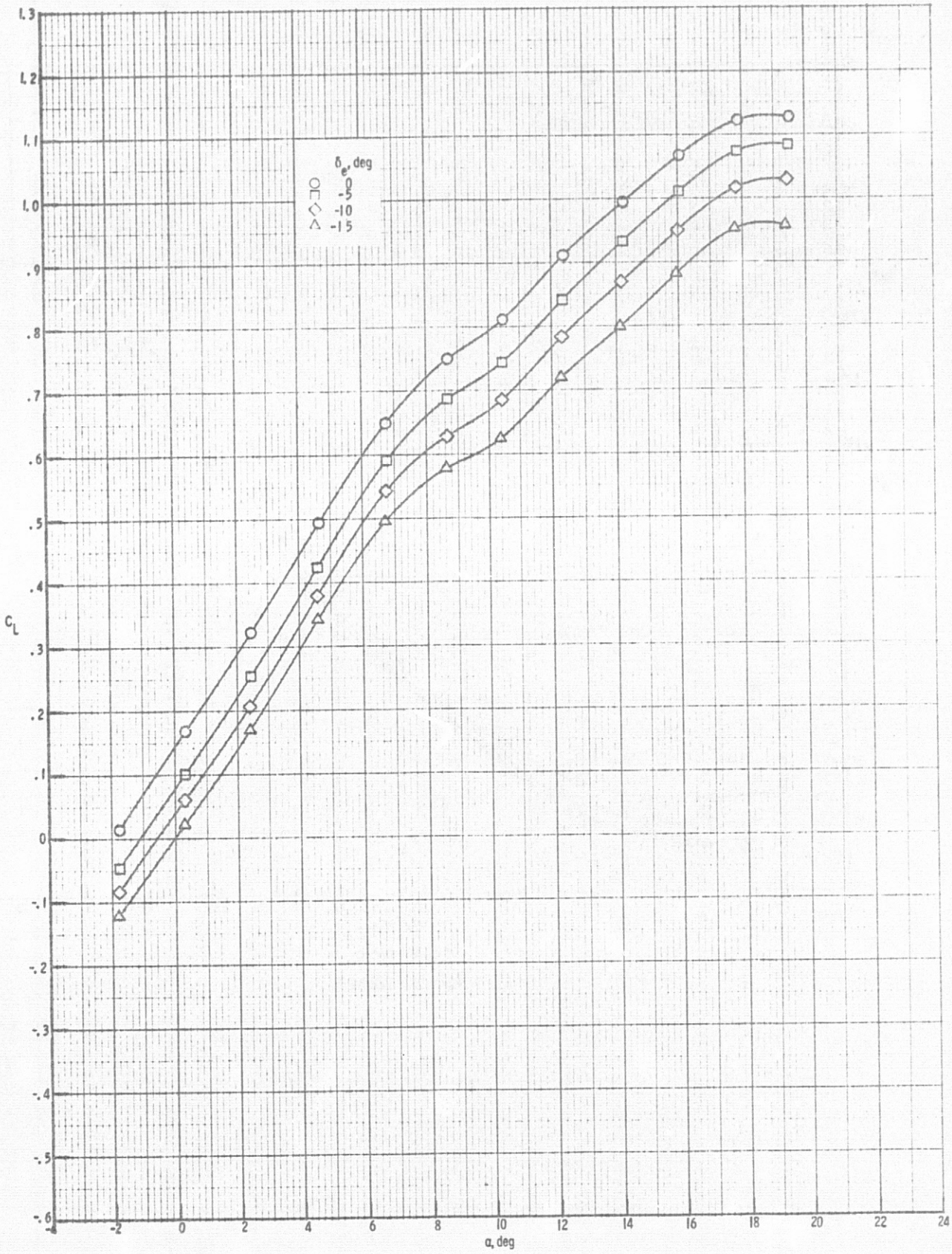

M = .80; δ_f = 15°

Figure 6. Continued.

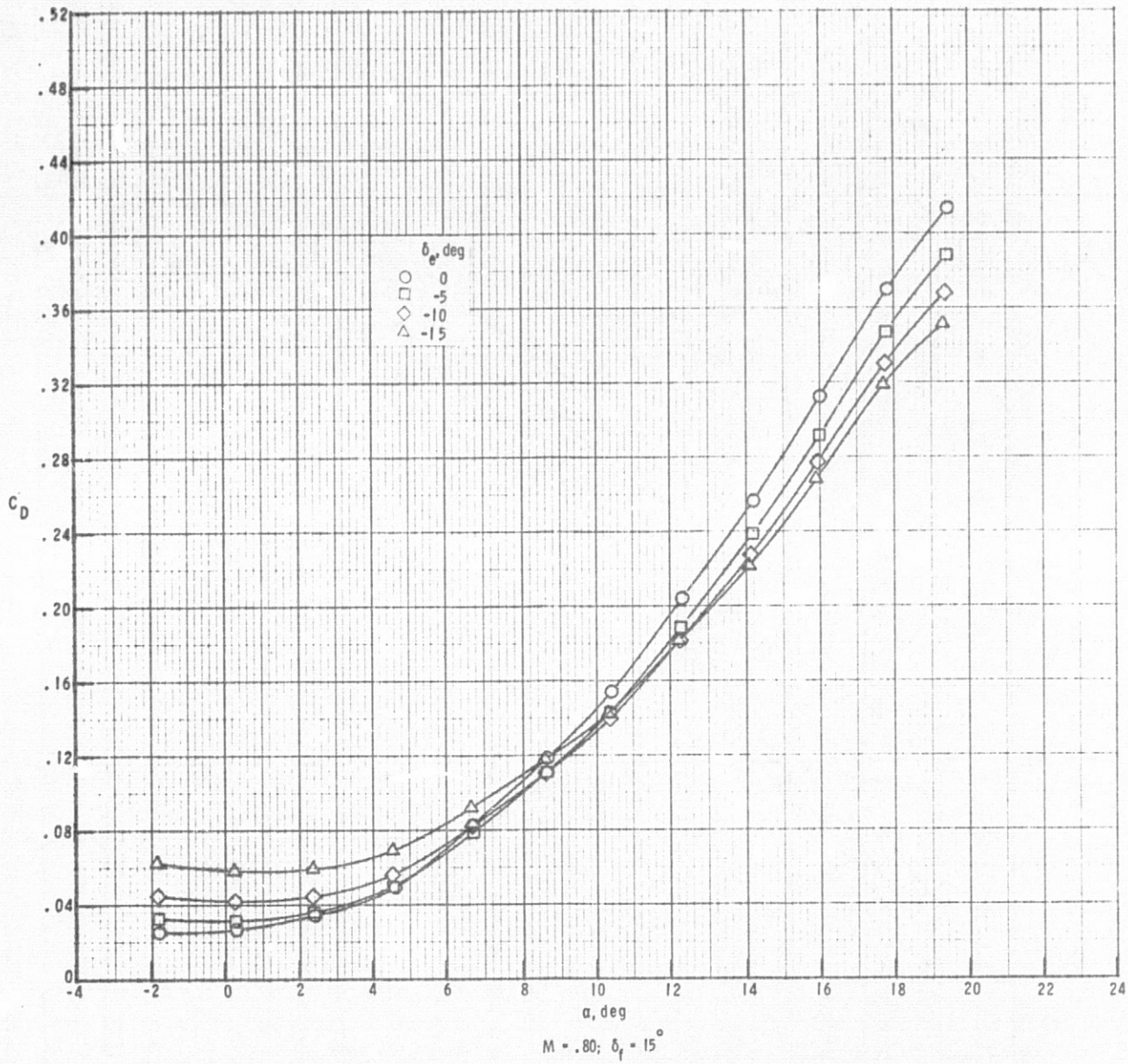

M = .80; δ_f = 15°

Figure 6. Continued.

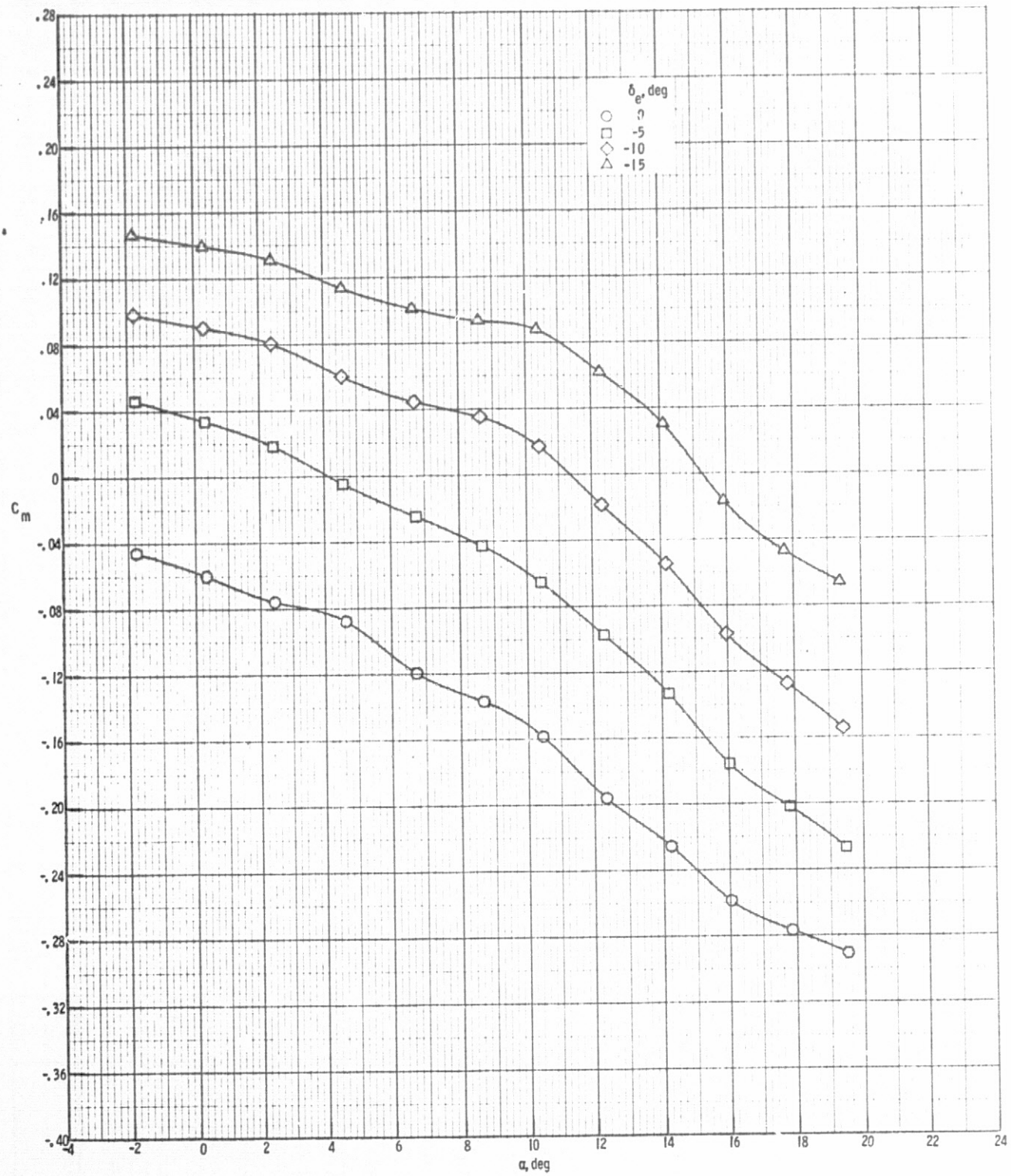

M = .80; δ_f = 15°

Figure 6. Continued.

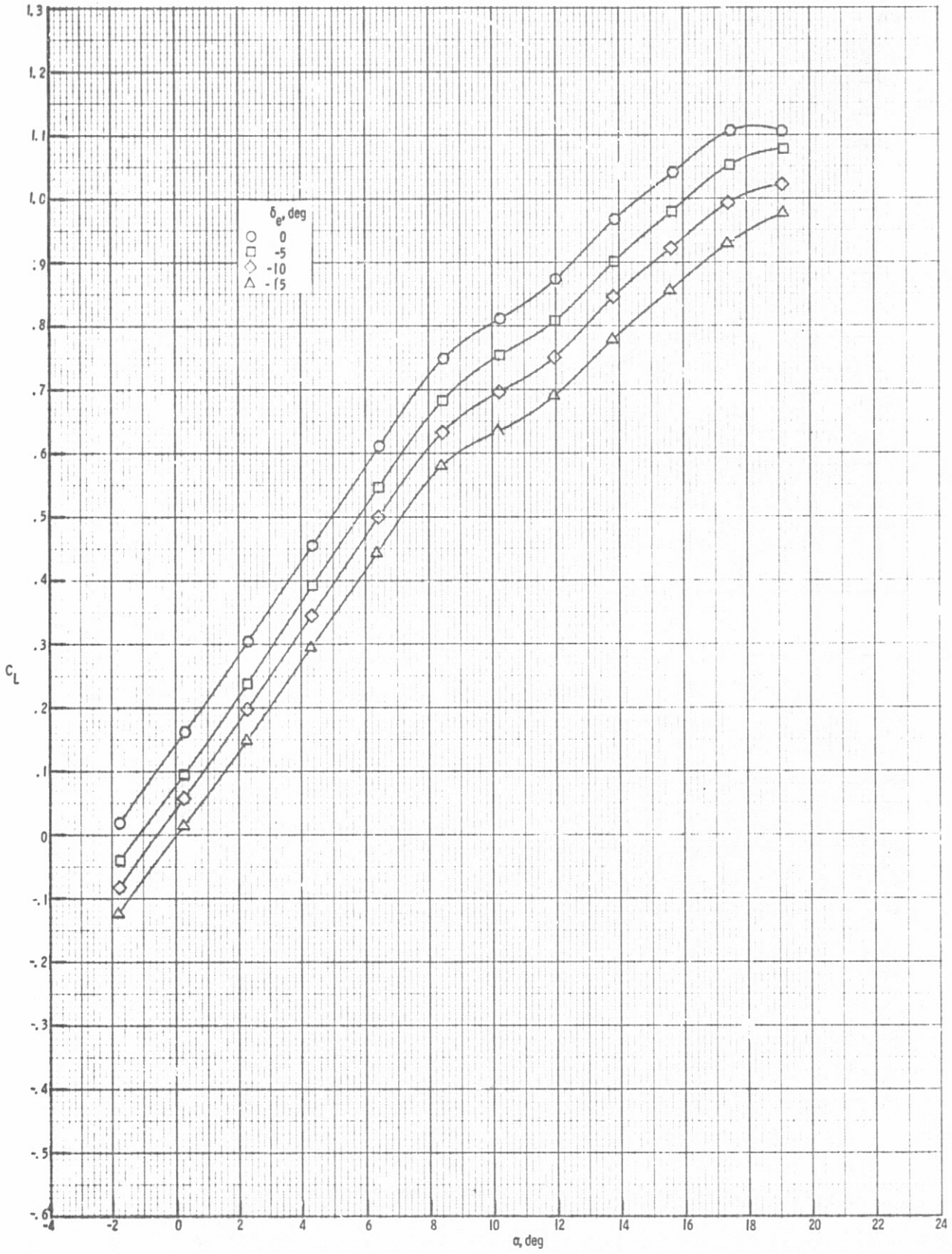

M = .70; δ_f = 15°

Figure 6. Continued.

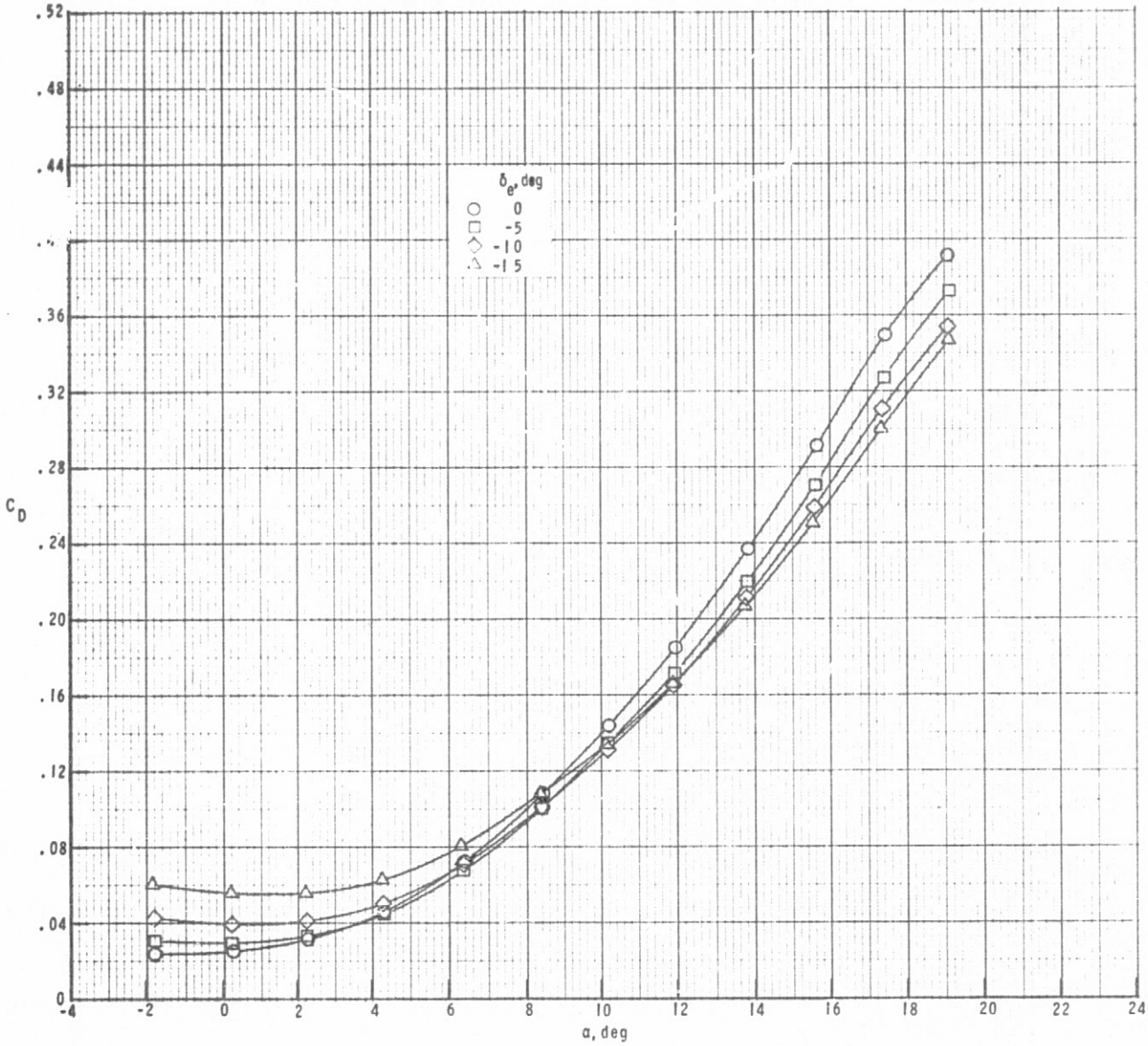

M = .70; δ_f = 15°

Figure 6. Continued.

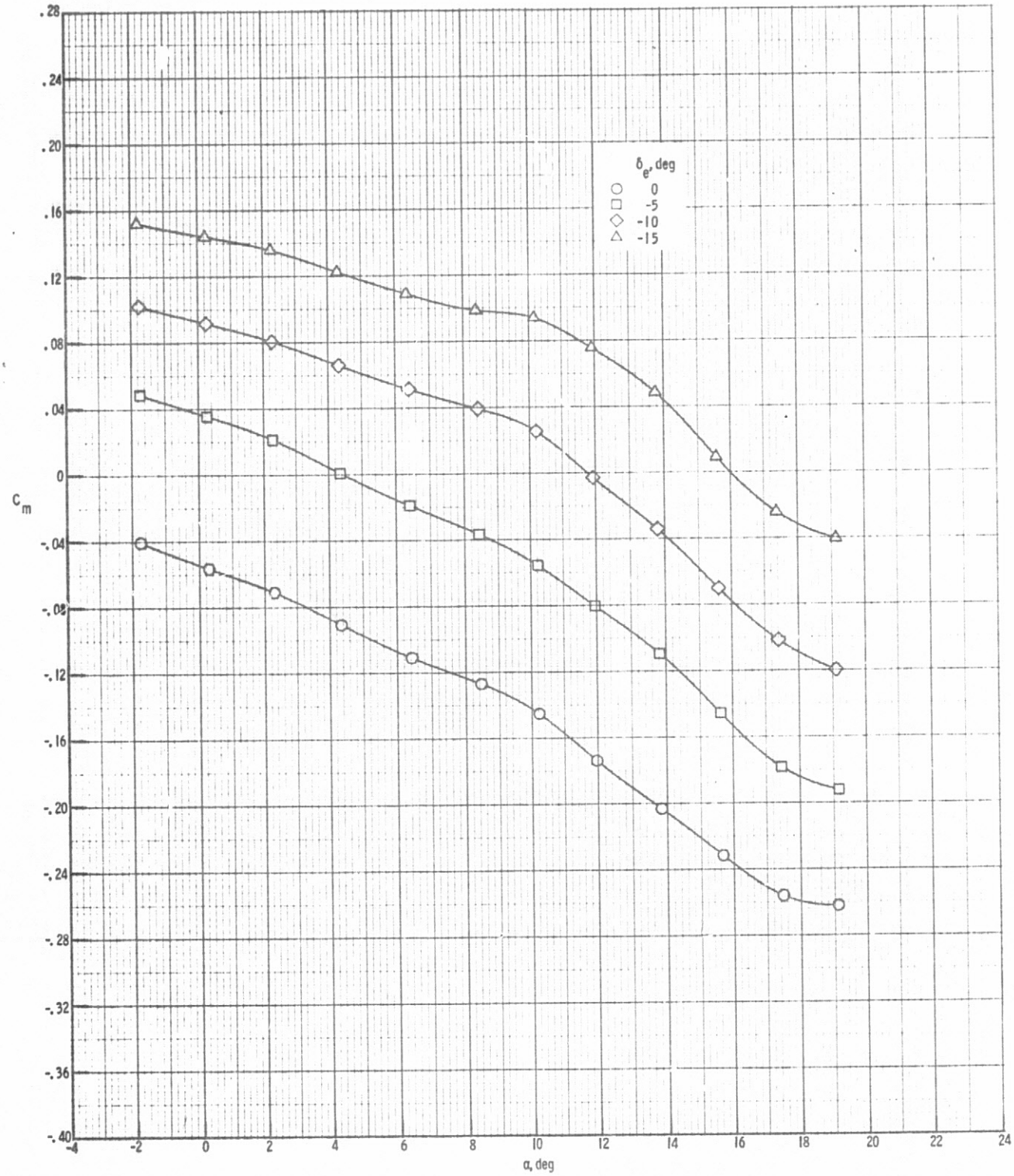

M = .70; δ_f = 15°

Figure 6. Concluded.

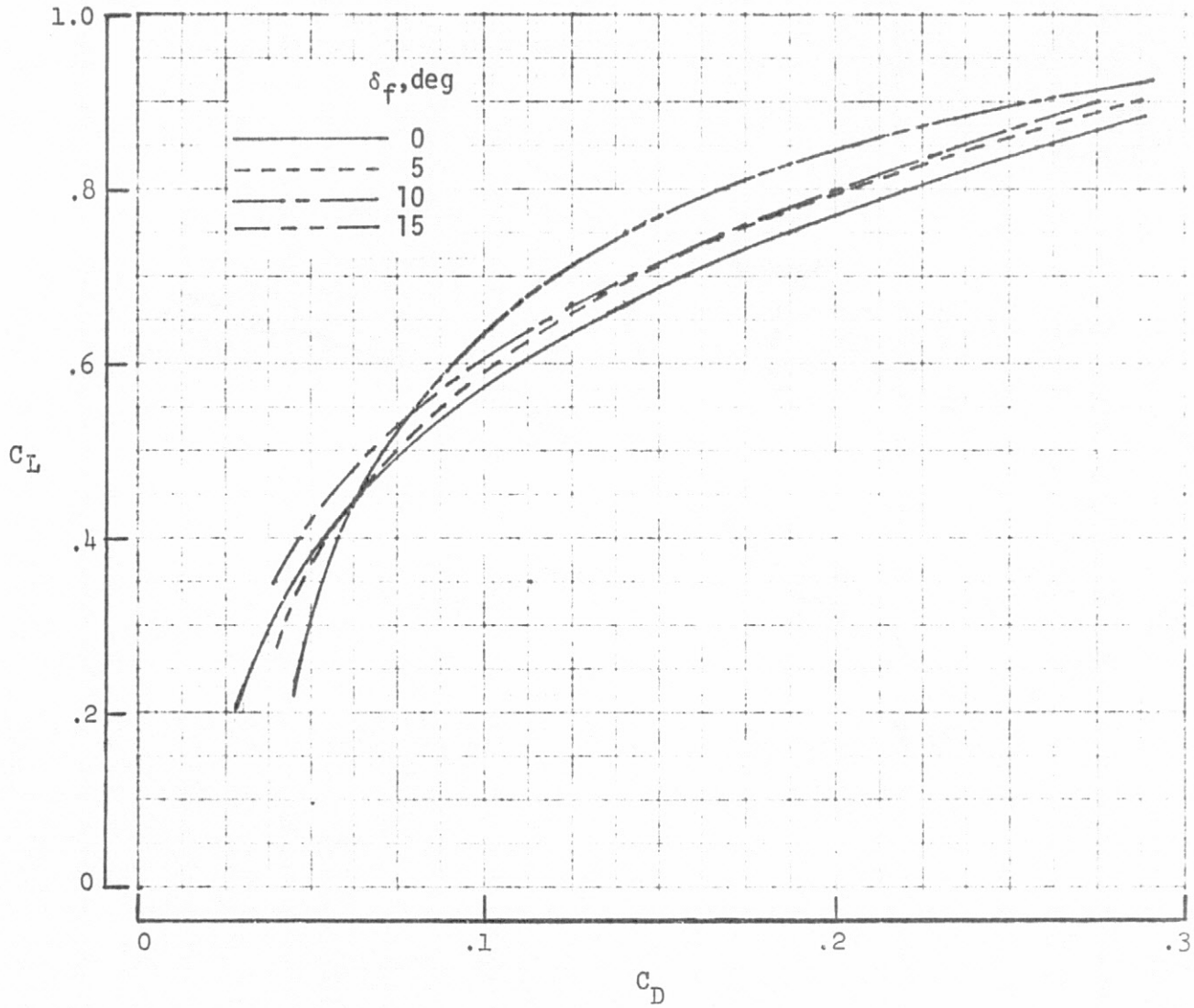

M = .93

Figure 7.- Trimmed drag polars at various flap settings.

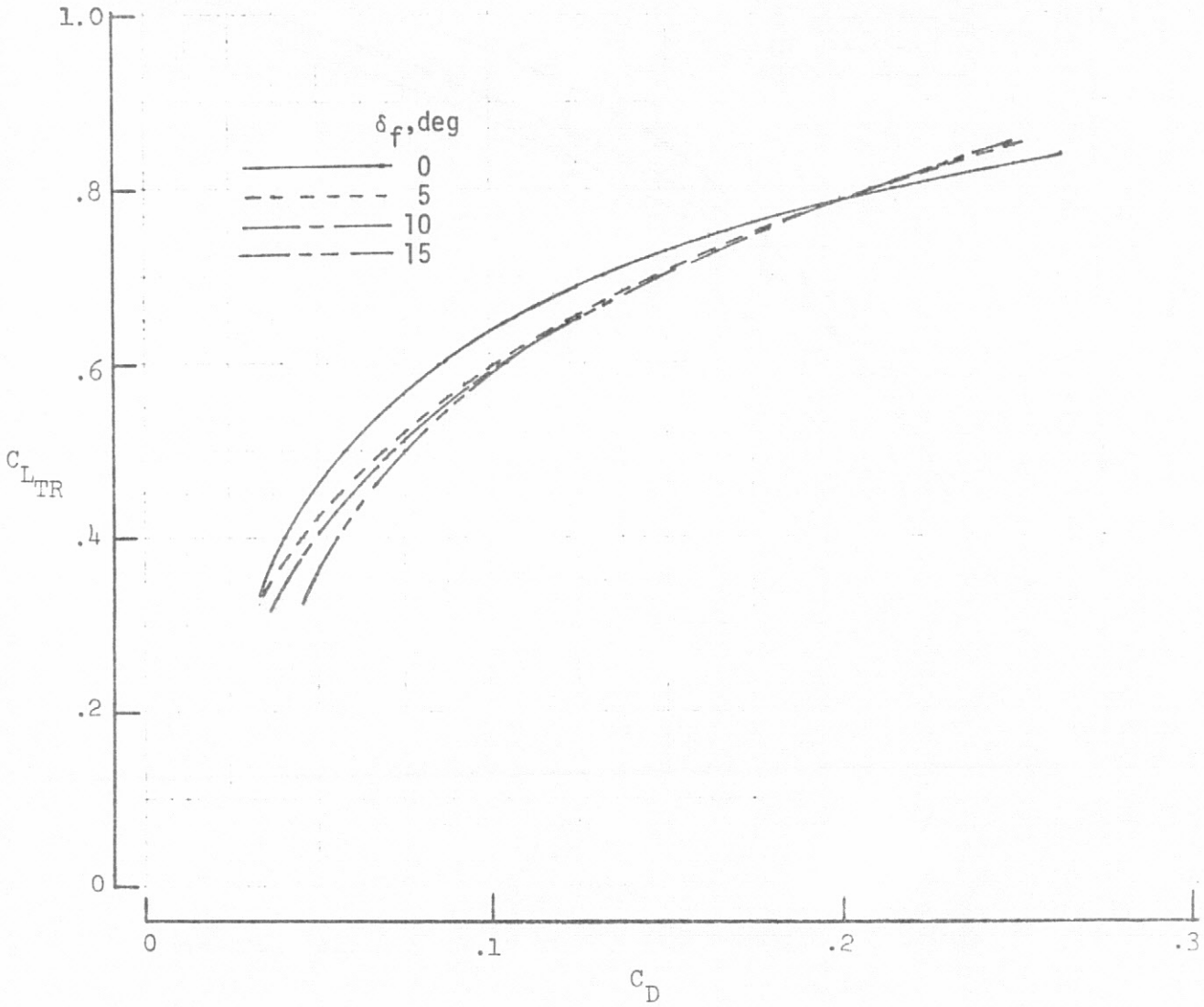

M = .90

Figure 7.- Continued.

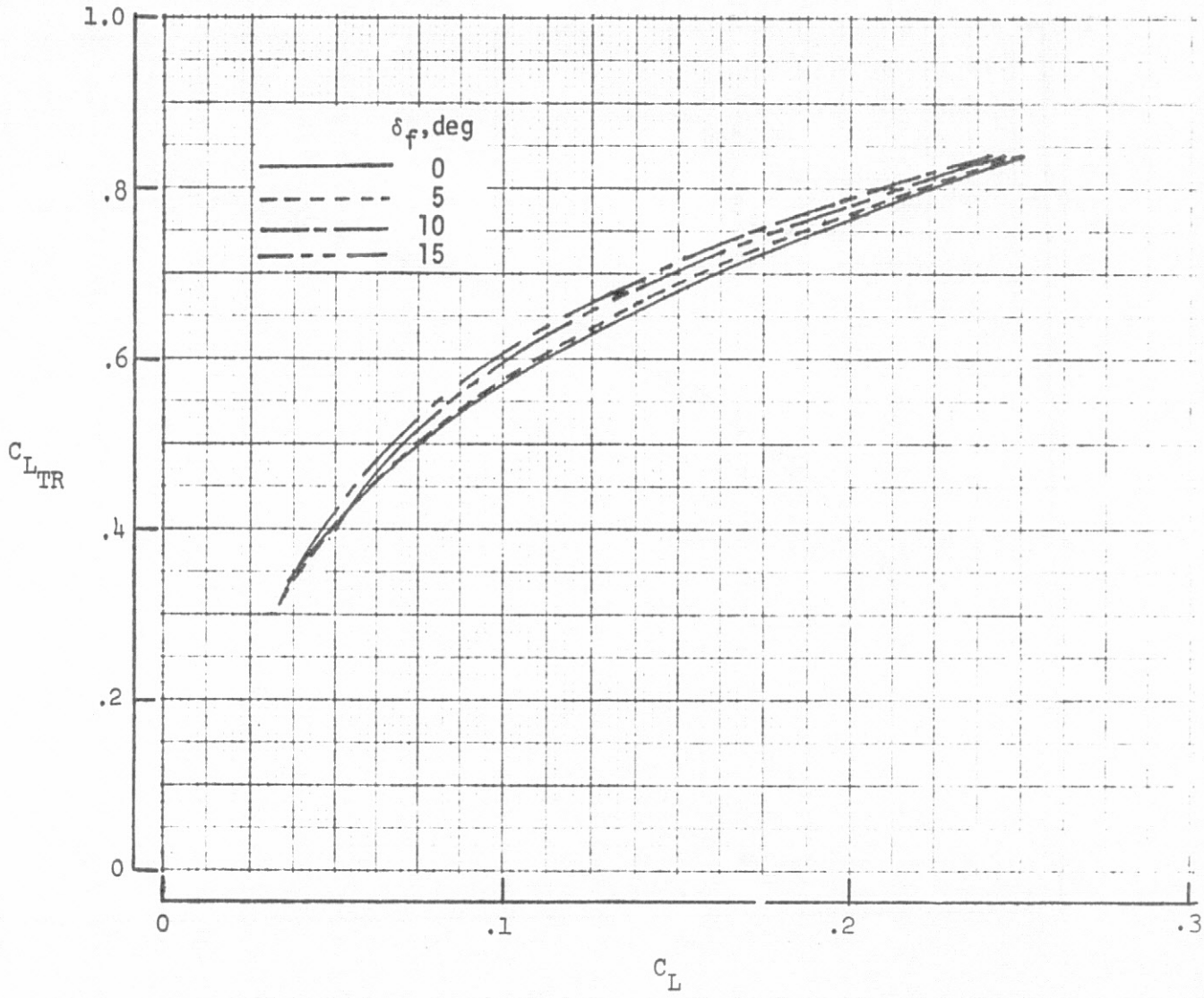

M = .85

Figure 7.- Continued.

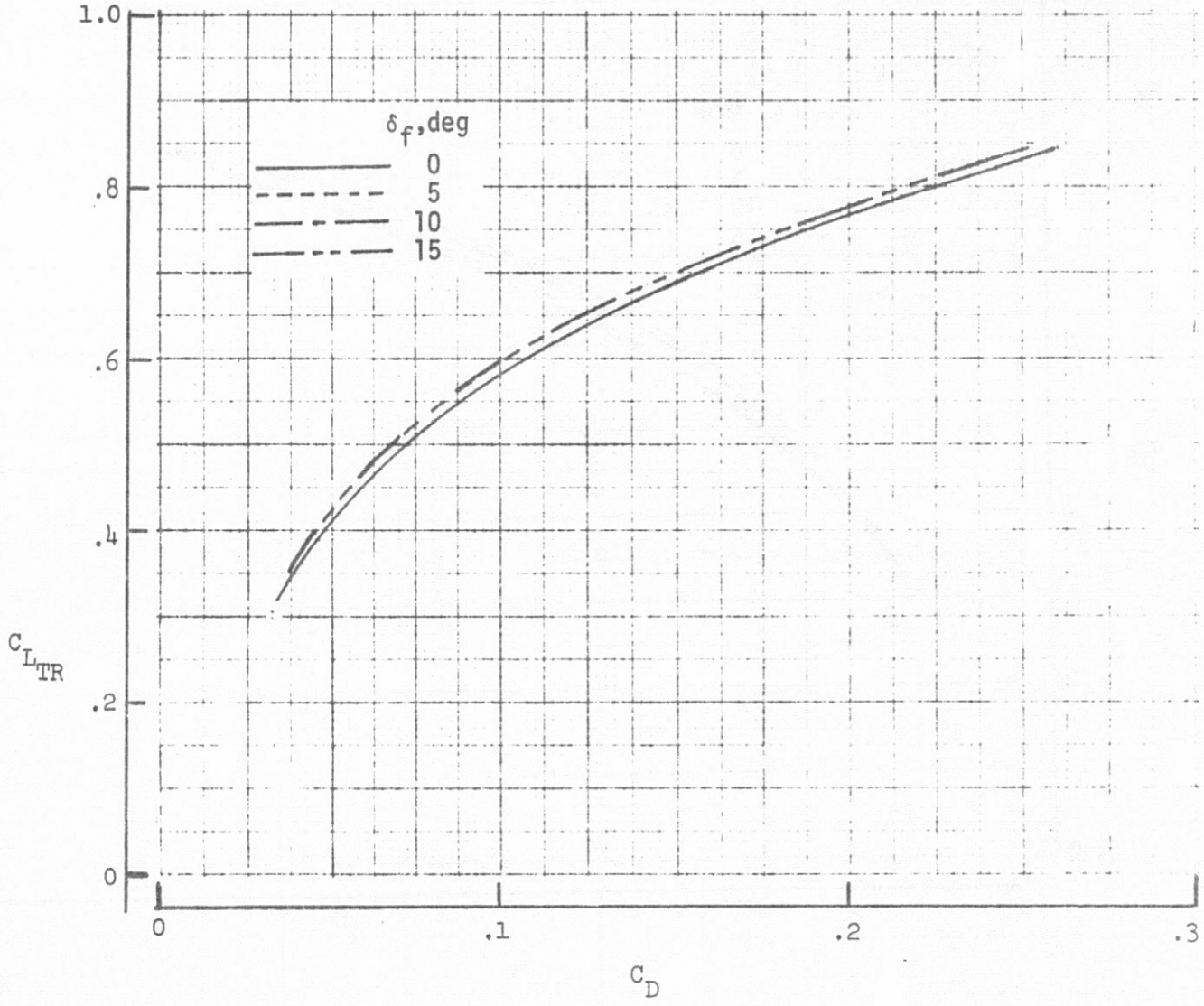

M = .80

Figure 7.- Continued.

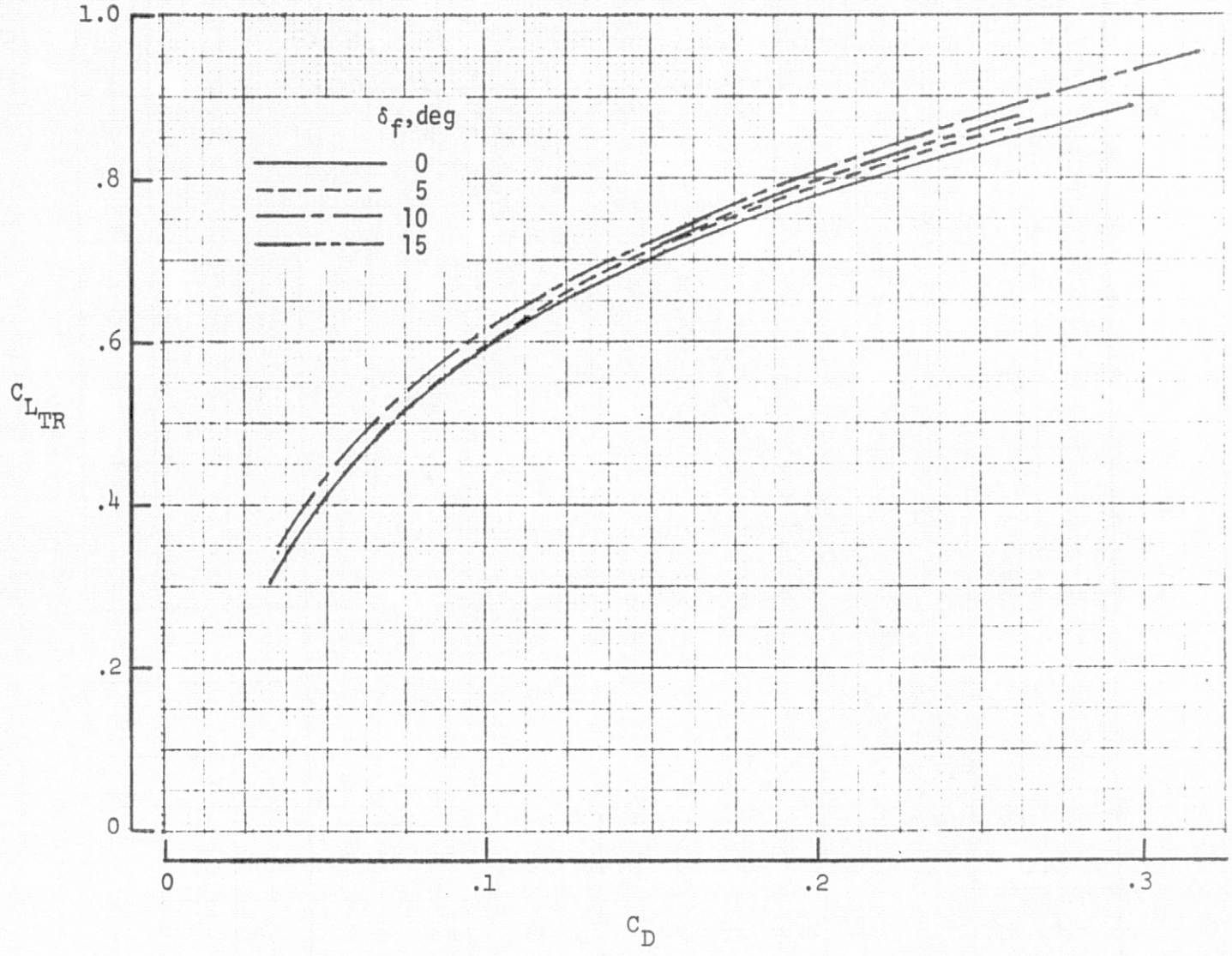

M = .70

Figure 7.- Concluded.

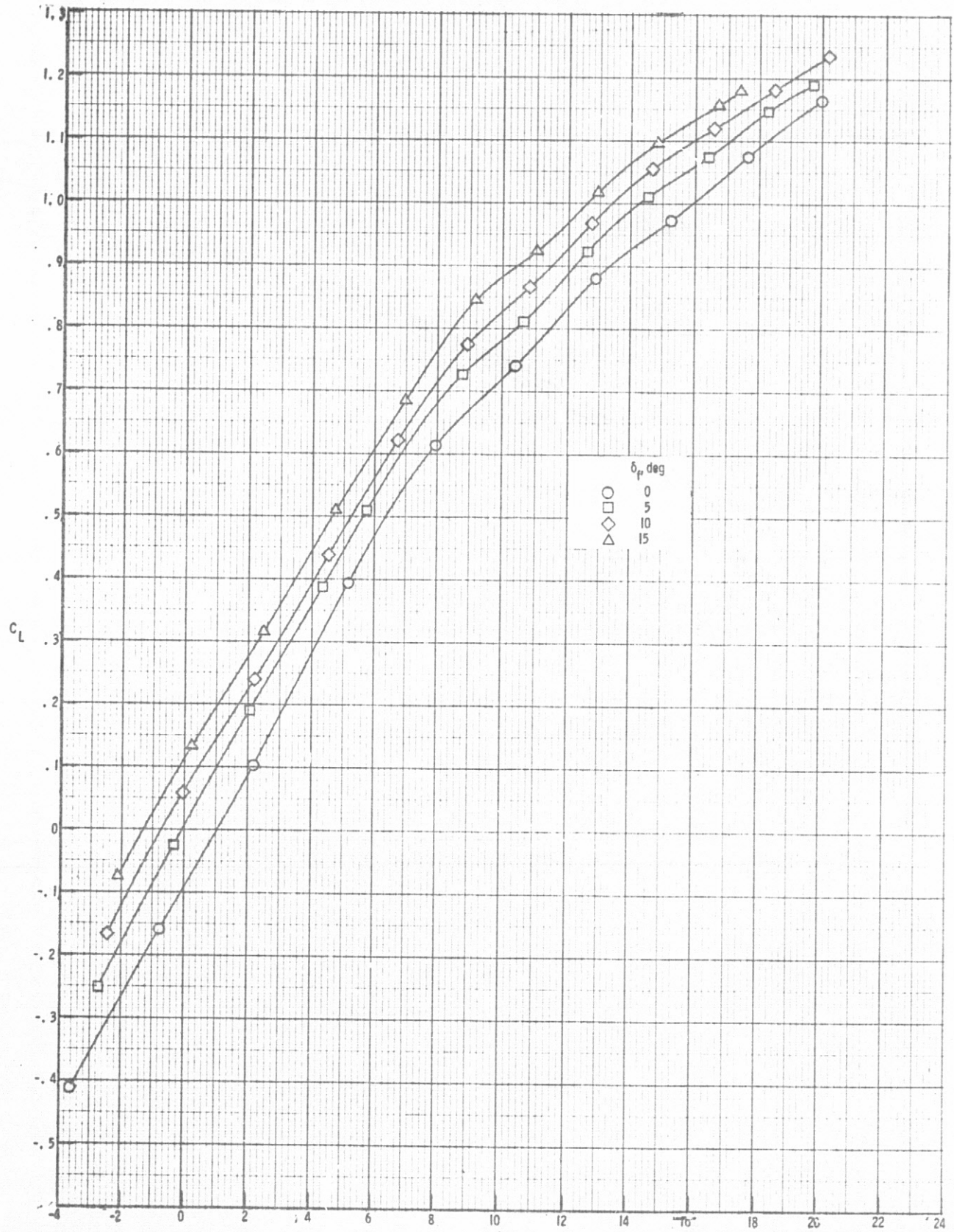

M = .93; δ_e = 0°

Figure 8. Effect of flap deflections on lift, drag and pitching moment coefficients. Horizontal tail is at zero degree.

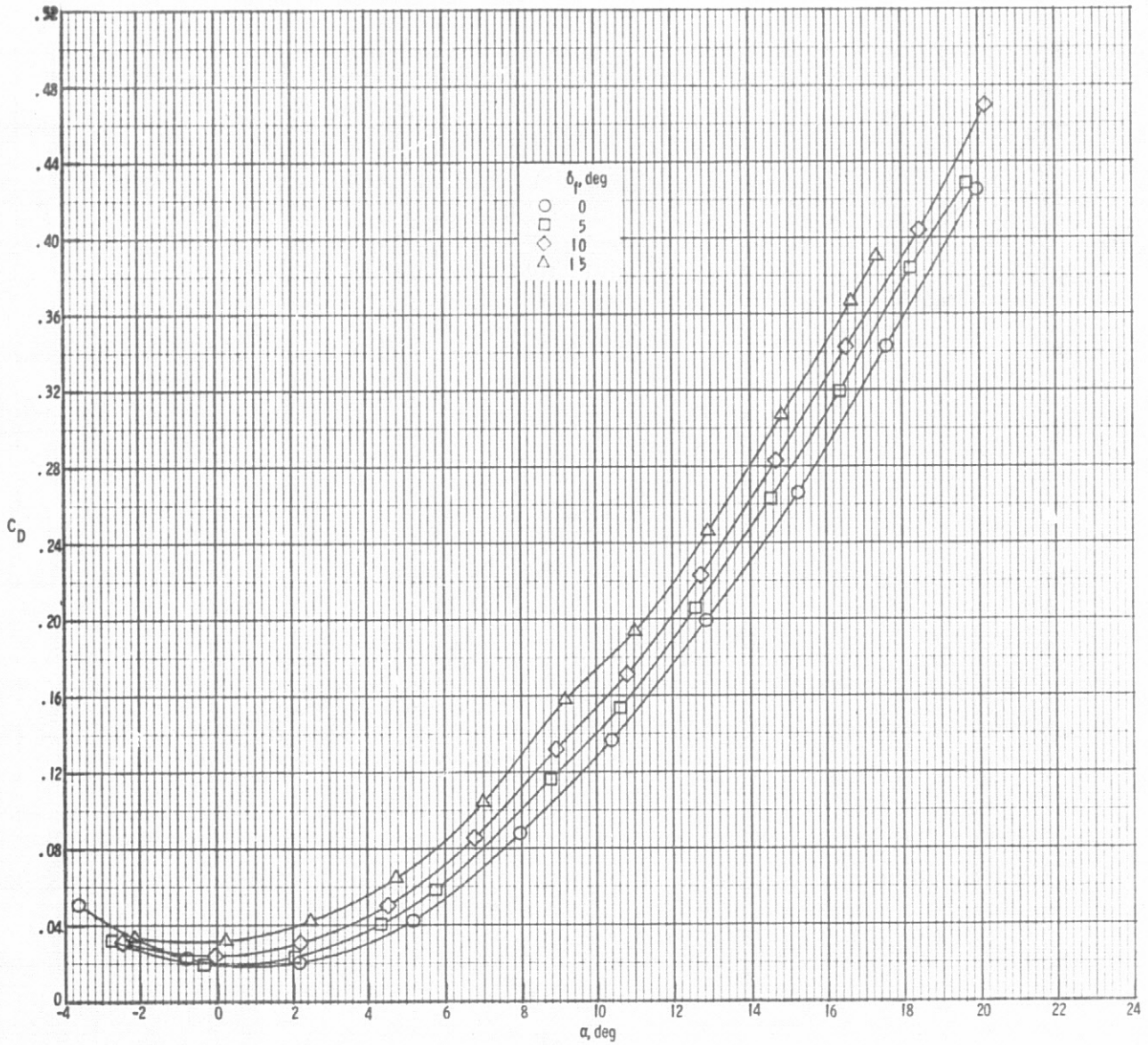

M = .93; δ_e = 0°

Figure 8. Continued.

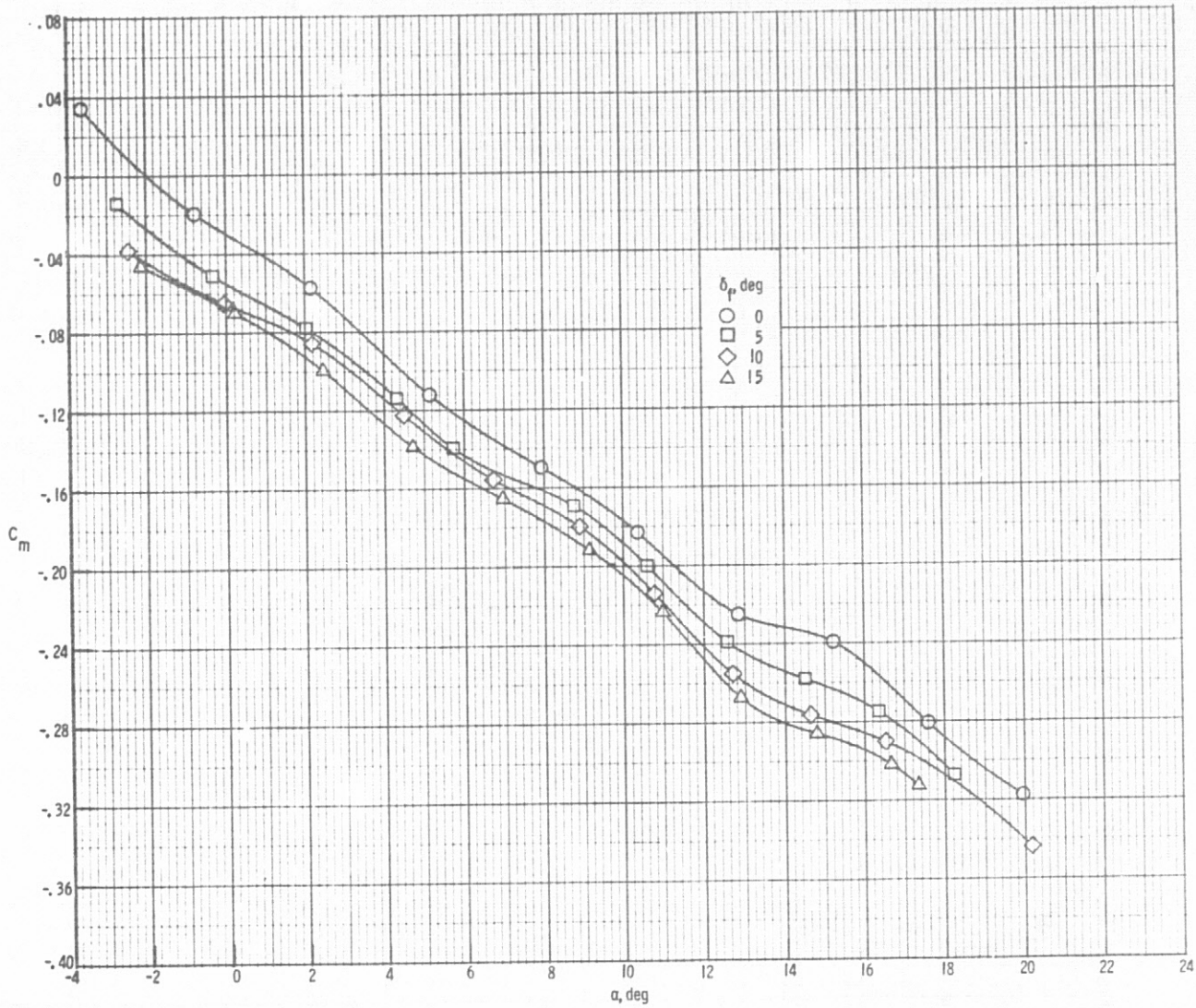

M = .93; $\delta_e = 0^\circ$

Figure 8. Continued.

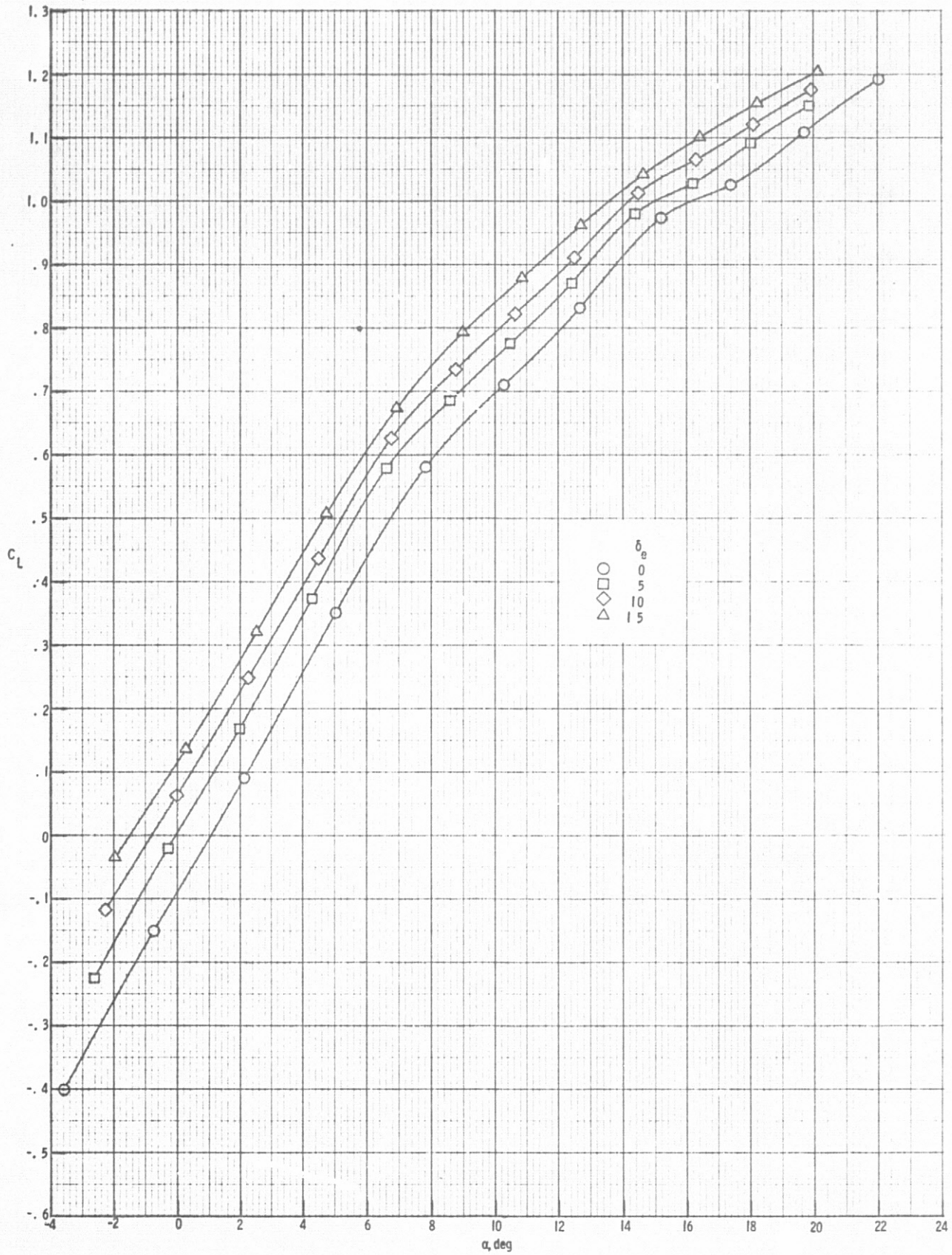

M = .90; $\delta_e = 0°$

Figure 8. Continued.

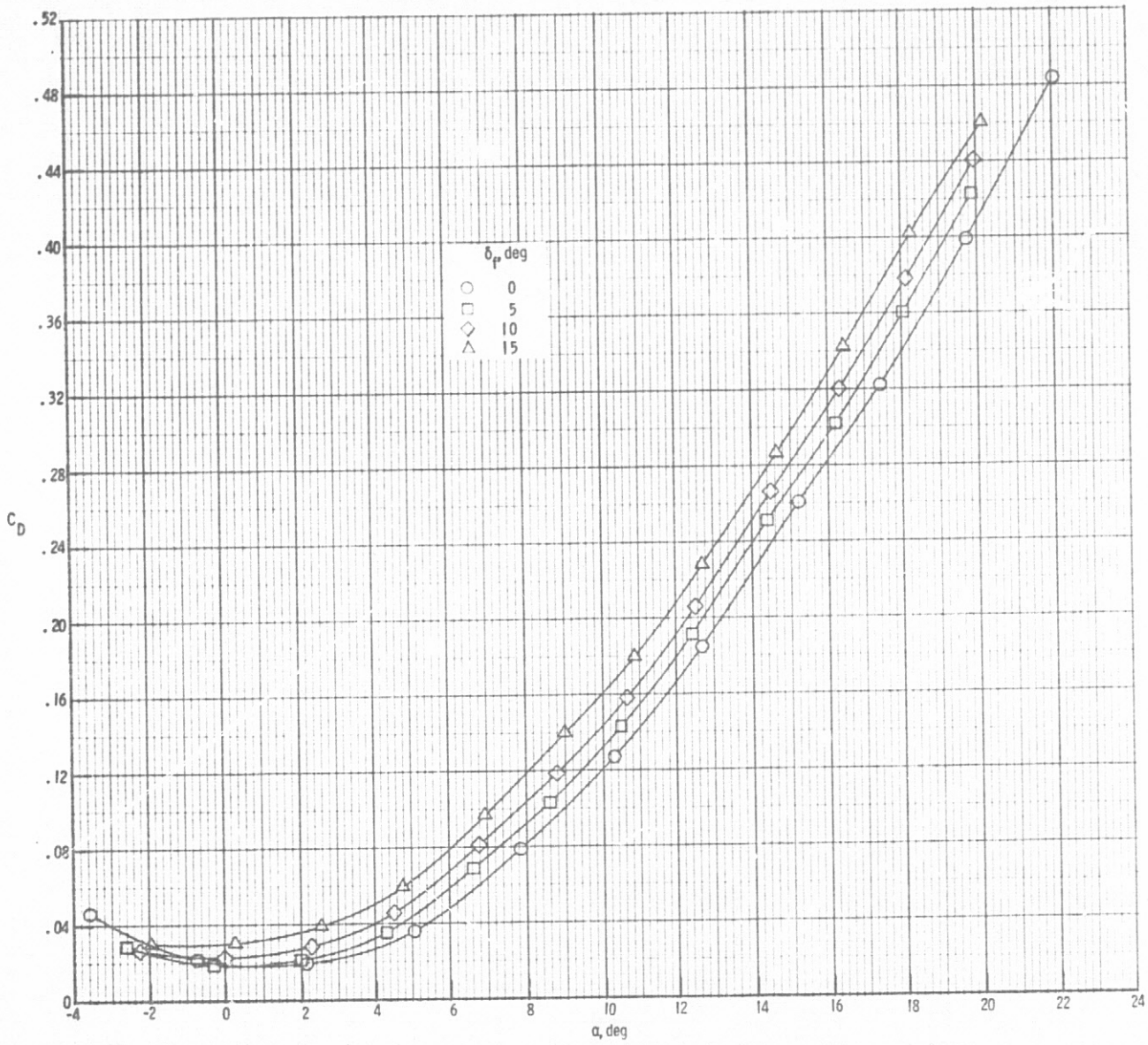

M = .90; δ_e = 0°

Figure 8. Continued.

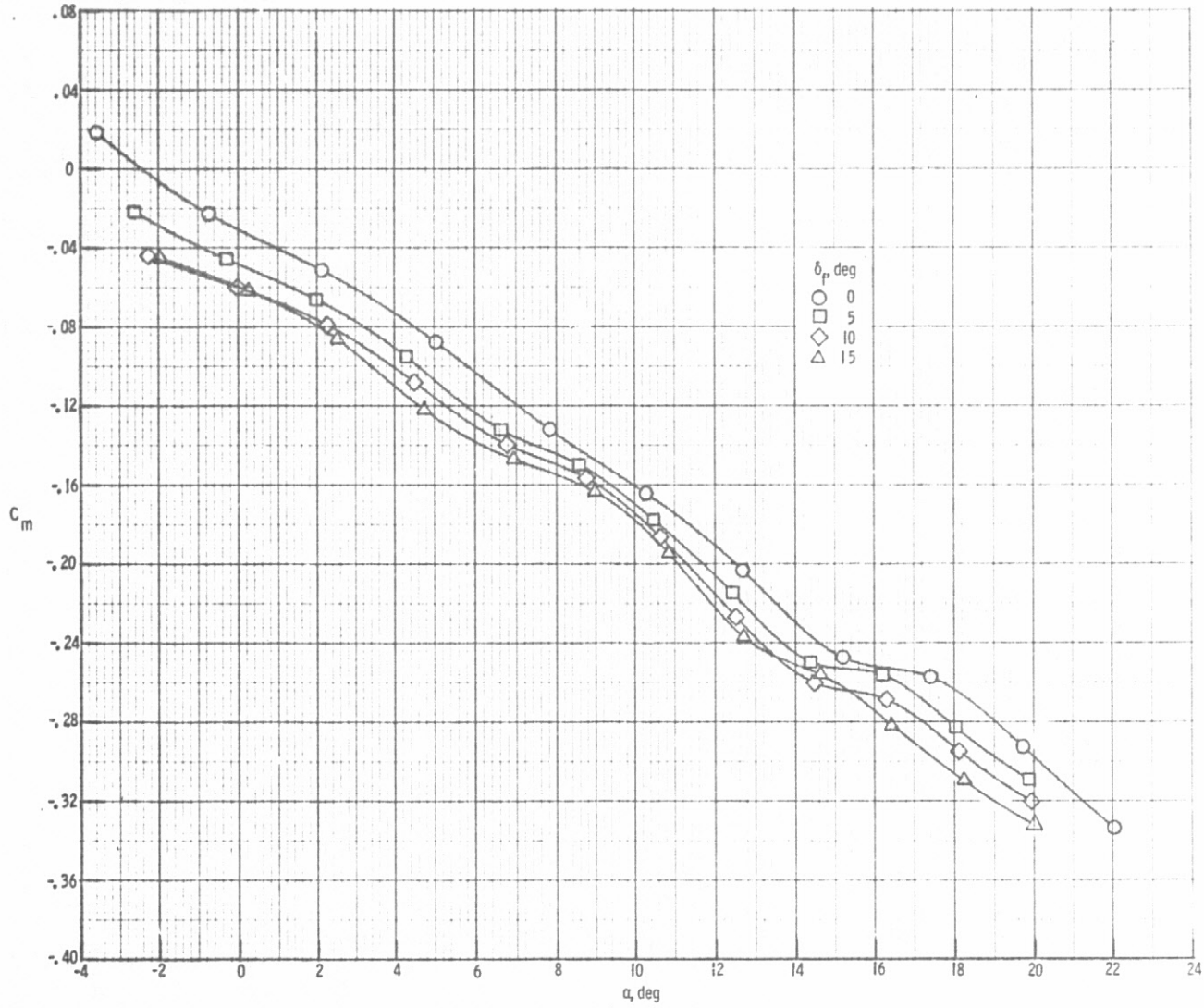

M = .90; δ_e = 0°

Figure 8. Continued.

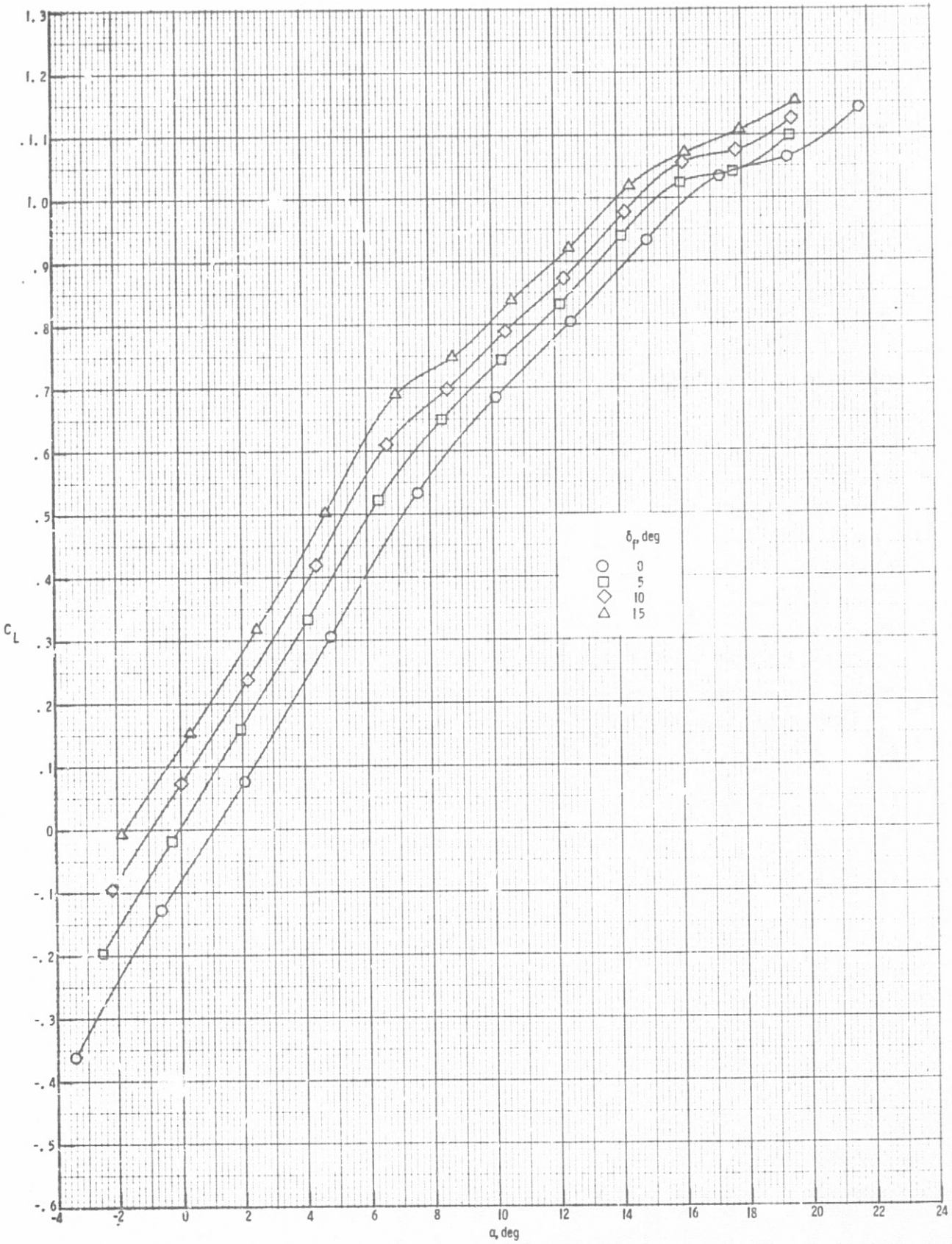

M = .85; δ_e = 0°

Figure 8. Continued.

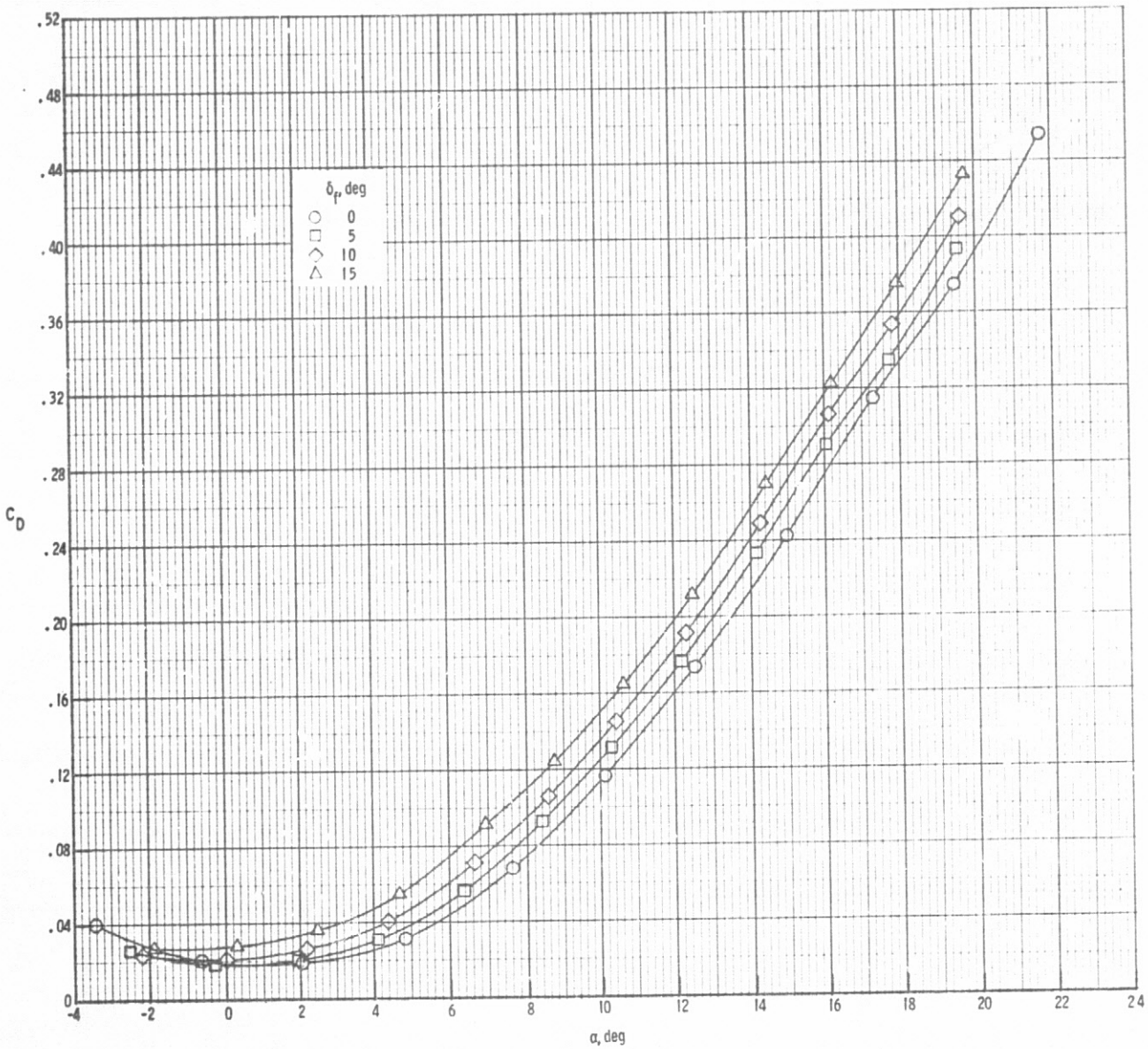

M = .85; δ_e = 0°

Figure 8. Continued.

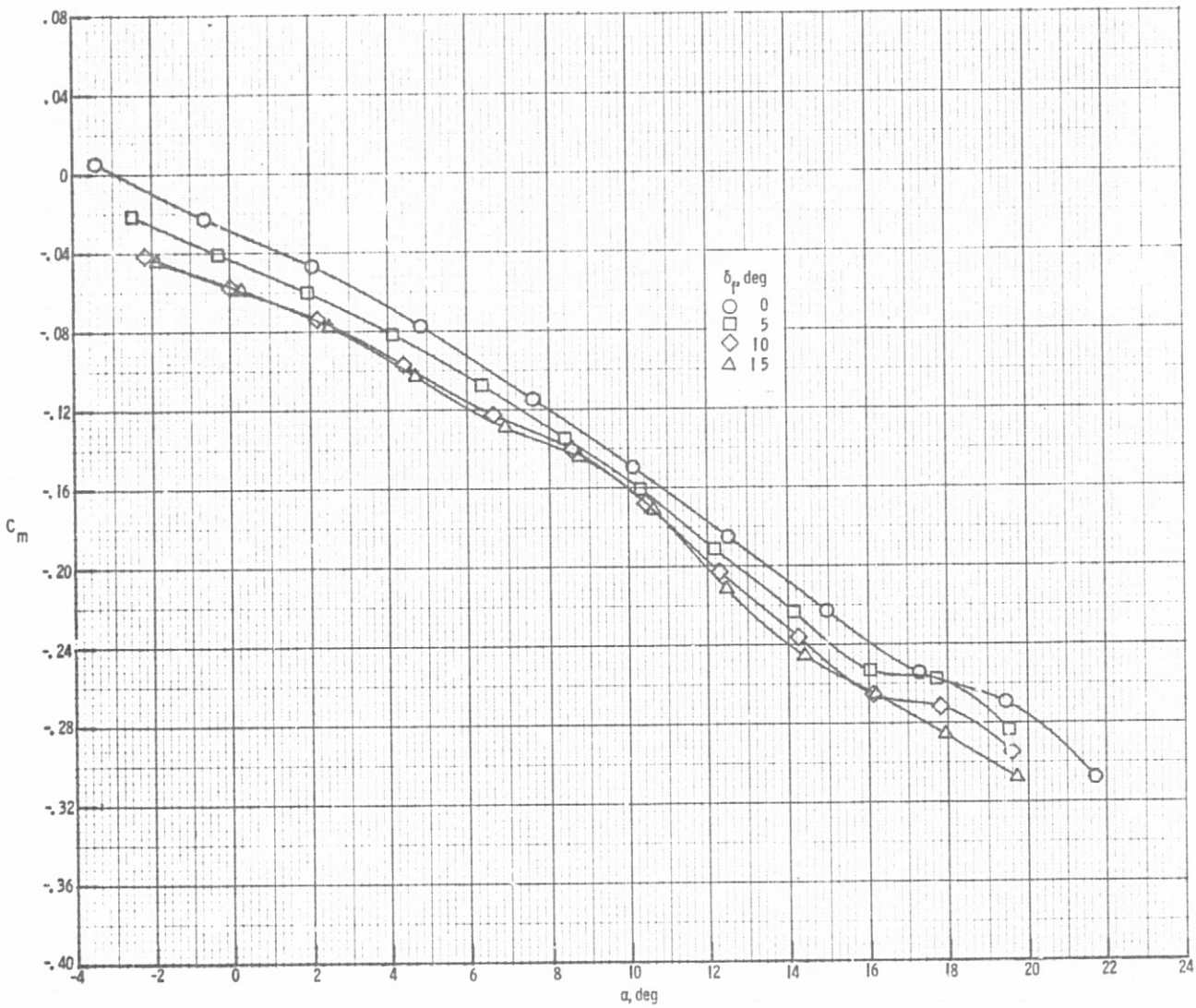

M = .85; δ_e = 0°

Figure 8. Continued.

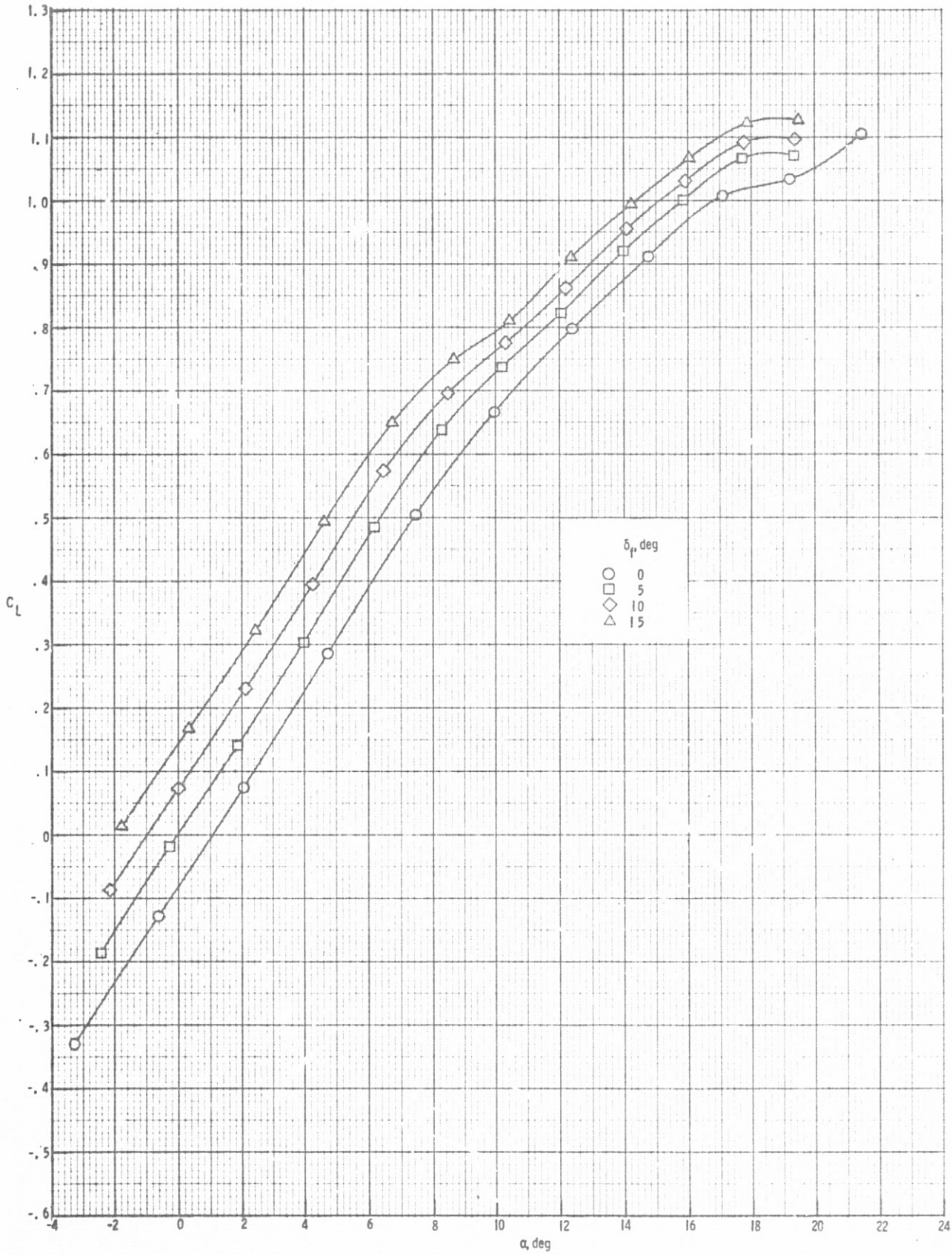

M = .80; $\delta_e = 0°$

Figure 8. Continued.

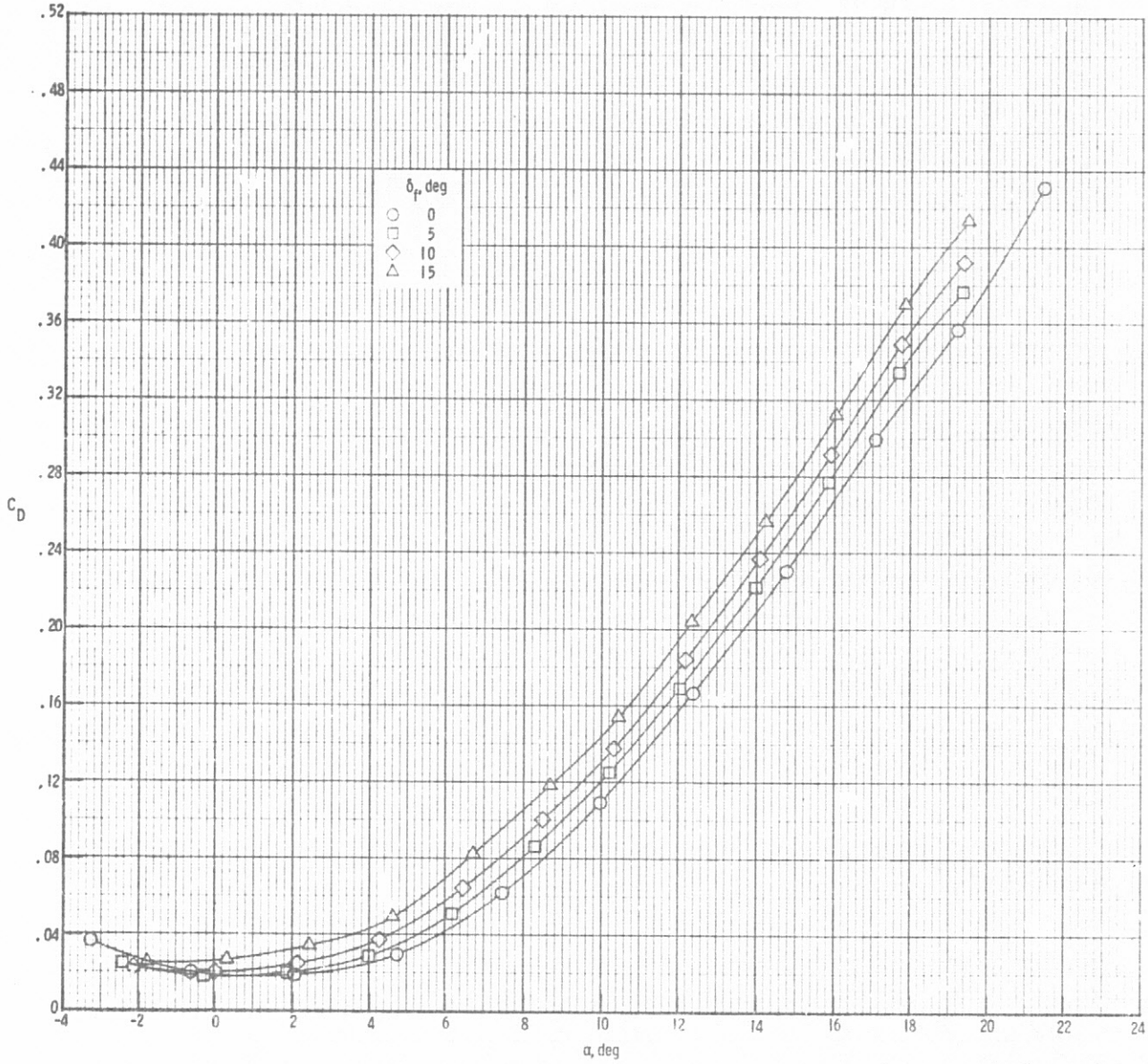

M = .80; $\delta_e = 0°$

Figure 8. Continued.

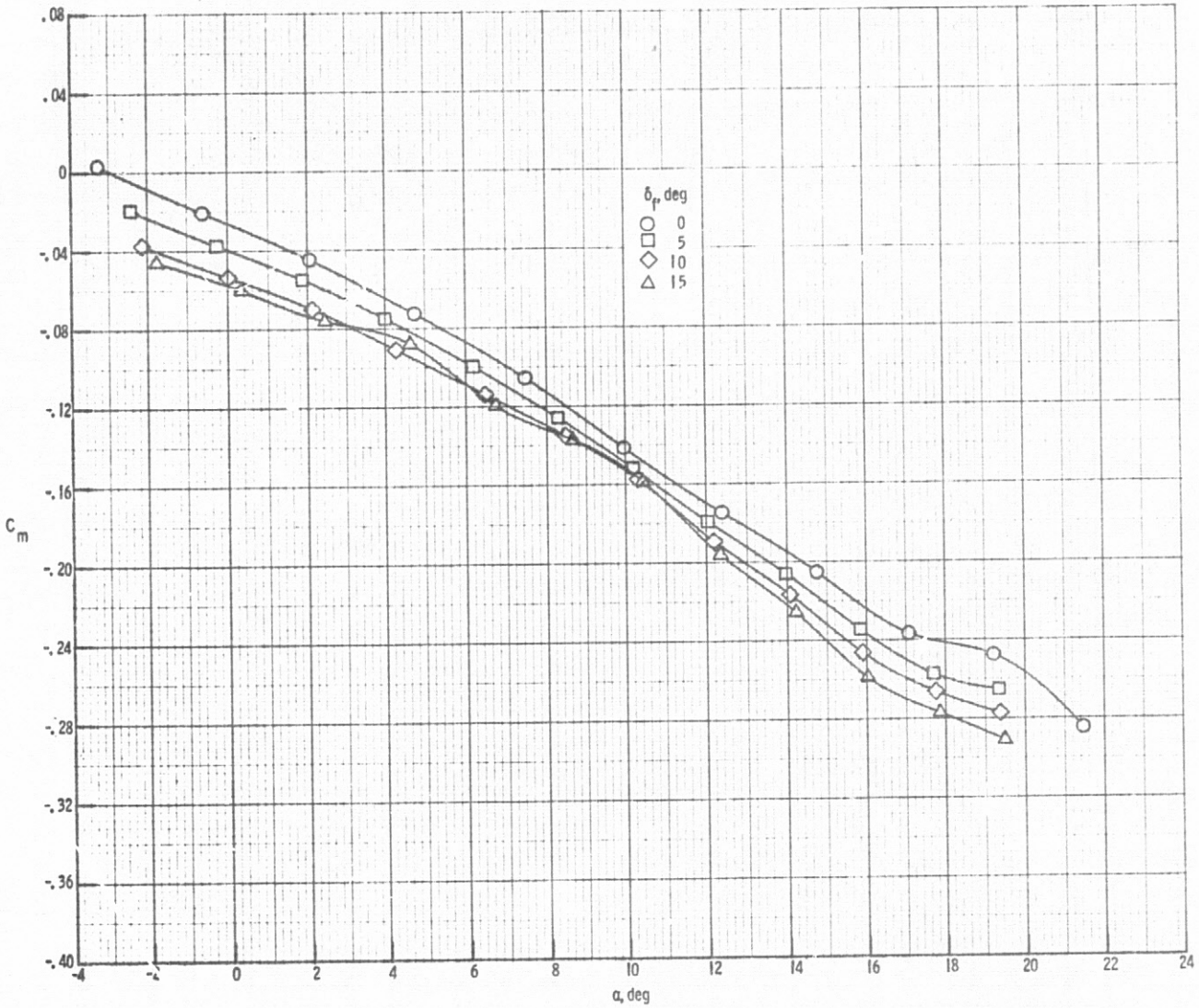

M = .80; δ_e = 0°

Figure 8. Continued.

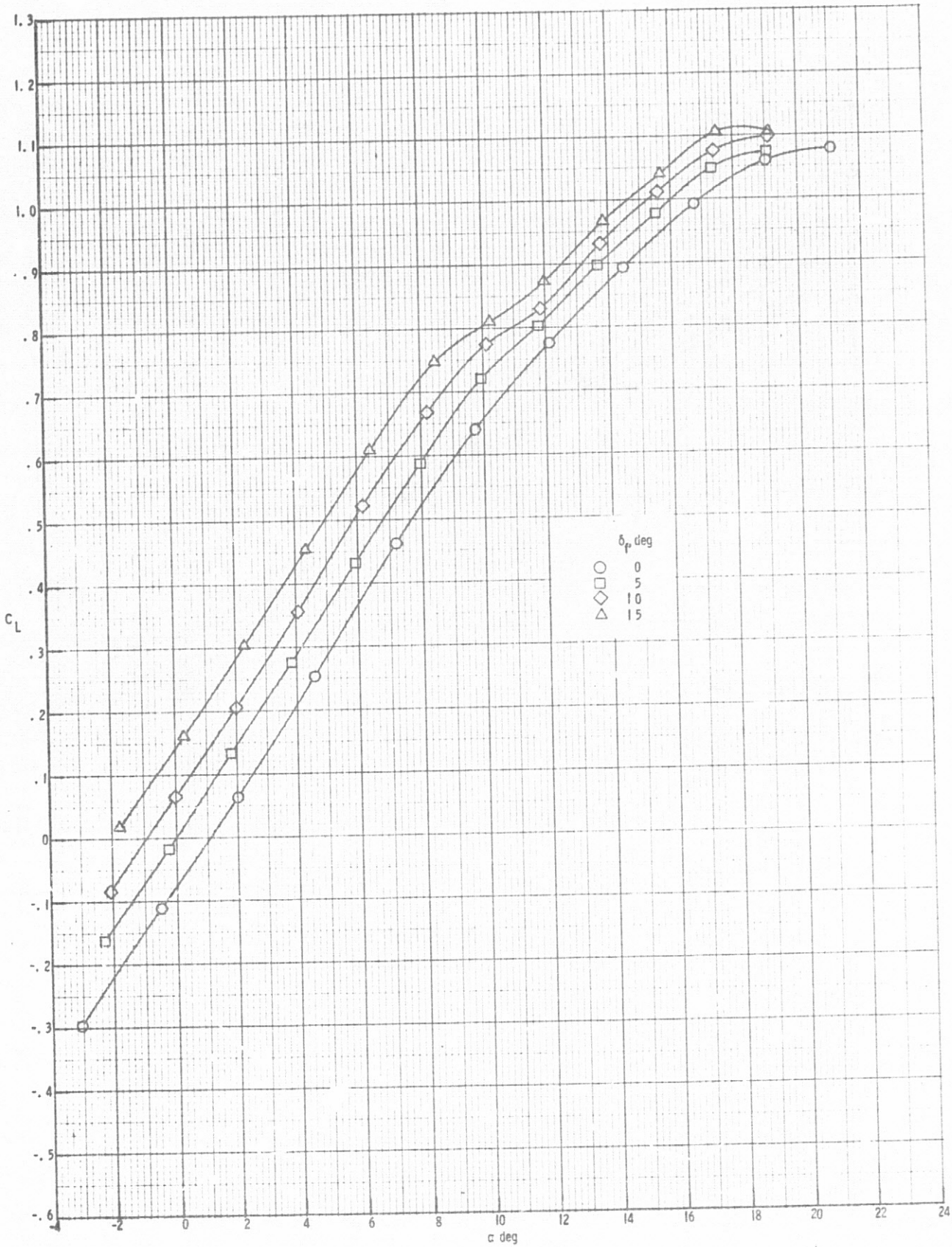

M = .70; δ_e = 0°

Figure 8. Continued

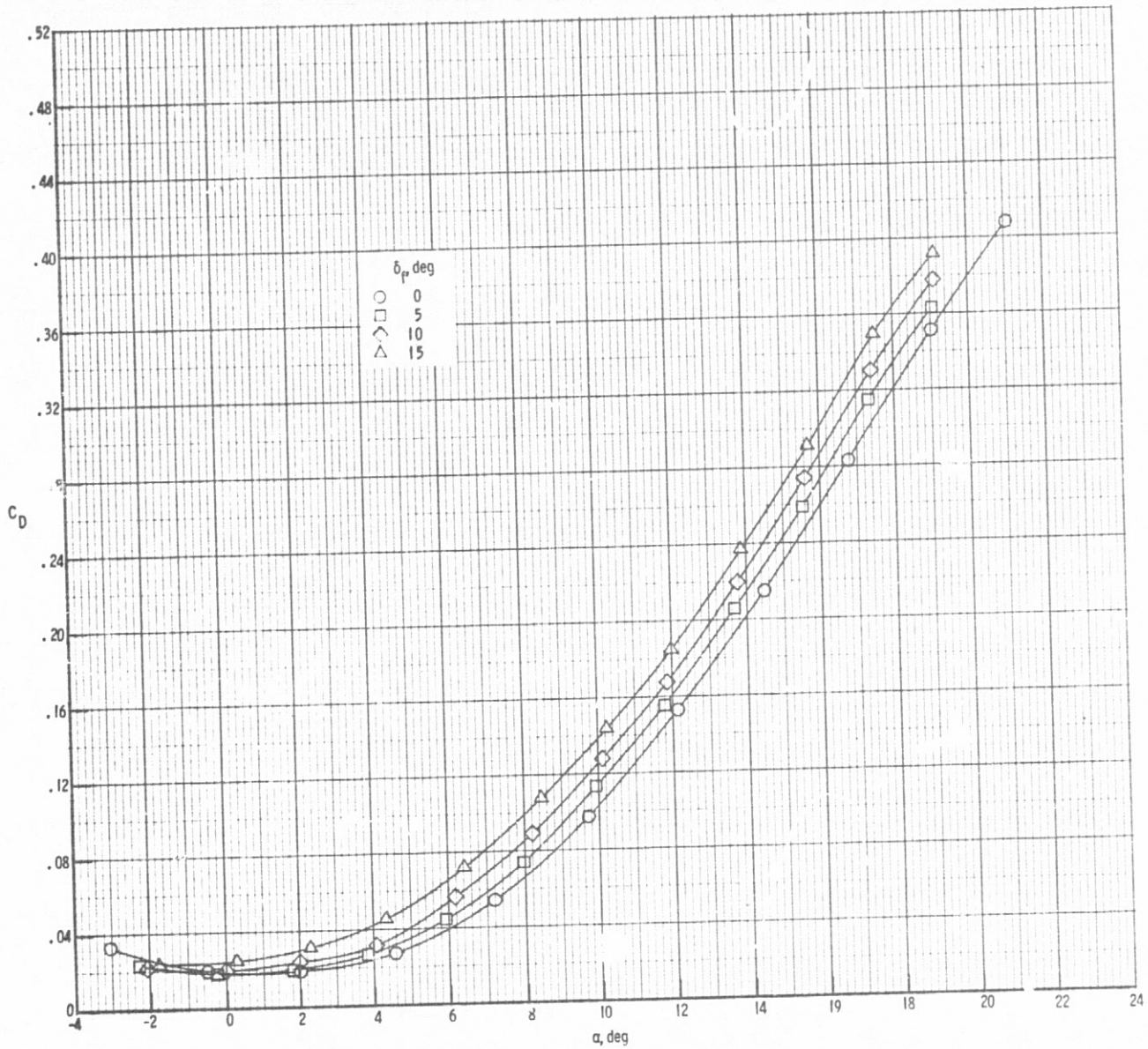

M = .70; δ_e = 0°

Figure 8. Continued.

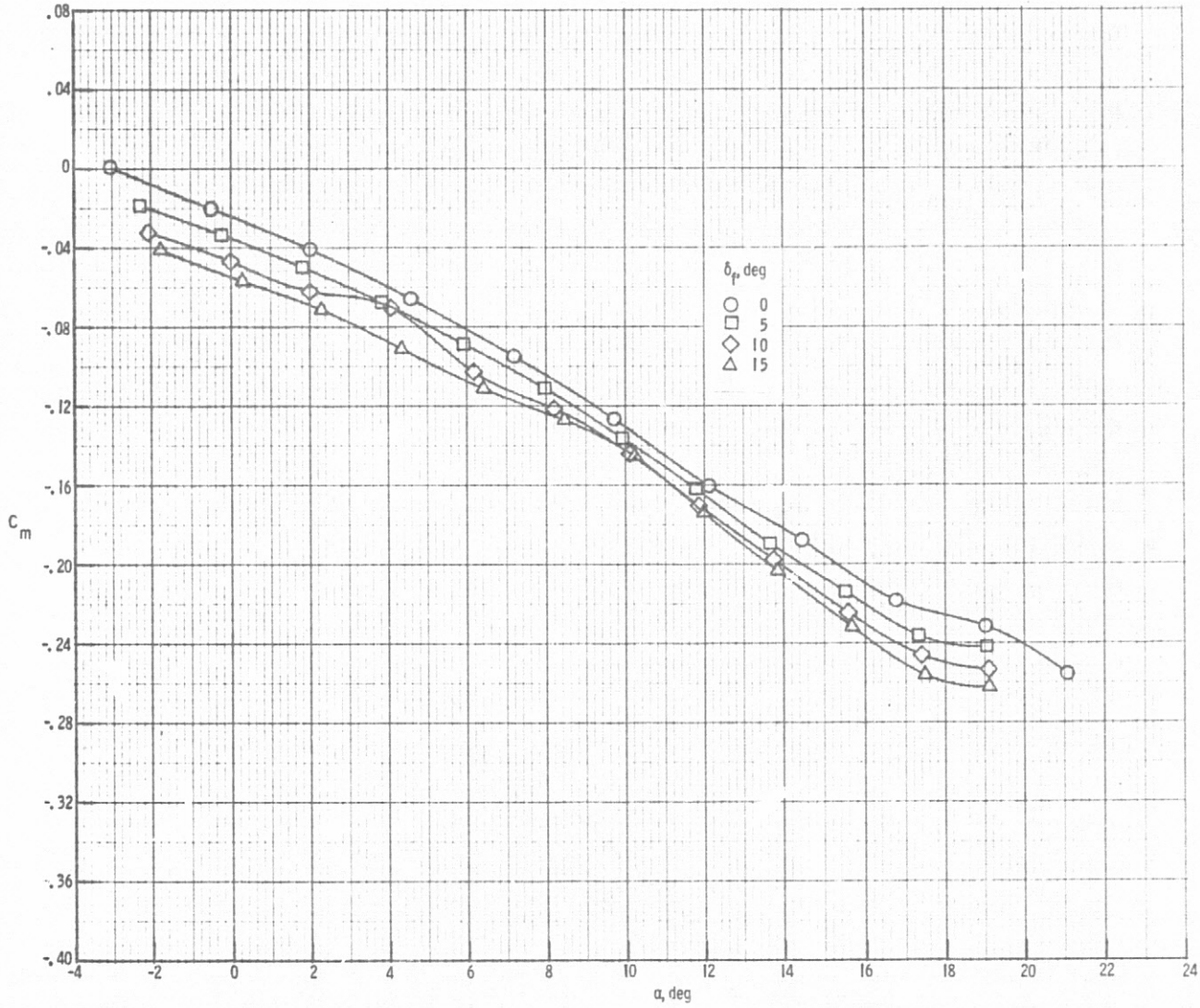

M = .70; δ_e = 0°

Figure 8. Concluded.

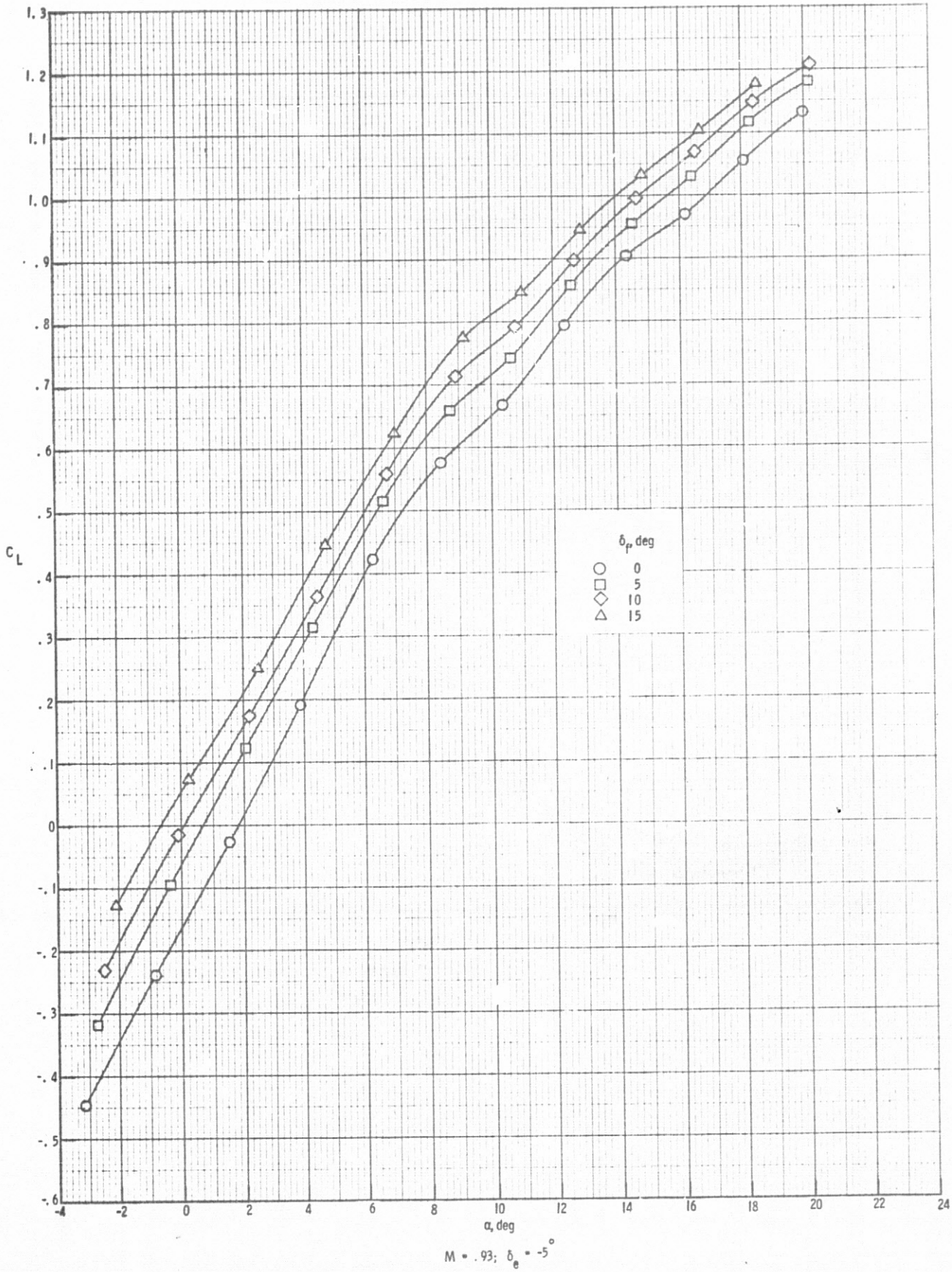

Figure 9. Effect of flap deflections on lift, drag, pitching moment coefficient. Horizontal tail is at minus five degree.

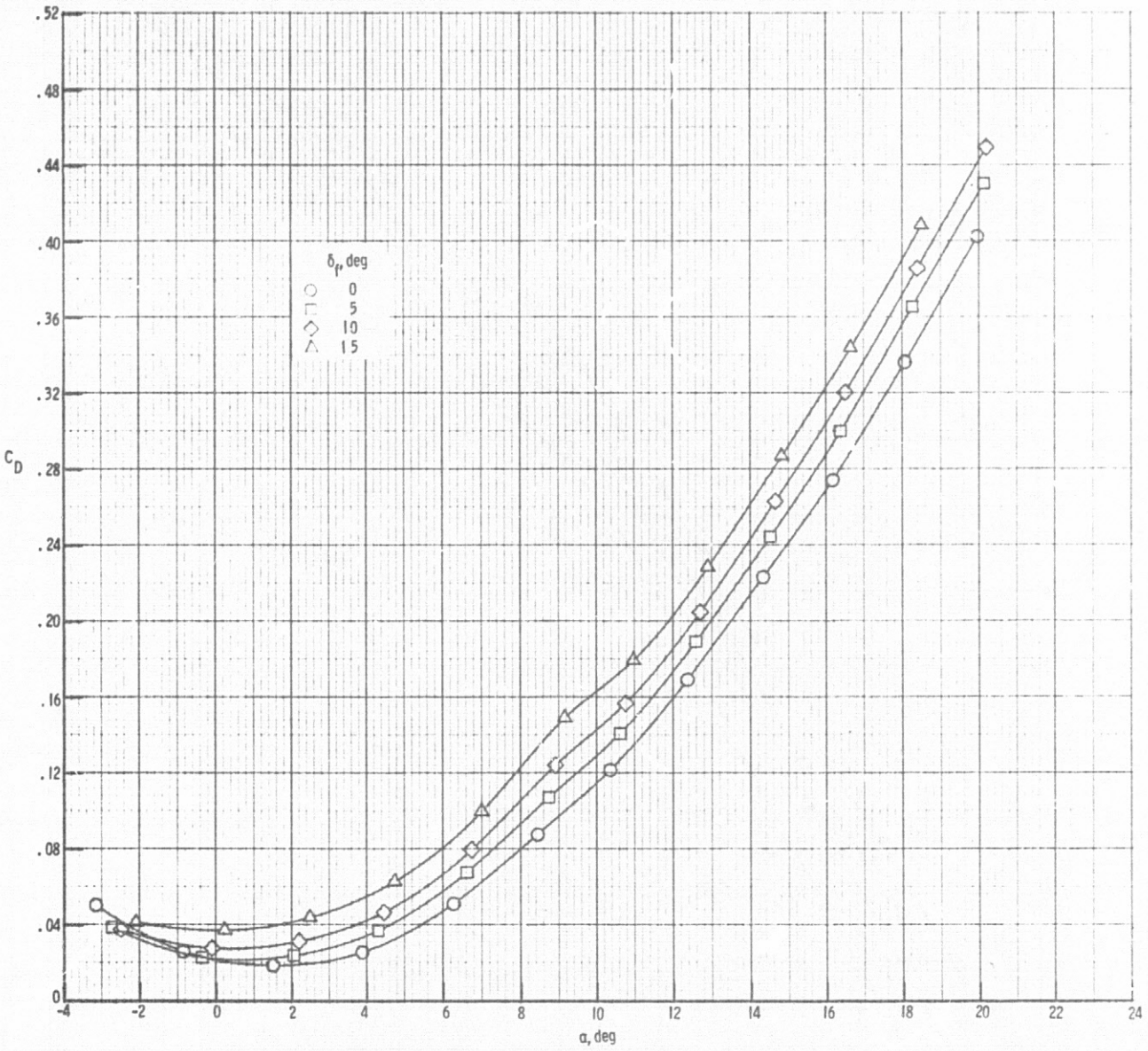

M = .93; $\delta_e = 0^\circ$

Figure 9. Continued.

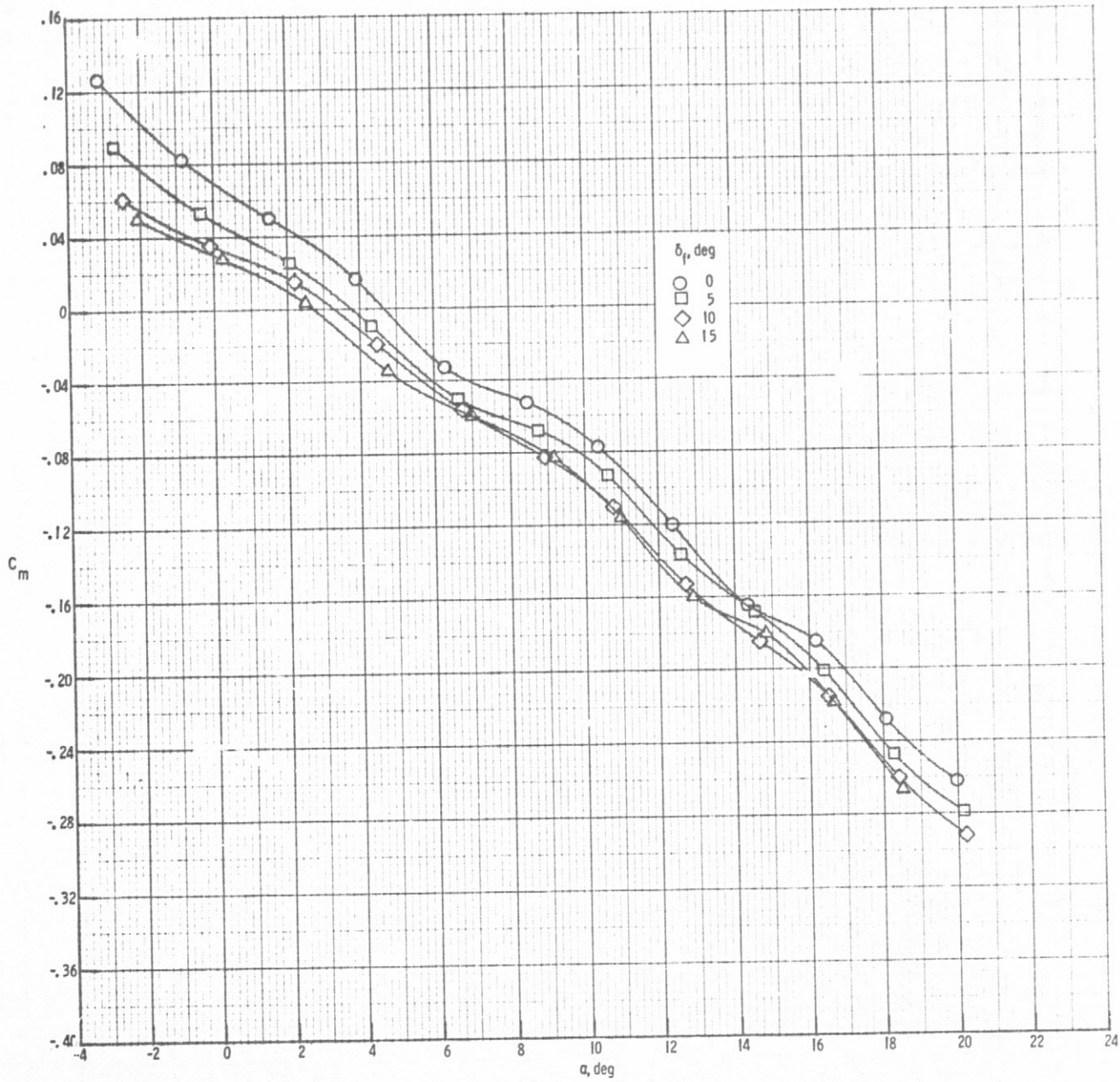

M = .93; δ_e = 0°

Figure 9. Continued.

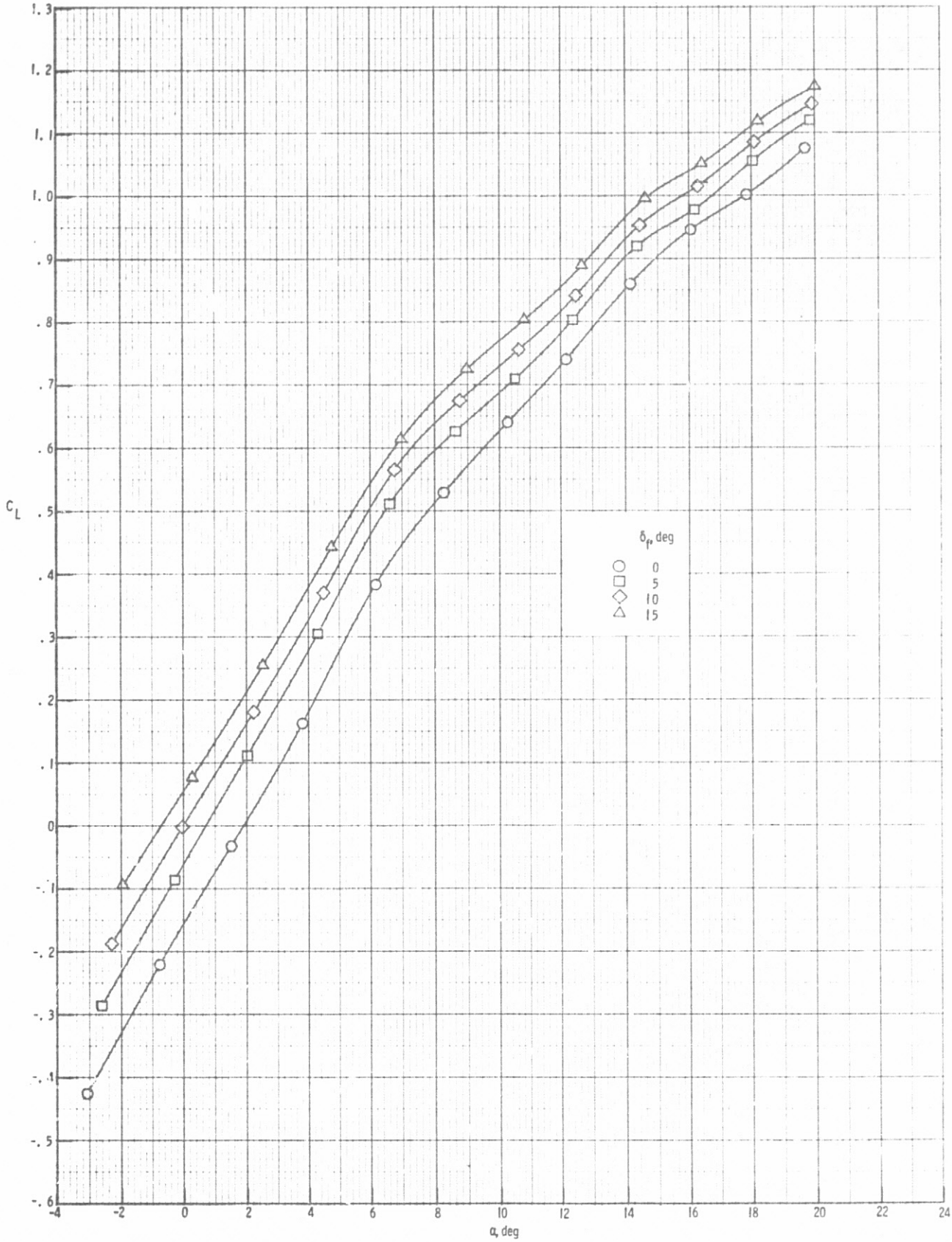

M = .90; δ_e = 0°

Figure 9. Continued.

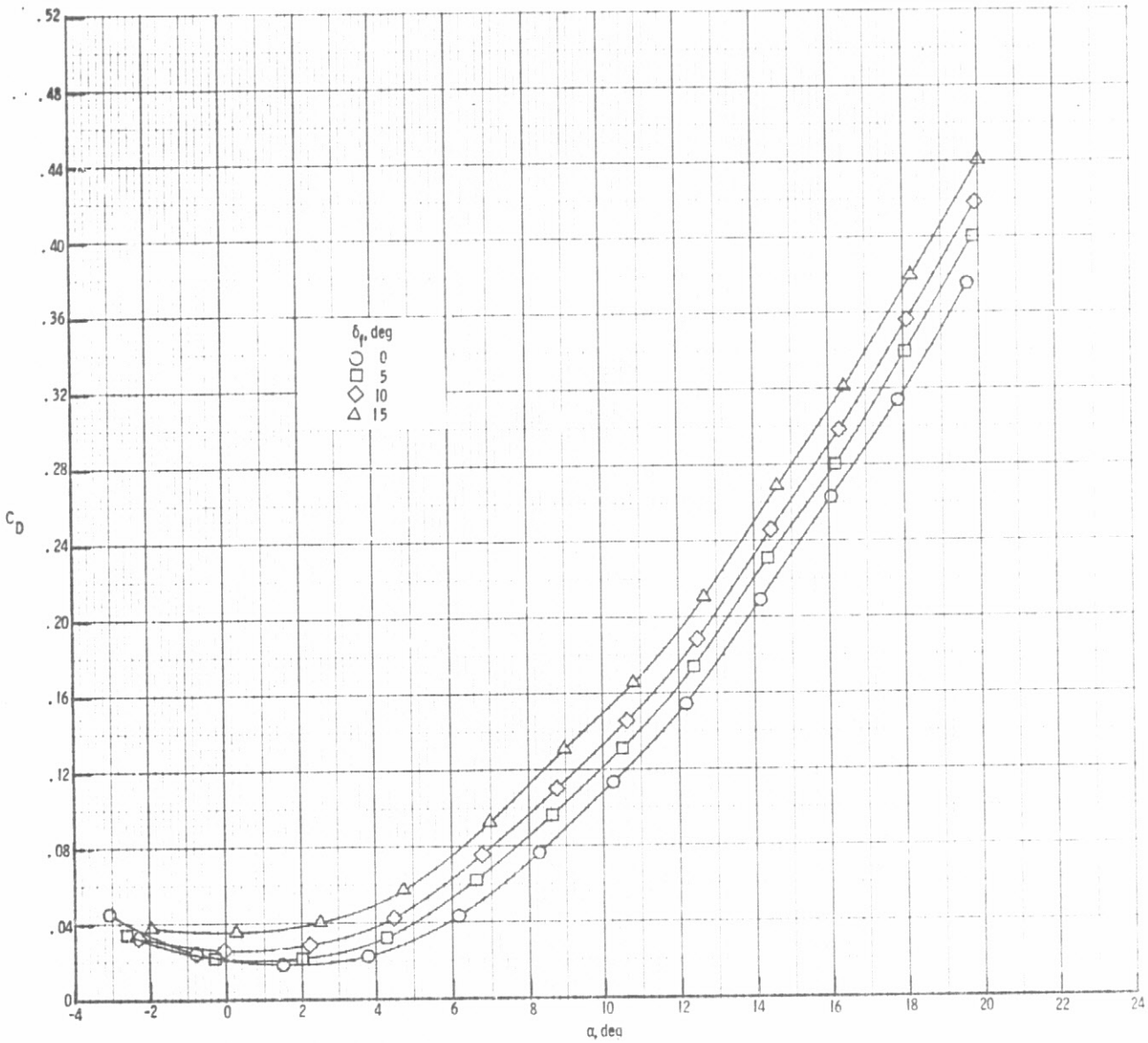

M = .90; $\delta_e = 0^\circ$

Figure 9. Continued.

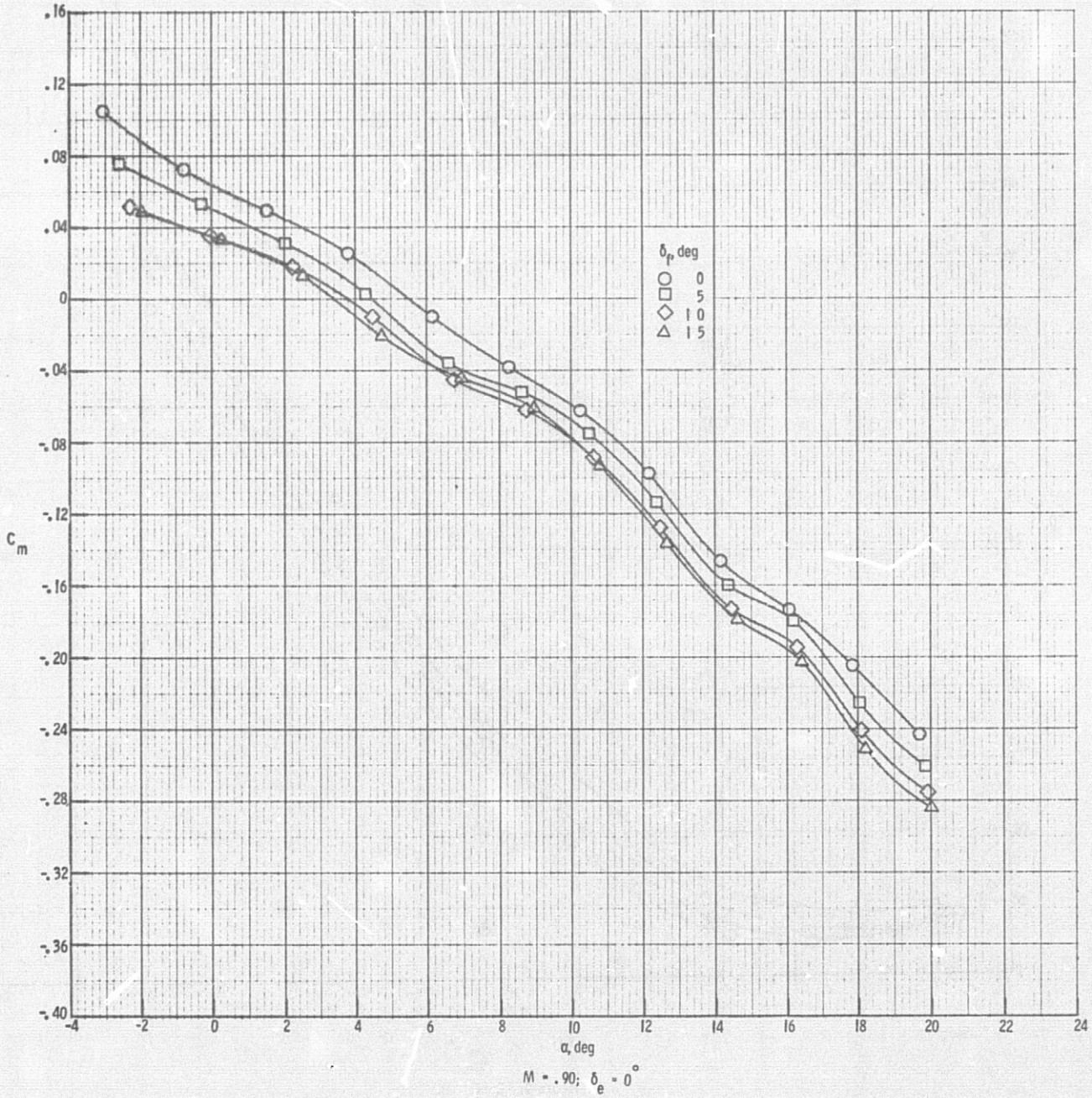

Figure 9. Continued.

C.2

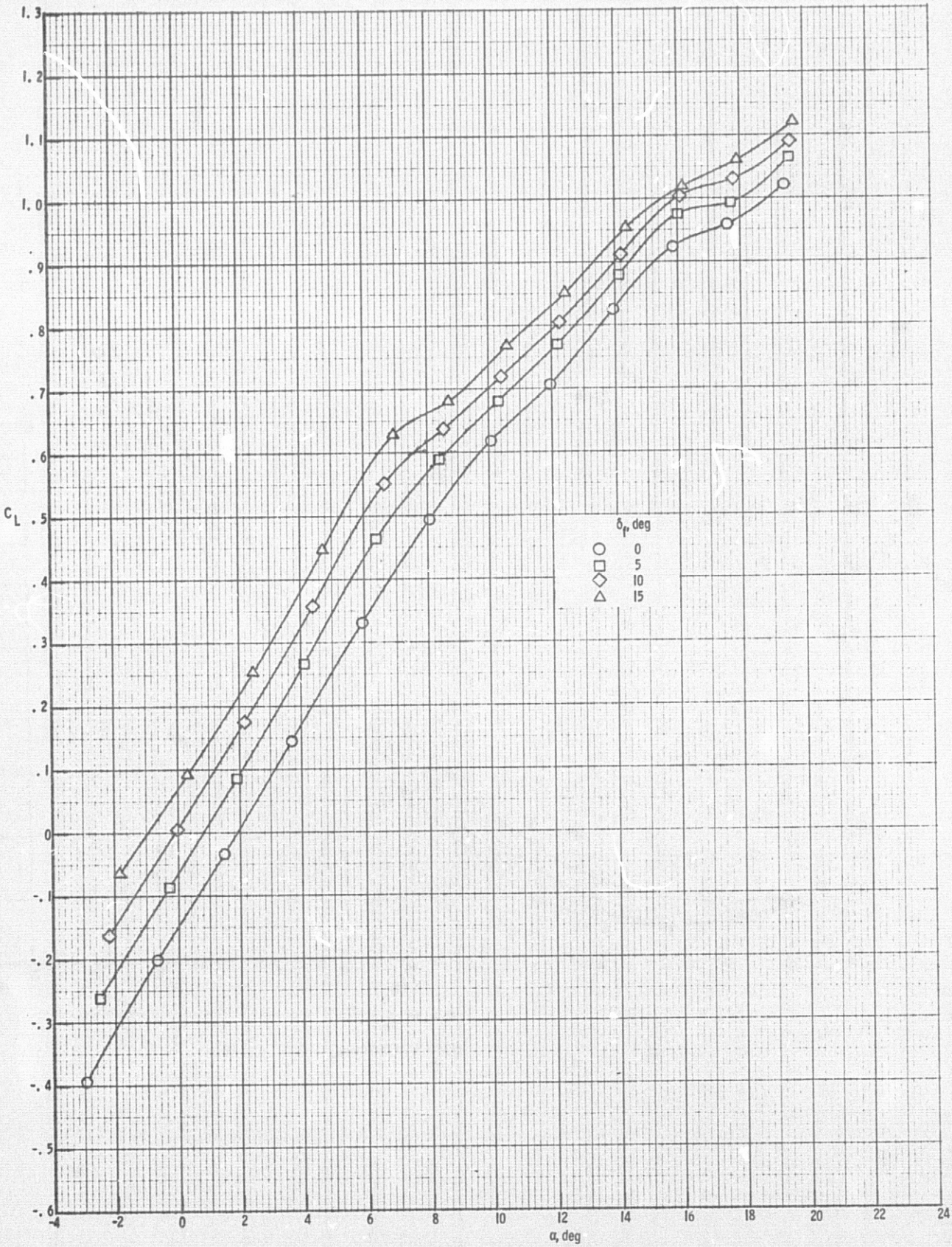

M = .85; $\delta_e = 0°$

Figure 9. Continued.

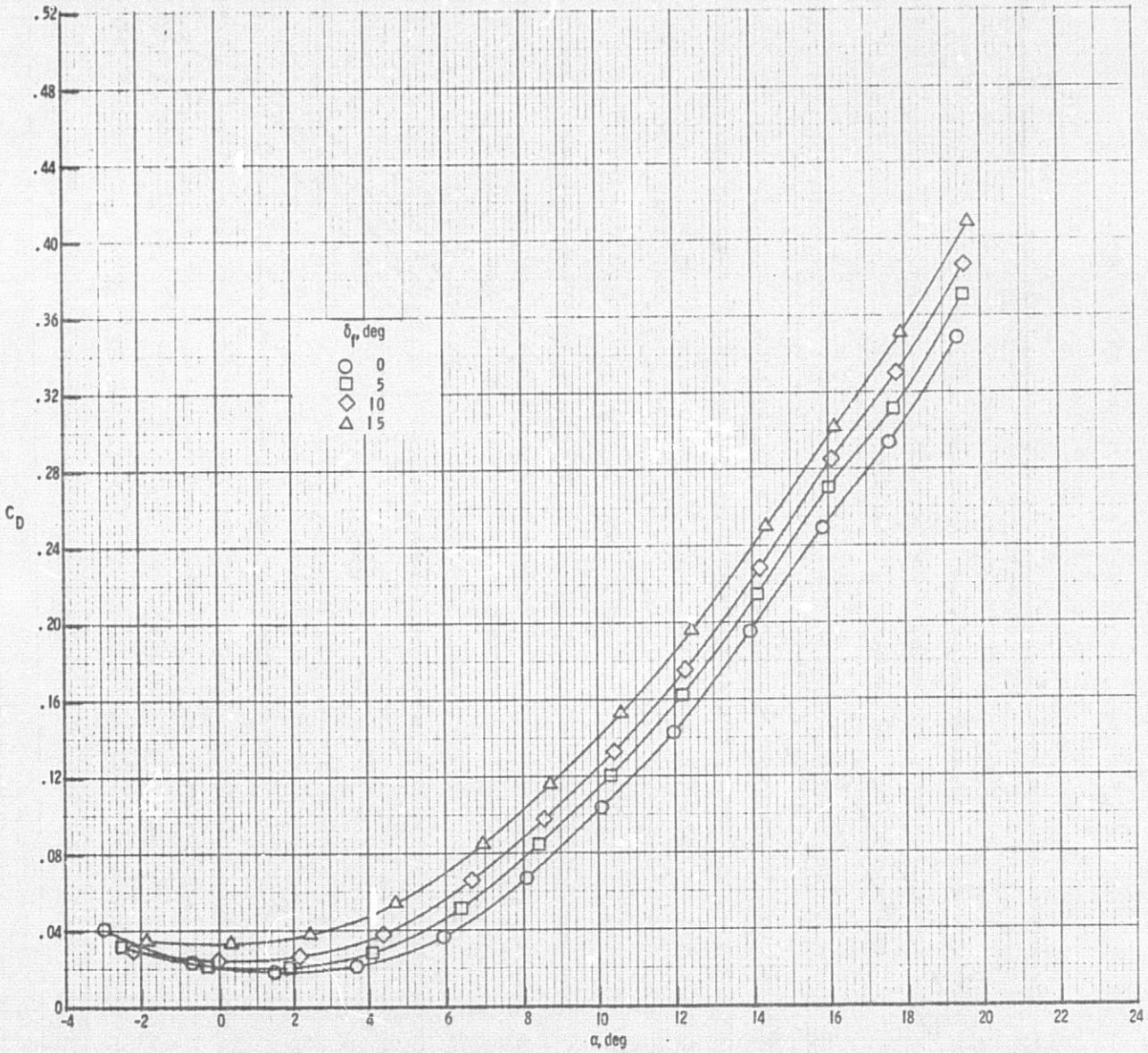

M = .85; $\delta_e = 0^\circ$

Figure 9. Continued.

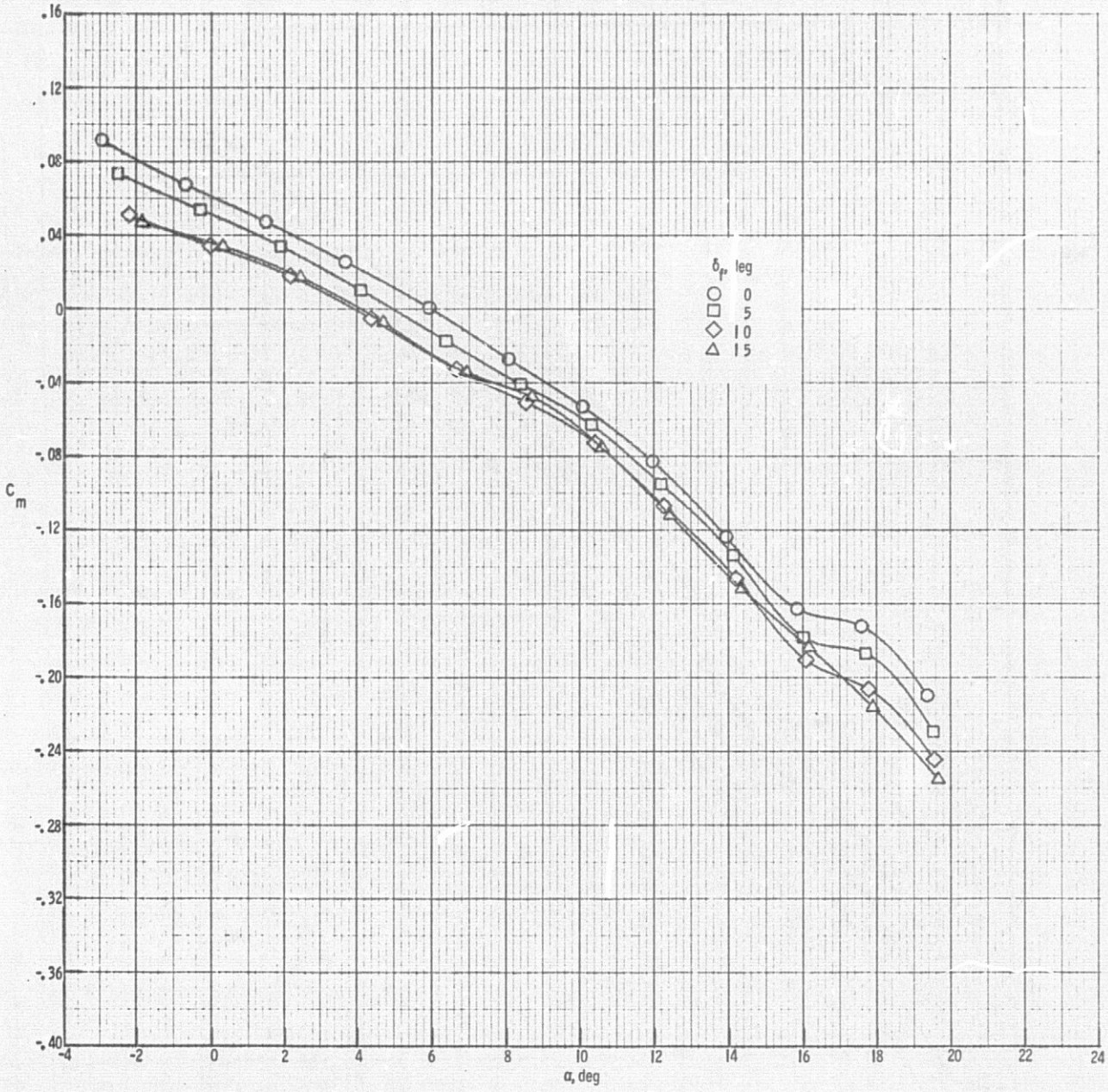

M = .85; $\delta_e = 0^\circ$

Figure 9. Continued.

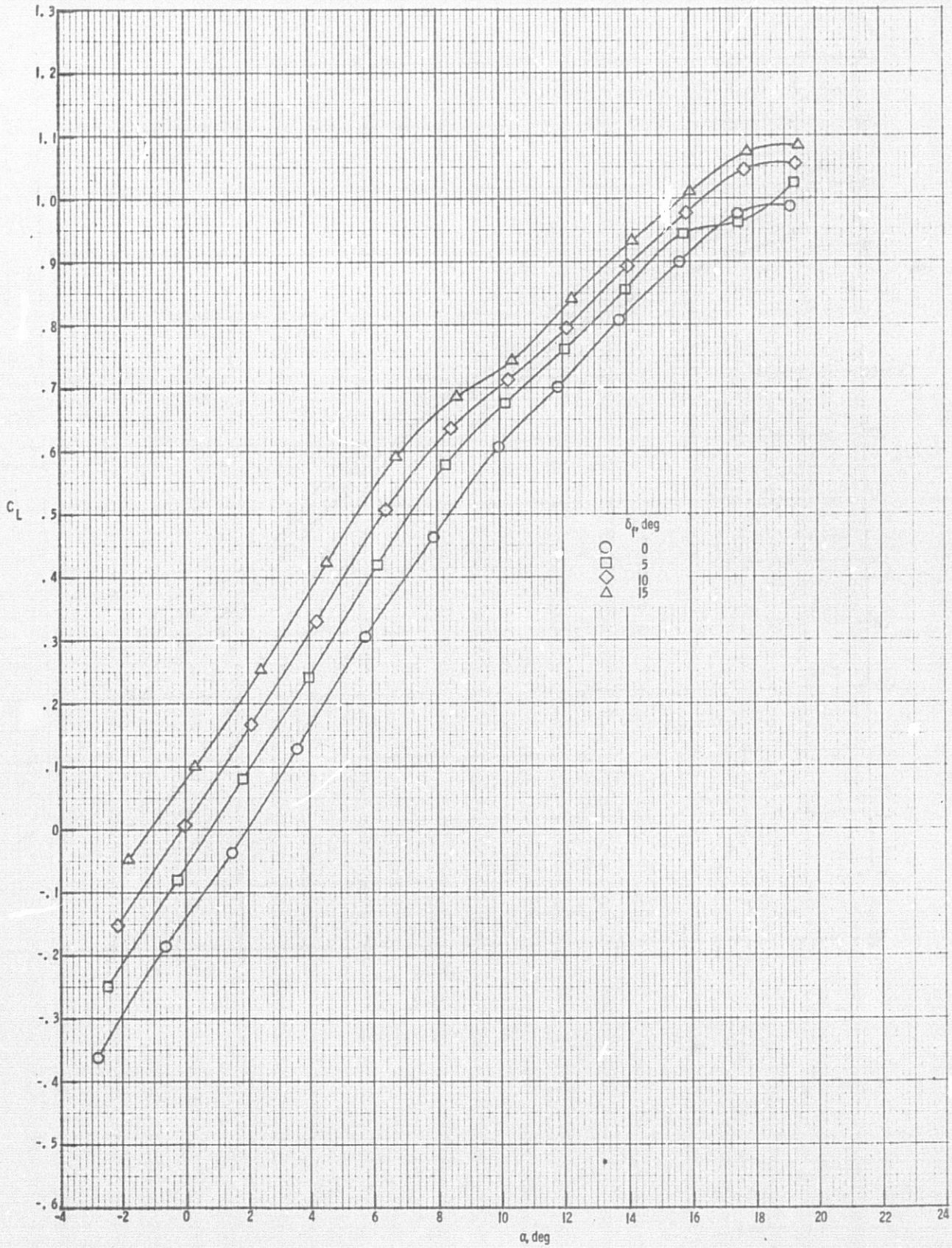

M = .80; $\delta_e = 0^\circ$

Figure 9. Continued.

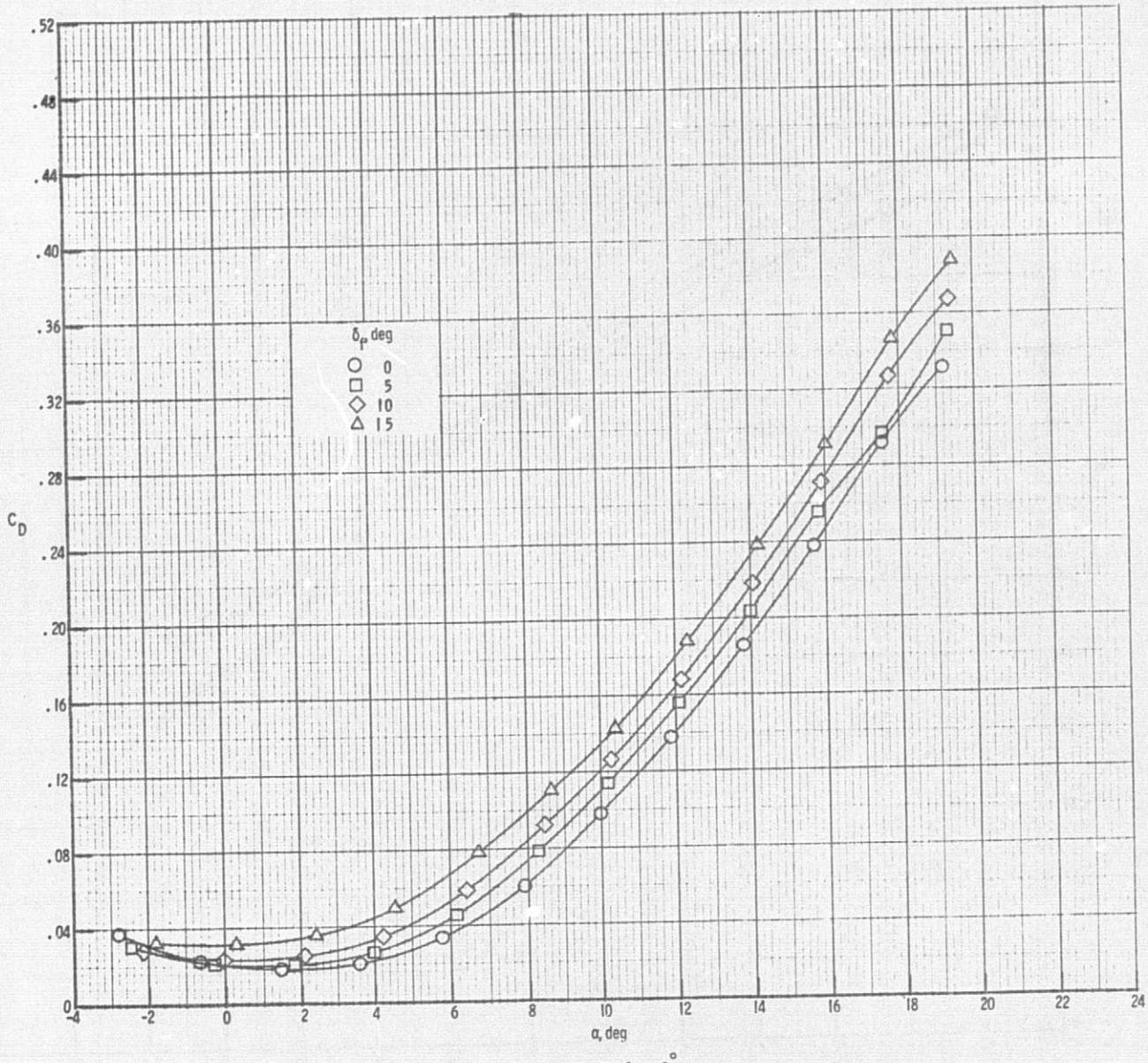

M = .80; $\delta_e = 0^\circ$

Figure 9. Continued.

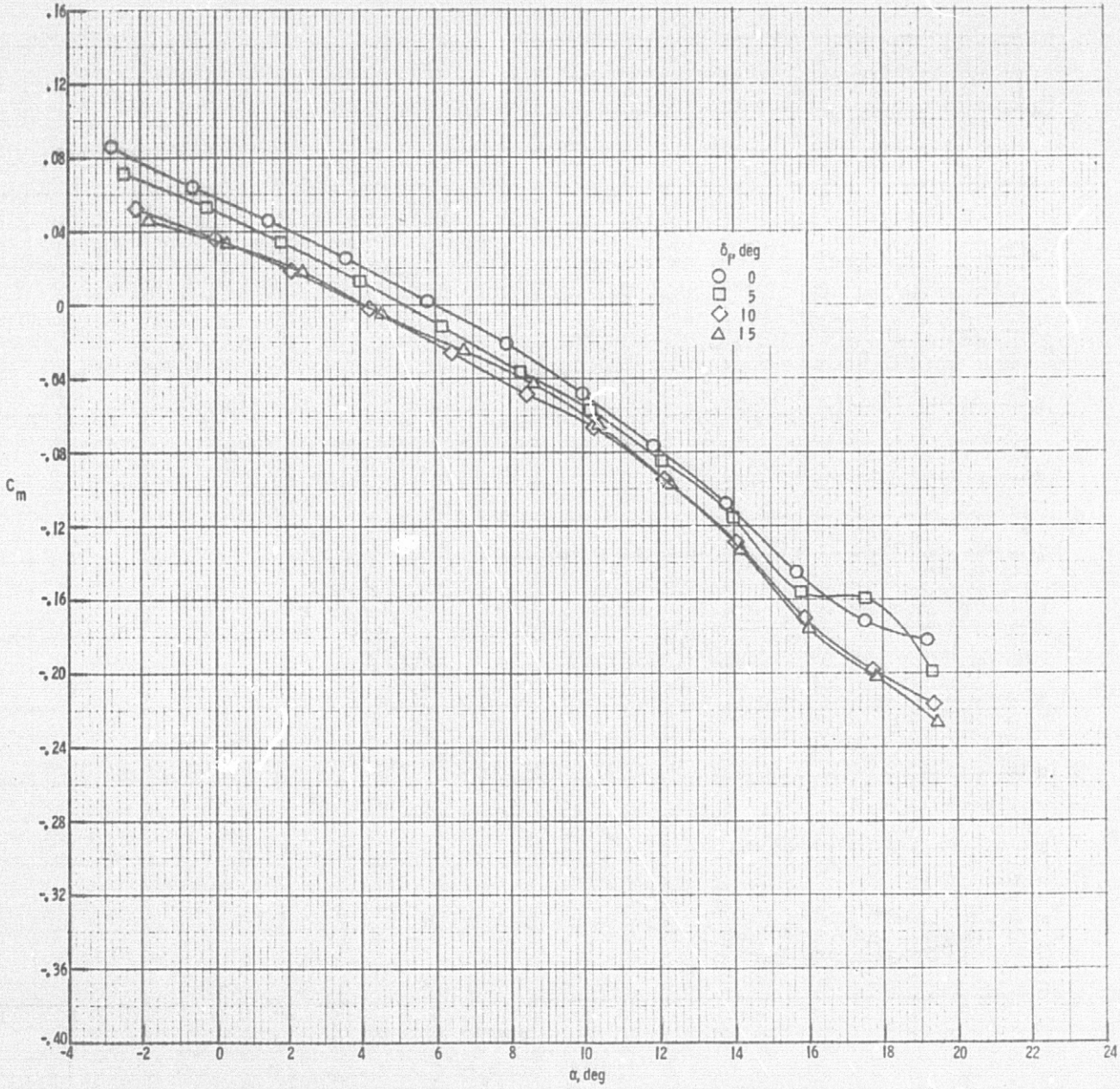

M = .80; $\delta_e = 0^\circ$

Figure 9. Continued.

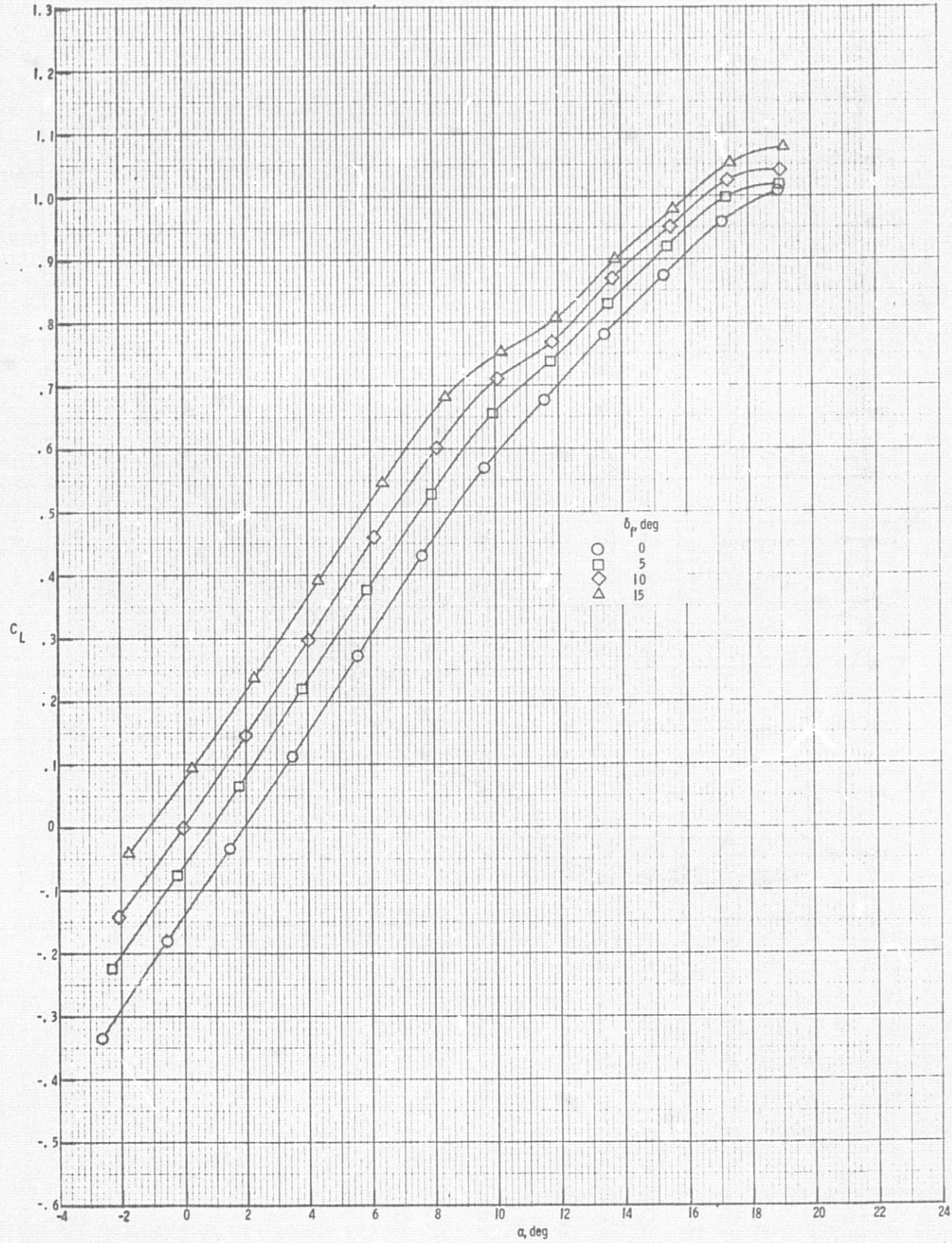

$M = .70$; $\delta_e = 0^\circ$

Figure 9. Continued.

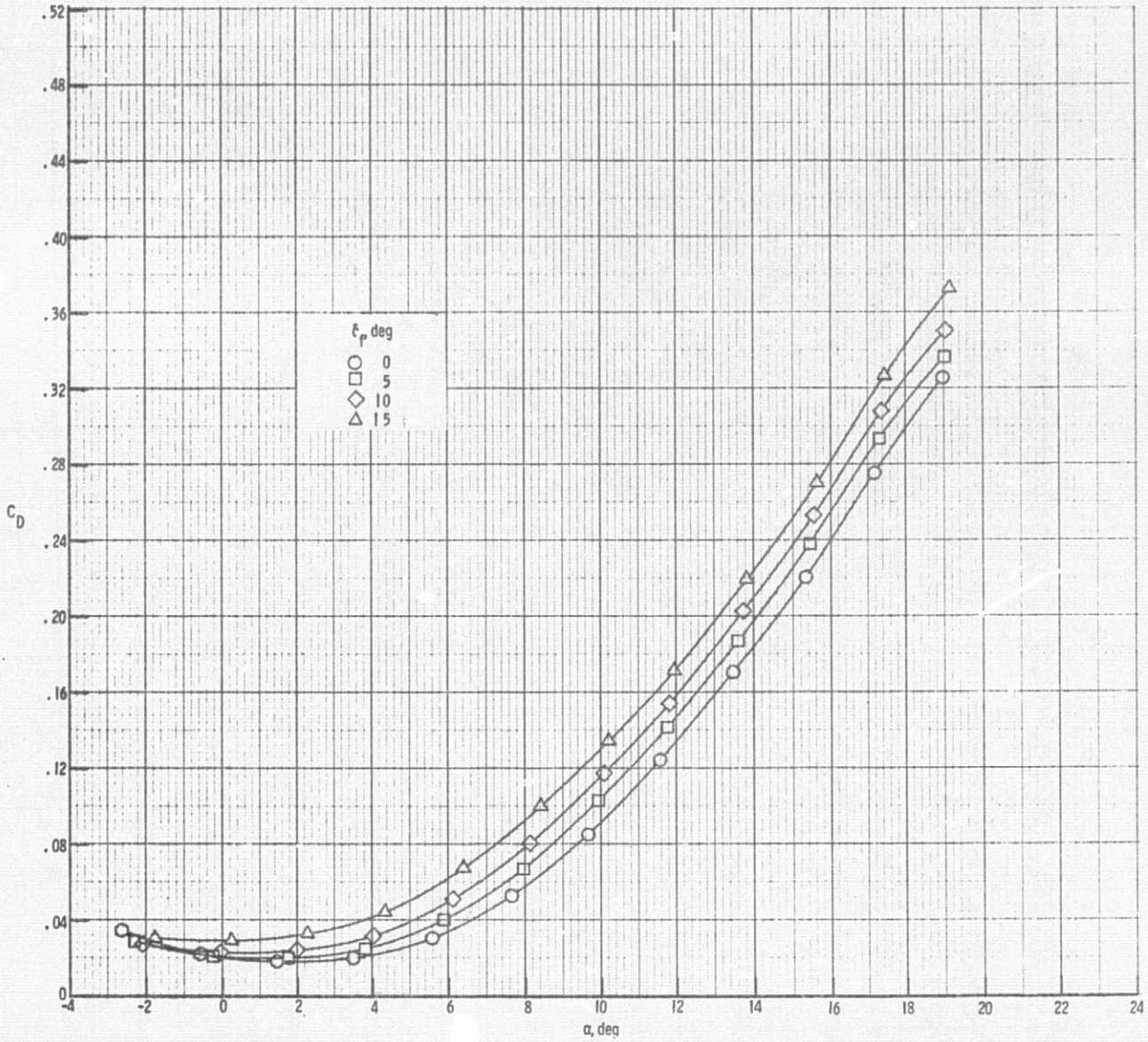

M = .70; $\delta_e = 0^\circ$

Figure 9. Continued.

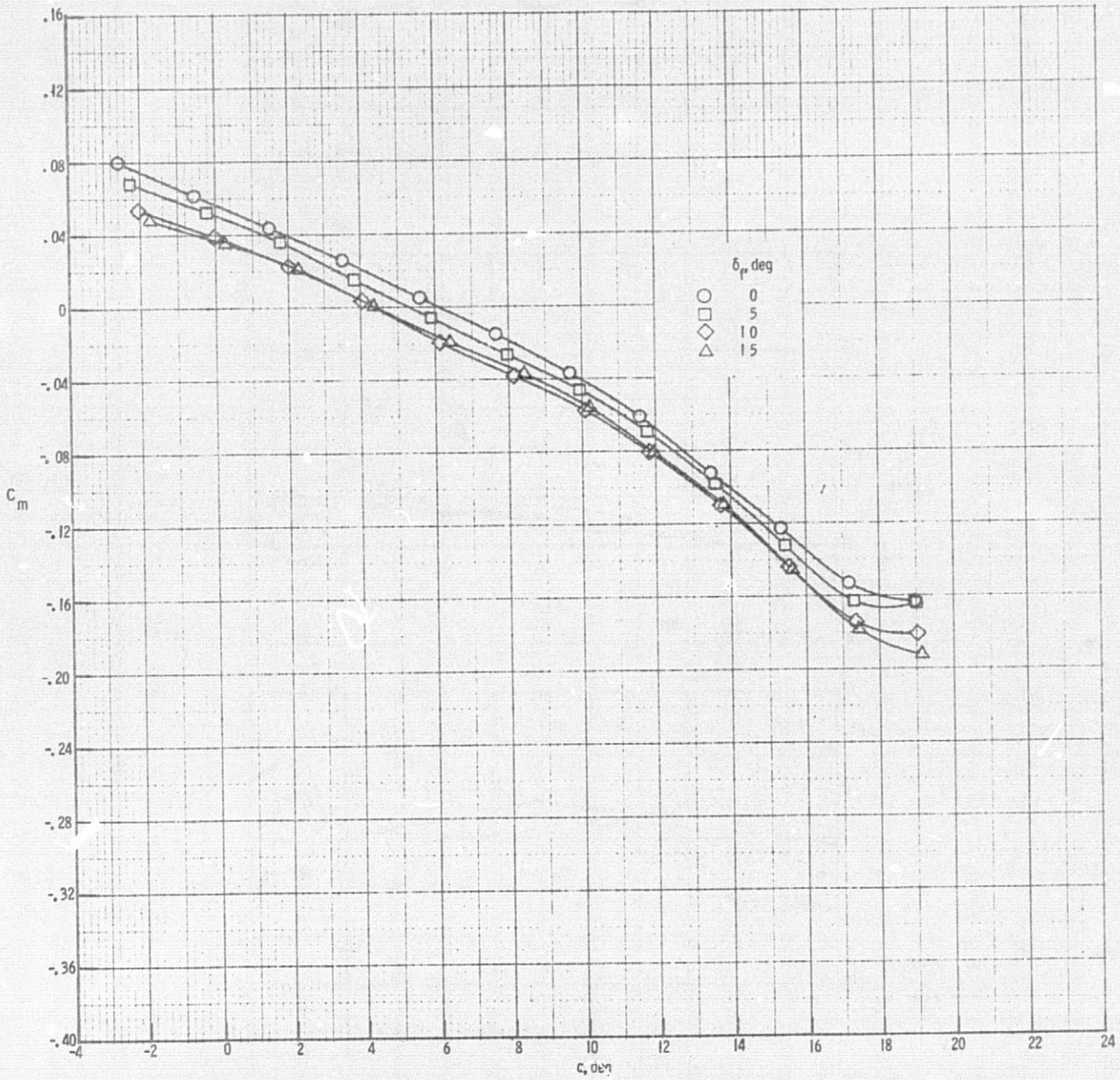

M = .70; δ_e = 0°

Figure 9. Concluded.

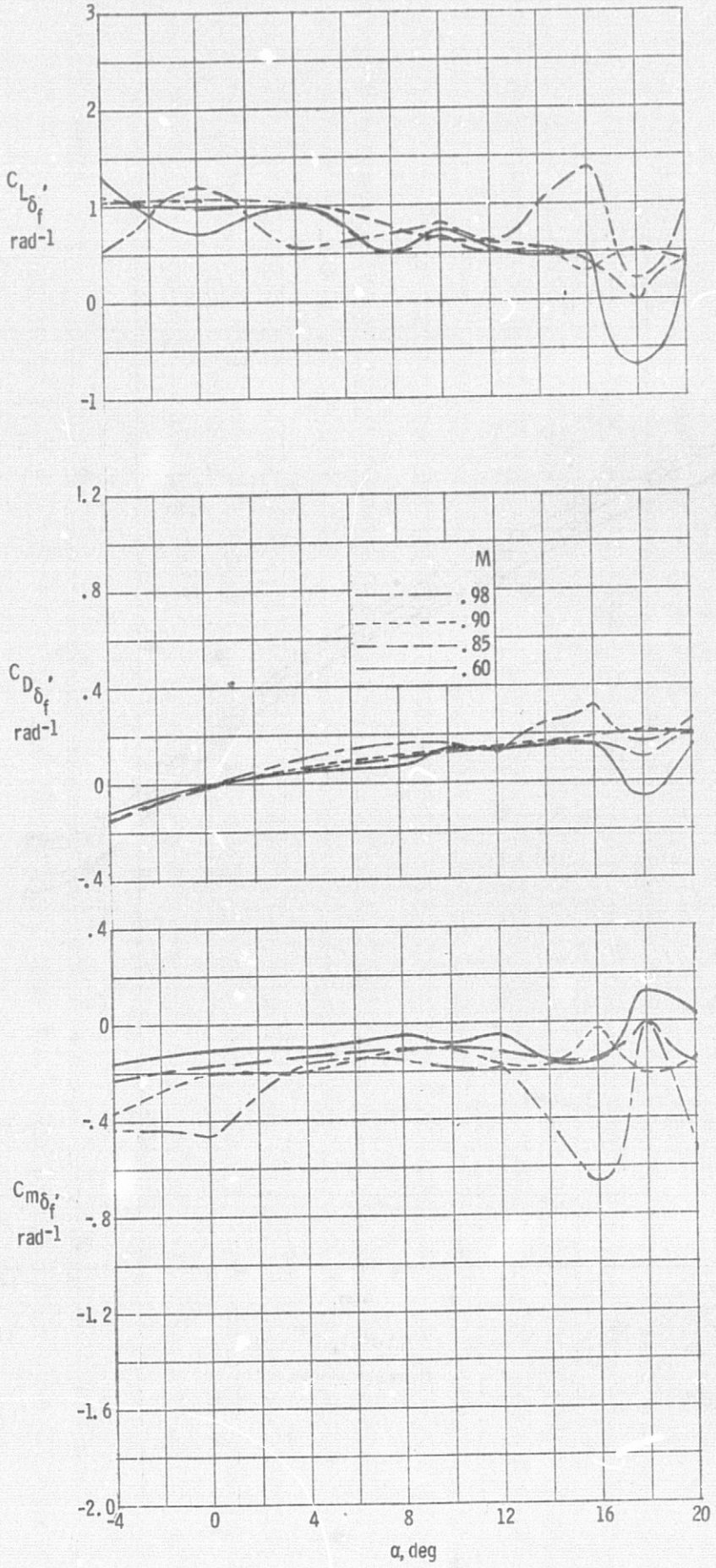

Figure 10. Summary of flap effectiveness.

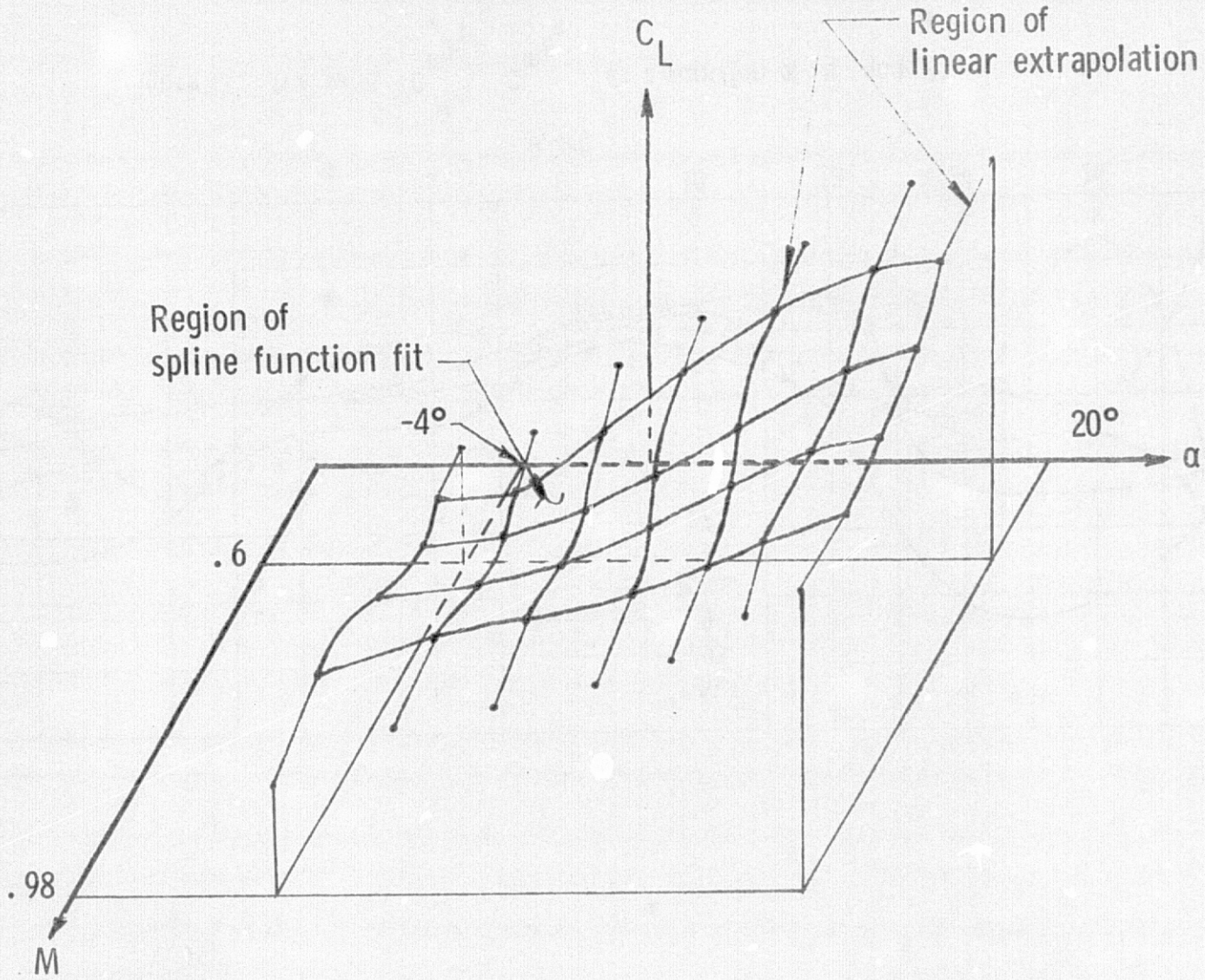

Figure II. Curve fitting and extrapolation scheme.

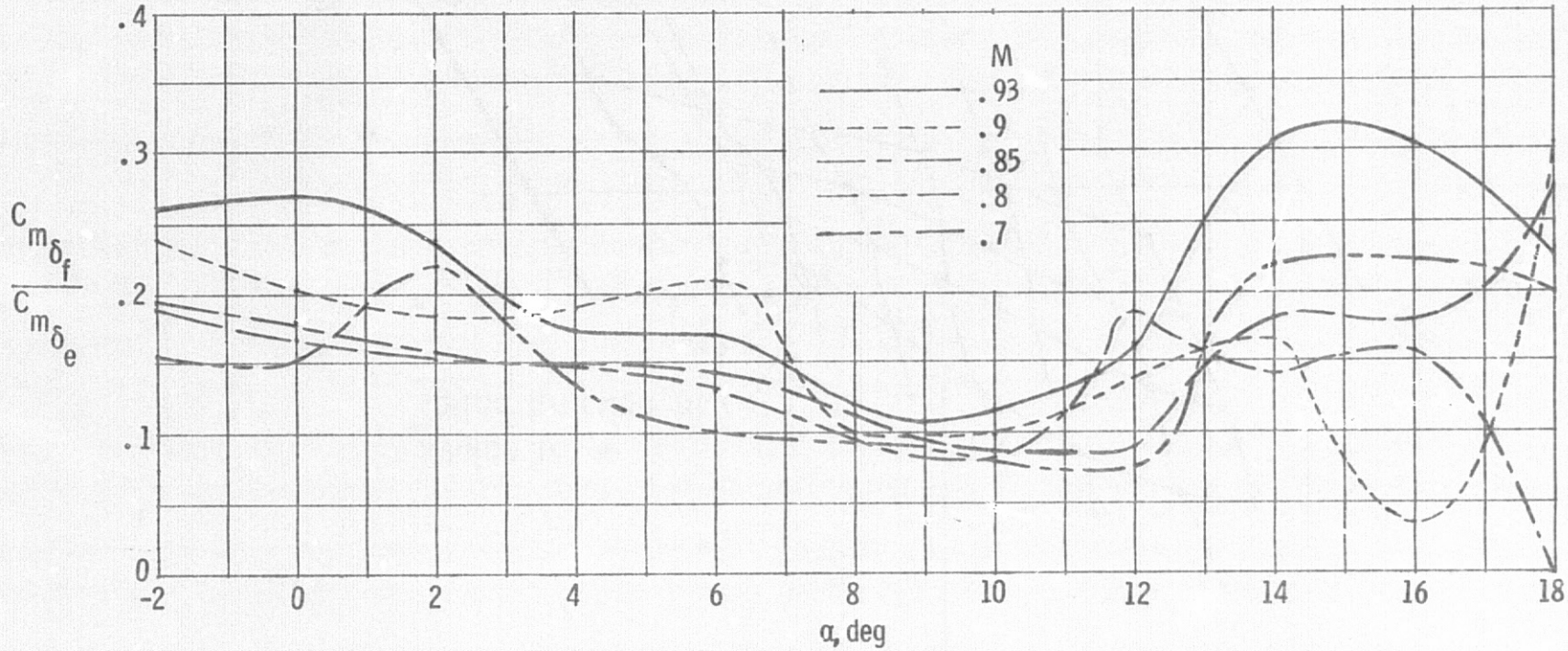

Figure 12. The ratio $\frac{C_{m_{\delta_f}}}{C_{m_{\delta_e}}}$ as a function of α and M.

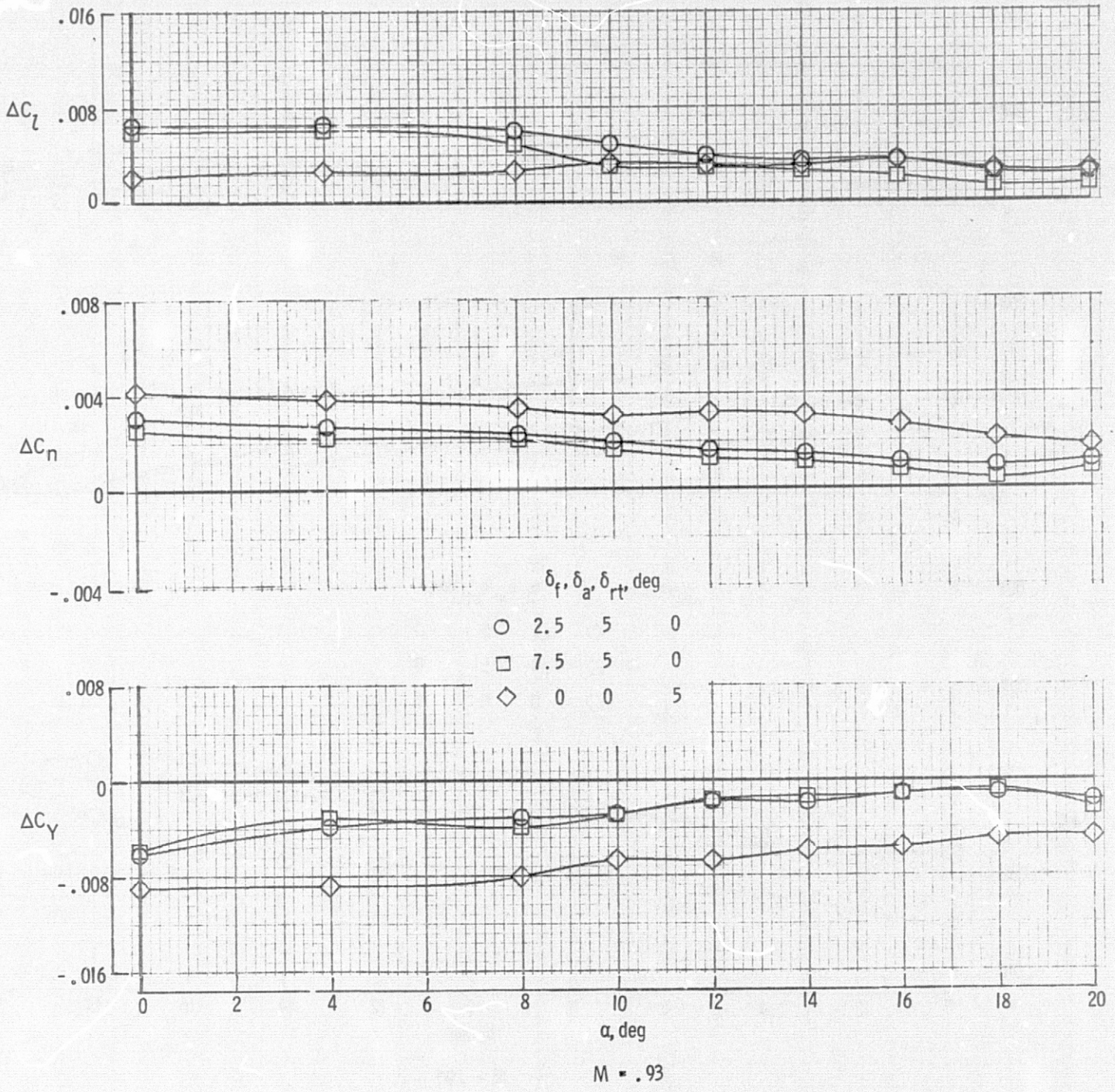

Figure 13. The effect of symmetric displacement of the ailerons on lateral-directional characteristics. Also note effectiveness of rolling tail (mean horizontal displacement, $\delta_e = -7.5^\circ$).

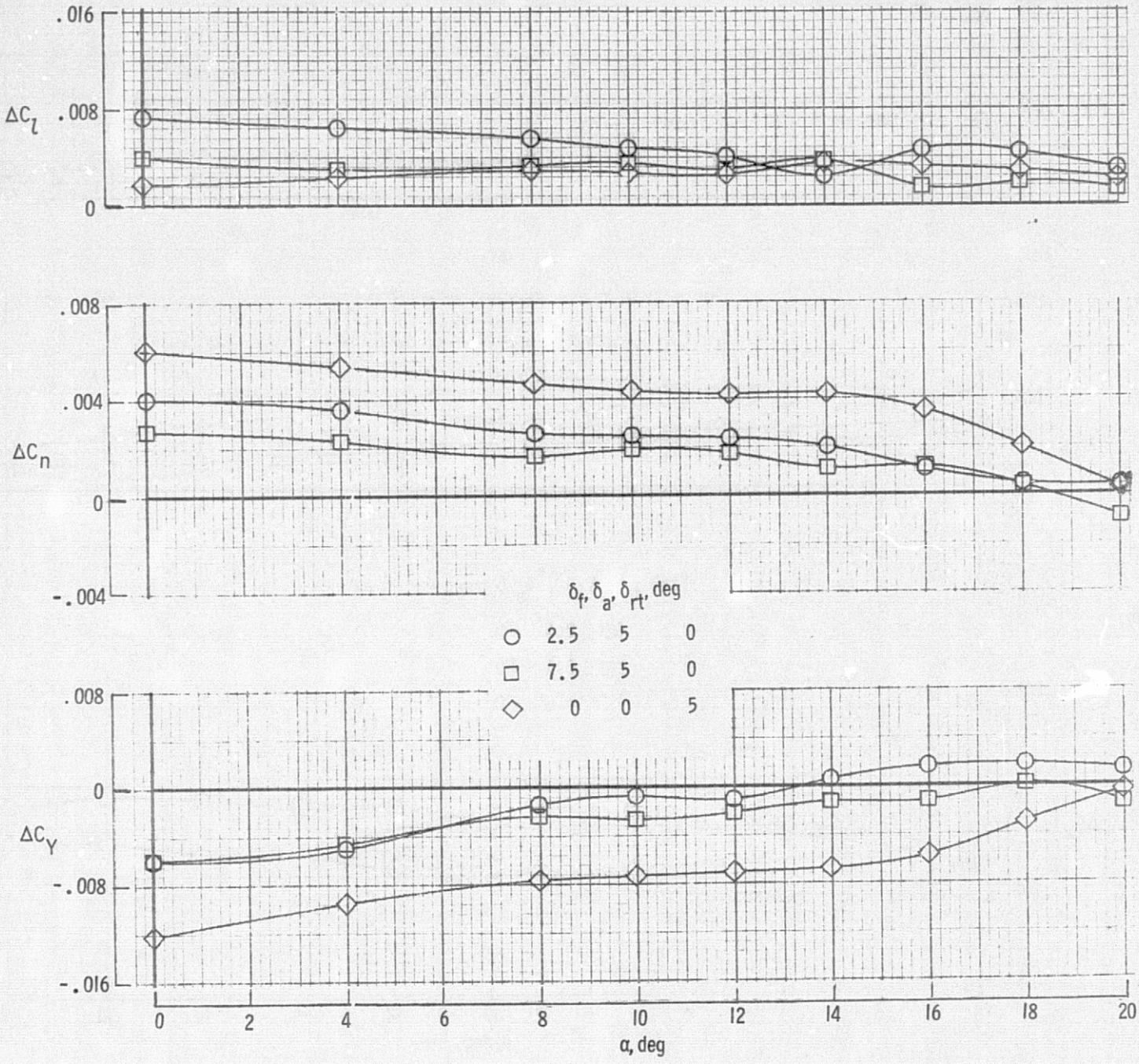

M = .90

Figure 13. Continued.

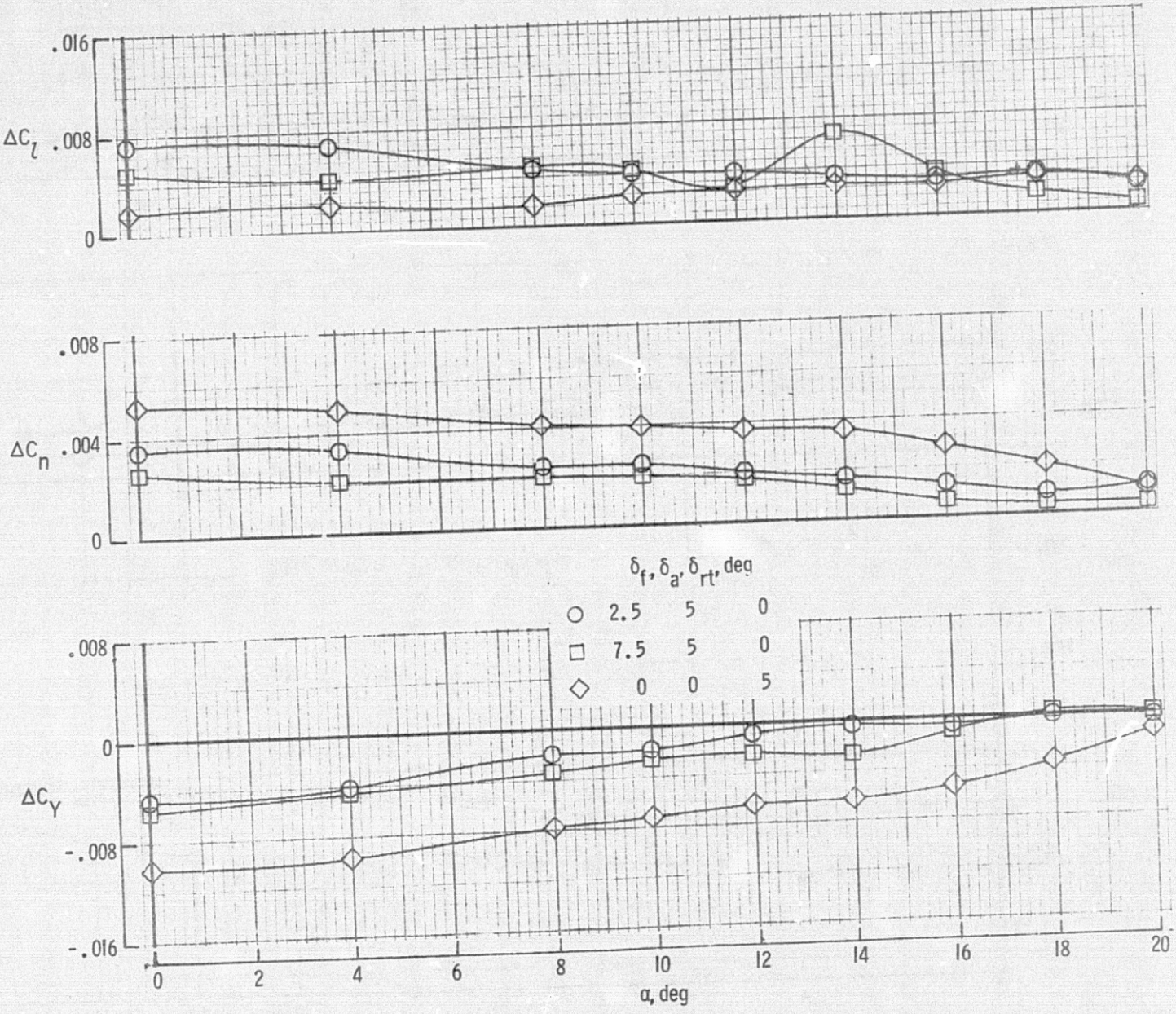

M = .85

Figure 13. Continued.

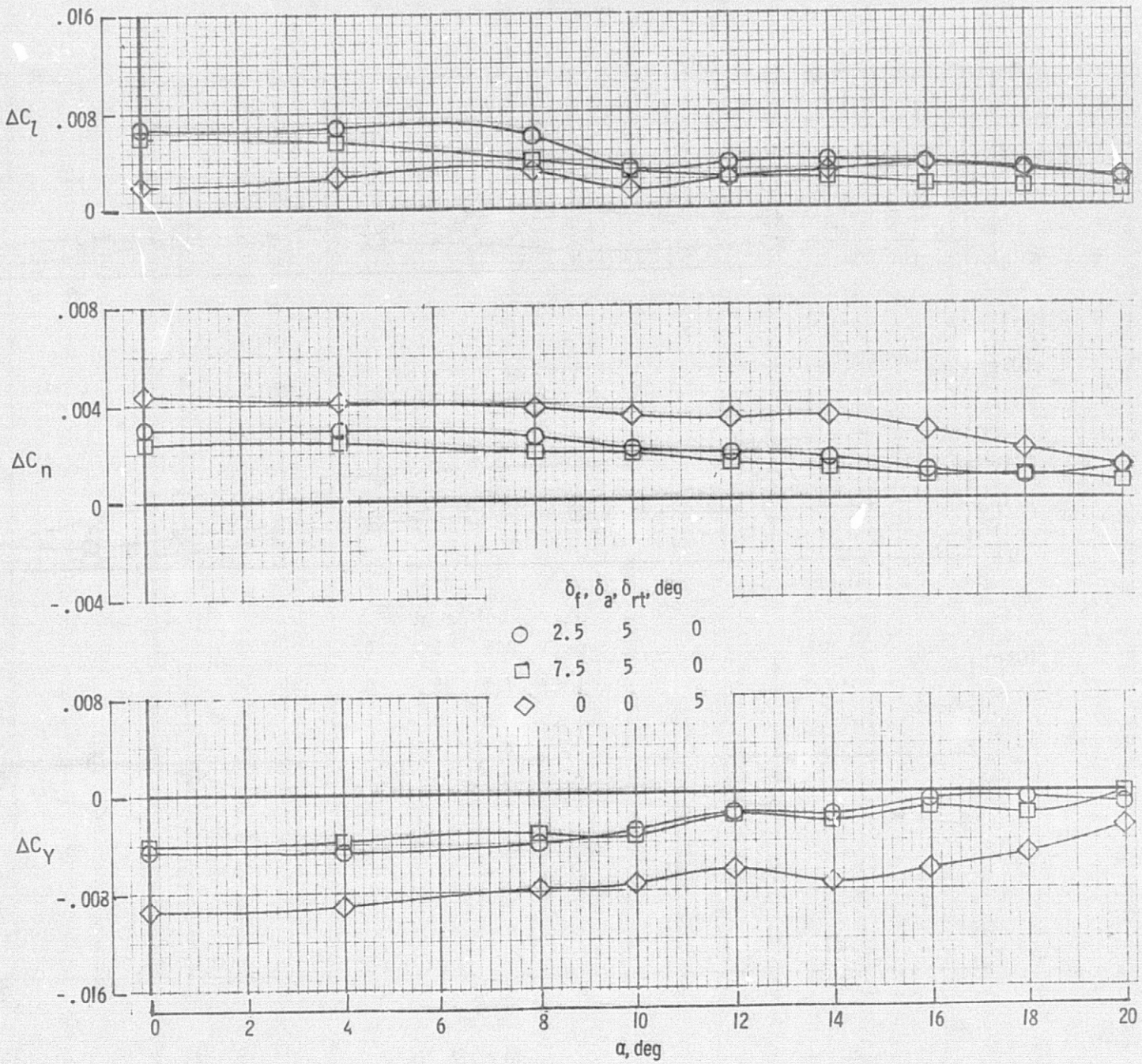

M = .80

Figure 13. Continued.

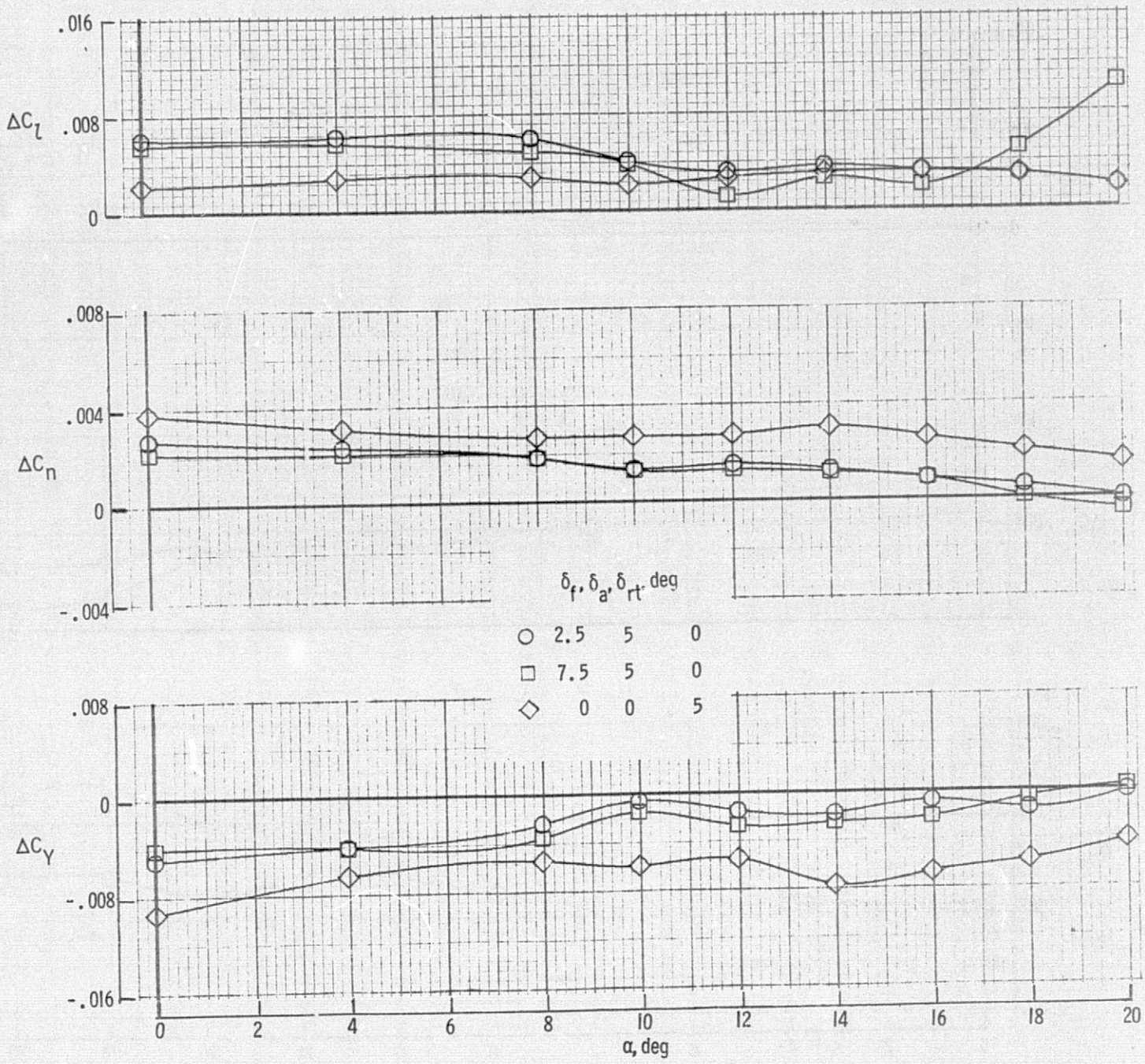

M = .70

Figure 13. Concluded.

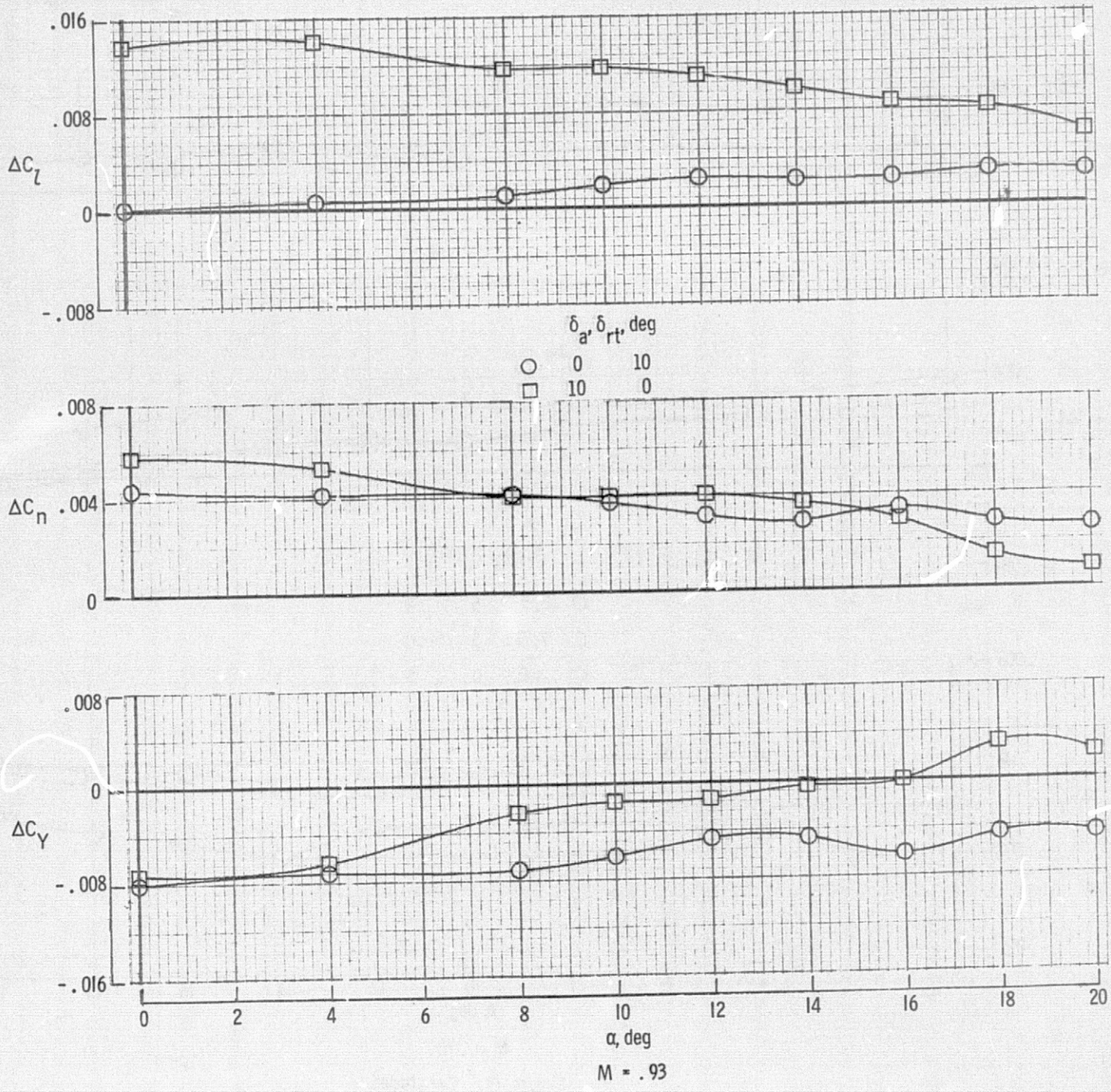

Figure 14. Comparison of the control effectiveness of the aileron and asymmetric horizontal tail deflection (for the latter data, the mean horizontal tail setting or δ_e is -10 degrees).

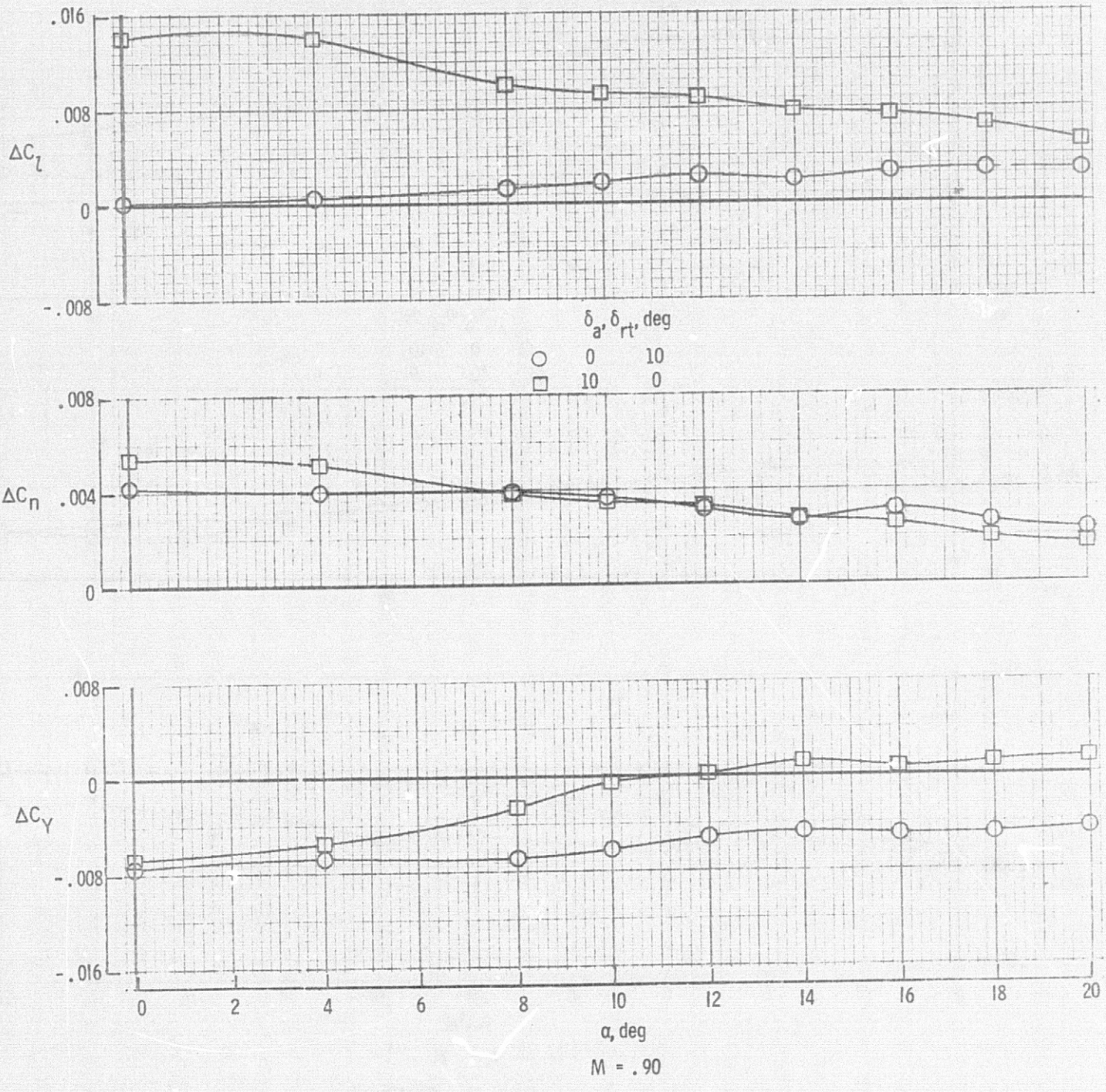

Figure 14. Continued.

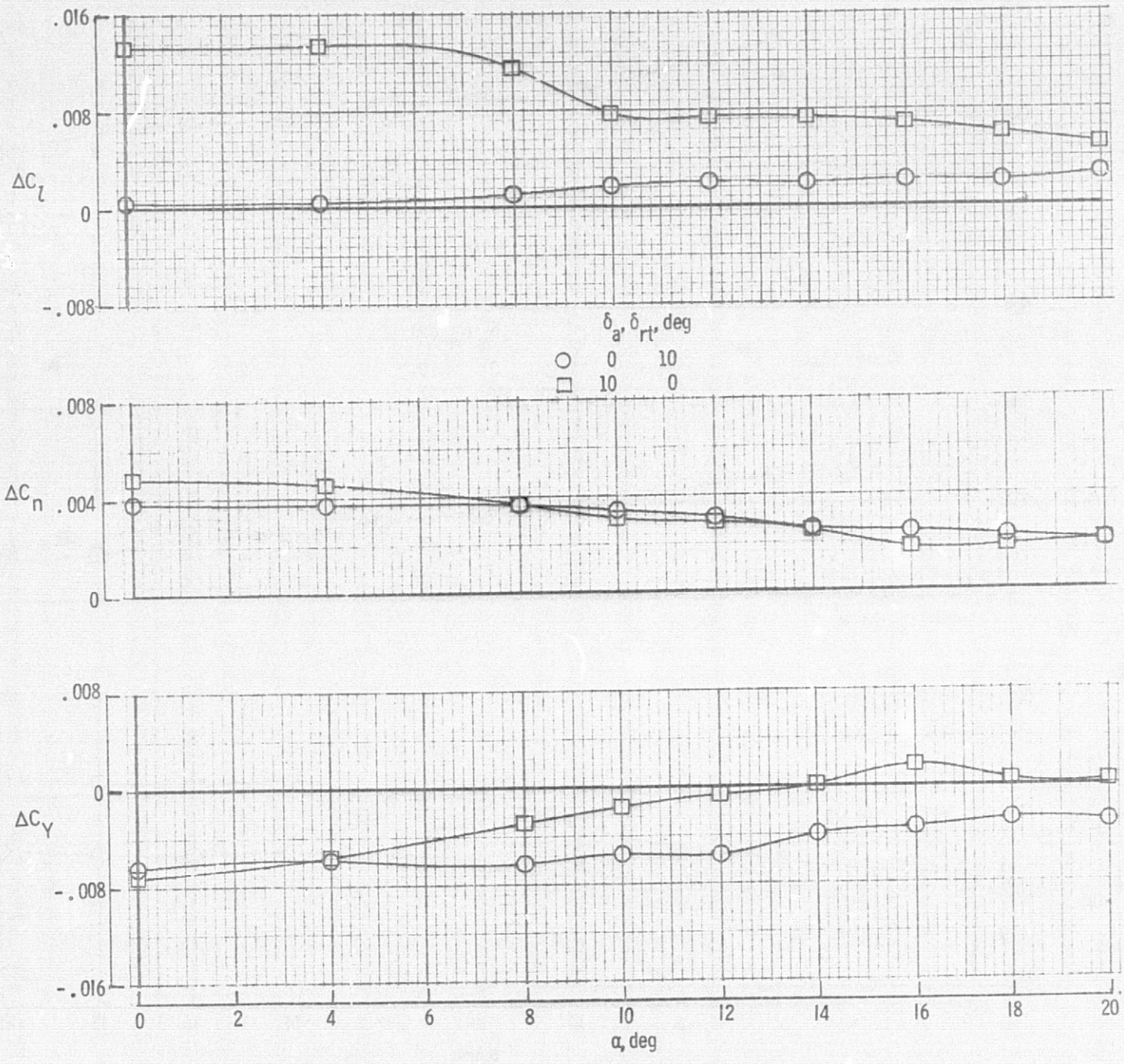

M = .85

Figure 14. Continued.

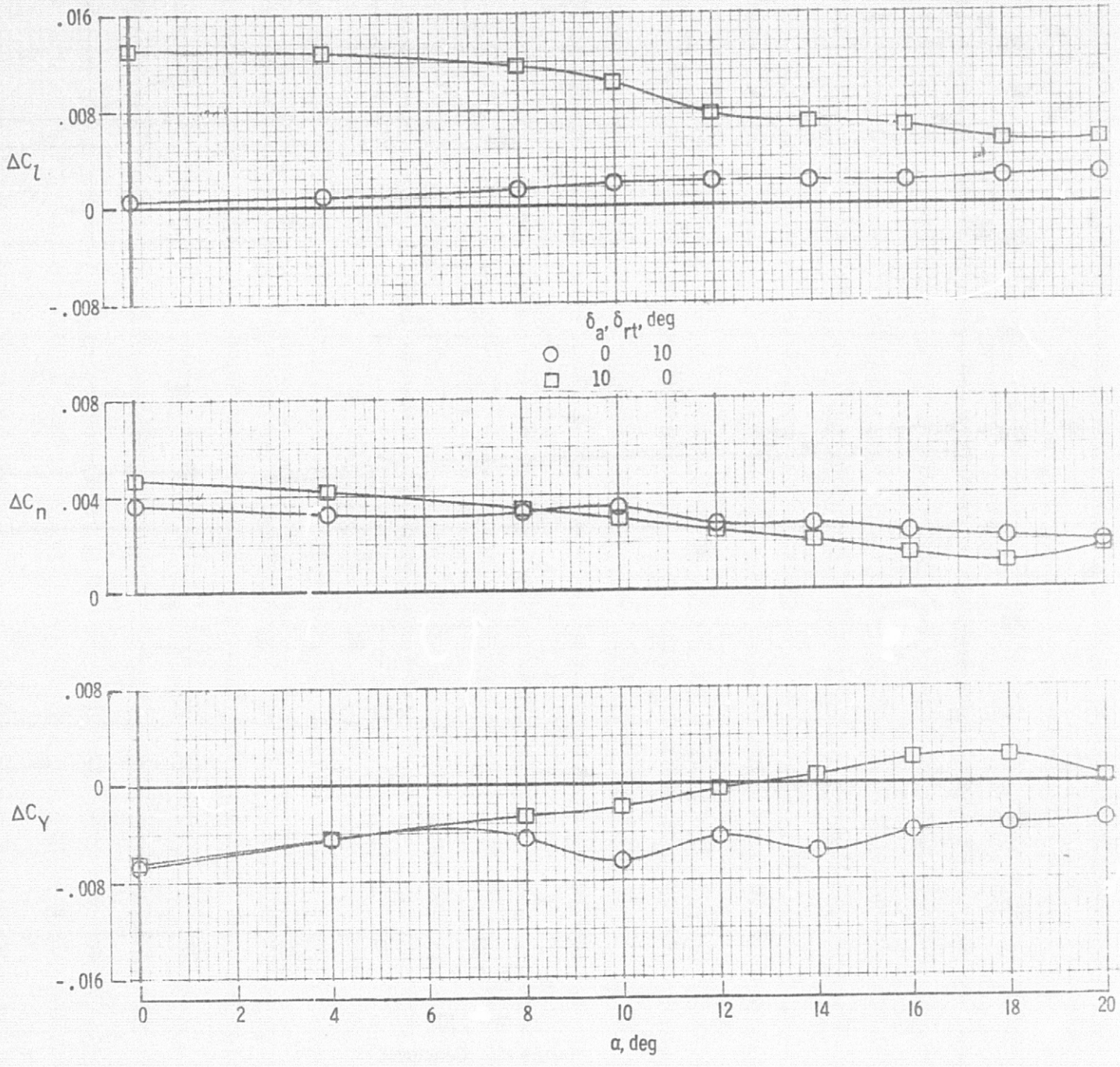

M = .80

Figure 14. Continued.

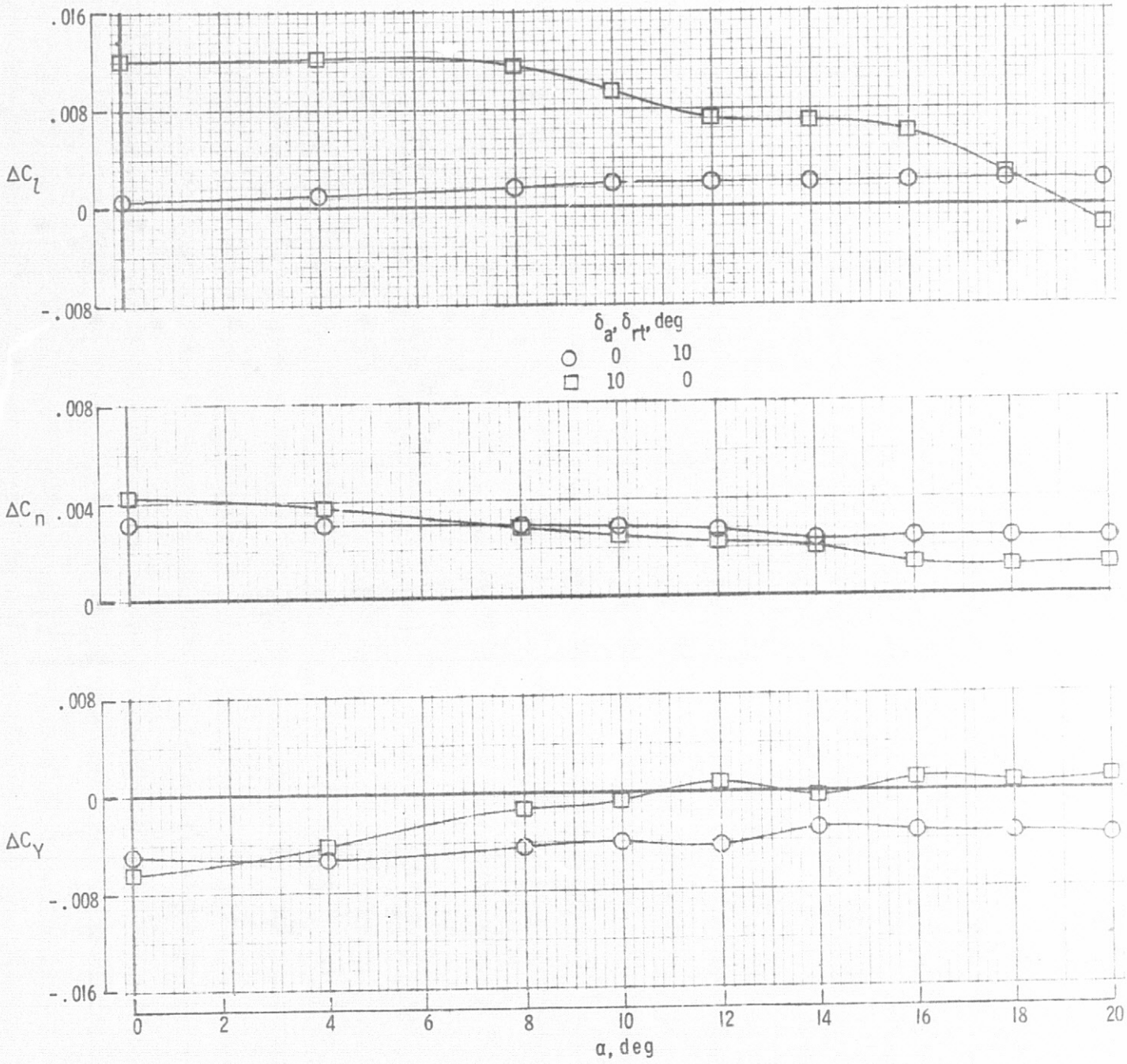

M = .70

Figure 14. Concluded.